UNIVERSITI PUTRA MALAYSIA

# *FINITE VISCOELASTIC BEHAVIOUR OF OIL PALM FRESH* FRUITLETS

CHIN MOON CHI

# FINITE VISCOELASTIC BEHAVIOUR OF OIL PALM FRESH FRUITLETS

CHIN MOON CHI

193850

PROJECT REPORT SUBMITTED IN PARTIALLY FULFILLMENT OF THE

REQUIREMENTS FOR THE DEGREE OF

BACHELOR OF ENGINEERING PROCESS AND FOOD WITH HONOURS

DEPARTMENT OF PROCESS AND FOOD ENGINEERING

FACULTY OF ENGINEEERING

UNIVERSITI PUTRA MALAYSIA

2021

## ACKNOWLEDGEMENT

First of all, I would like to express my sincere gratitude to my supervisor, Dr. Mohd Afandi P. Mohammed for his guidance, patience, support and assistance in helping me to complete my final year project throughout these two semesters.

I would also like to appreciate the effort from Dr. Intan Syafinaz Mohamed Amin Tawakkal as the coordinator of the course (EPF4949). Thanks for always providing information related to the course and guiding students to make sure everything follow the schedules smoothly.

## ABSTRACT

Studying the mechanical behaviour of oil palm fruitlet could be helpful in oil palm grading operation. This work investigates the mechanical behaviour of oil palm fruitlet by using finite element method. An axisymmetric model of a single oil palm fruitlet was developed to simulate the pin puncture test, drop test and compression test. The parameters were varied to investigate their effect on the stress-displacement curve. The stress relaxation test results showed the evidence of the viscoelastic behaviour of the oil palm mesocarp. A parametric study of the mesocarp-kernel interface properties was also carried out. The results showed that the model is not sensitive to the varying parameters due to the boundary conditions that limited the movement of the fruitlet. The model has potential in fruit maturity detection application.

## TABLE OF CONTENTS

## LIST OF TABLES

## LIST OF FIGURES

# CHAPTER 1

# INTRODUCTION

## 1.1 Background

In Malaysia, palm oil industry is very important to the economy of the country. Malaysia produces approximately 20 million tons of palm oil every year, valued at around 72 billion Malaysia ringgit. According to MPOC, Malaysia is one of the world's largest palm oil exporter which currently accounts for 28% of world palm oil production and 33% of world exports. Malaysia is also responsible for 9.5% and 19.7% of the world's total production and exports when considering the oils and fats produced in the country. In Malaysia, the palm oil industry provides employment directly and indirectly for over 0.8 million people. Malaysia plays an important role in fulfilling the growing global need for oils and fats sustainably because it is one of the biggest producers and exporters of palm oil and palm oil products. (*Malaysian Palm Oil's Worldwide Significance*, n.d.; *Malaysian Palm Oil Industry – MPOC*, n.d.)

In order to maximize the quality of oil, the oil palm fresh fruit bunch (FFB) should be harvested at optimum maturity stage. When the oil palm fruits abscised, their oil content would start to deteriorate. The harvested FFB are delivered to palm oil mill within shortest time by using an organized collection and transport system to ensure that

the oil extraction process can start before the oil quality deteriorate to an unacceptable limit.

Grading of FFB refers to the process of evaluating and inspecting the quality of oil palm fresh fruit bunch. This is done by selecting samples of FFB randomly from a consignment at the mill. Around 50-100 bunches are selected from the top, middle and bottom portions of the consignment. (Murah, n.d.)

Oil palm Fresh Fruit Bunch (FFB) can be generally classified and graded into four ripeness grades which include ripe, underripe, unripe and overripe. A ripe FFB is a bunch which has reddish orange colour fruits and has at least 10 sockets of detached fruits with more than 50% of fruits still attached to the bunch. An underripe FFB has reddish orange colour fruits and has less than 10 sockets of detached fruitlets. An unripe FFB is a bunch which has purplish black colour fruits and without any socket of detached fruitlets. An overripe FFB is darkish red in colour and has more than 50% of detached fruitlets but with at least 10% of the fruits still attached to the bunch. (Murah, n.d.)

FFB grading plays a significant role in oil palm industry to ensure good quality and large quantity of production of crude palm oil (CPO) and crude palm kernel oil (CPKO) in Malaysia. The purpose of FFB grading is to improve the quality of oil palm FFB arrived at the mill as well as improving the quality of oil extracted from the FFB. Besides, the efficiency of oil extraction at the mills can be increased by proper FFB grading. Moreover, FFB grading helps to ensure a fair deal between the suppliers and

millers. FFB grading is also responsible in determining the purchase price based on the quality of the oil palm FFB.

Oil extraction rate (OER), refer to the percentage of oil recovered per FFB processed, is used to assess the performance of a palm oil mill as well as the profitability. The quality of FFB is one of the factors that contributed to low oil extraction rate. According to Misron et al. (2020), many palm oil mills have been facing issues where low quality FFB are delivered to them frequently , thus resulting in low OER of mill and consequently financial loss. Sometimes, FFBs are harvested even though they have not reached their optimum maturity stage. These unripe or underripe FFB are stored for few days to allow their colour to change to the same colour as ripe FFB. These FFB have less oil content and the oils extracted have low quality. It is very difficult for the workers to detect these low quality FFBs because their appearance are same as those ripe FFB.

In oil palm industry, quality of the fruits is very important because it contributes to most of the profit in a palm oil mill. High quality products were believed to be the key success in today's competitive market. Generally, the quality of fruits is categorized based on their texture, shape and colour. In Malaysia, conventional grading of oil palm FFB is still being carried out manually in palm oil producing industries. Oil palm FFB are divided into several grades by human eyes and observation based on the colour and loose fruits of FFB. (Shabdin et al., 2016; Utom et al., 2018)

## 1.2 Problem Statement

The current oil palm FFB grading method is using human graders to inspect the FFB visually. Human graders classify oil palm fruits into different ripeness standard by cutting a small part in the fruits to see the mesocarp colour and counting the number of loose fruits per bunch (Harun et al., 2013; Jaffar et al., 2009). These tasks must be done by skilled and experienced workers. Therefore, training programmes on FFB grading which emphasizes ripeness standards and good grading technique of FFB must be conducted.

This method has a lot of disadvantages including inaccuracy and inconsistent evaluation result. Furthermore, this method requires a lot of labour to do the task in which labour shortage would become another challenge faced by the oil palm processing industries. Besides, the manual grading of oil palm FFBs is time-consuming and tends to biased appraisal and human error, thus affecting the profitability of a palm oil mill. According to A.R et al. (2009), the conventional grading method of oil palm has more disadvantages than advantages. The long-practiced routine is time-wasting and tedious.

Due to the current grading practice, Malaysian oil palm industries have been facing problem of grading the fruits accurately. Previous studies showed that the fruit ripeness could greatly influent the crude palm oil yield and the quality of oil extracted. Thus, it is important to grade the oil palm fruits according to their ripeness to improve the quality of the oil produced as well as the overall marketability.

Studying the mechanical behaviour of an oil palm fruitlet could help in oil palm FFB grading. The force or stress distribution against the fleshy structure of the mesocarp will vary depending on the maturity level of the oil palm fruitlet.

## 1.3 Objectives

The objectives of this project are:-

- To study the mechanical behaviour of a single oil palm fruitlet through different constitutive material models
- To simulate deformation of a single oil palm fruitlet when applying pin puncture, drop and compression tests
- To study the effect of different model parameters and mesocarp-kernel interface from the oil palm fruitlet model

## 1.4 Scope of Study

The project will be started by studying the anatomy of a single oil palm fruitlet. The linear dimensions such as length, width and diameter of the fruitlet and kernel are obtained from online sources. After obtaining those data, an average value would be decided to create the representative geometry. These values would then be used to create a geometric model of a single oil palm fruitlet by using Abaqus/CAE software. By including mechanical properties such as modulus of elasticity of the fruitlet in the CAE model, virtual test such as pin puncture test, drop test and compression test can be carried out to investigate the mechanical behaviour of the oil palm fruitlet.

# CHAPTER 2

# LITERATURE REVIEW

## 2.1 Study on the structure of oil palm single fruitlet

### 2.1.1 Anatomy of oil palm single fruitlet

The size of an individual oil palm fruitlet is usually between 15 and 30 mm. Figure 2.1 shows the structure of an oil palm fruitlet.

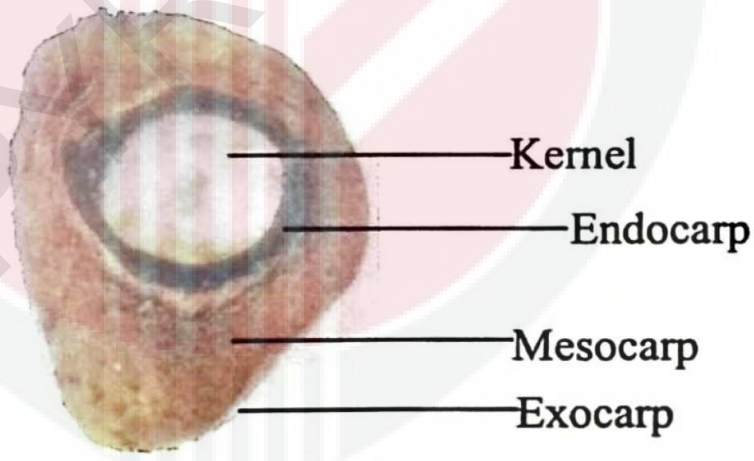


Figure 2.1: Anatomy of a single oil palm fruitlet. (Nwankwojike et al., 2011)

The pulp is made up of mesocarp and exocarp which contain the palm oil. The central nut is made up of endocarp (shell) and edible kernel which contain the palm kernel oil. (Nwankwojike et al., 2011)

Figure 2.2 shows the three main varieties of oil palm are *Dura, Pisifera* and *Tenera*. Due to the shelless nature of *Pisifera*, edible oils only could be processed from *Dura* and *Tenera* fruits. *Dura* fruits have 35-55% of pulp content and their shell thickness is generally between 2 and 8mm. Kernel of *Dura* fruits comprise about 4-20% of the fruit weight. For *Tenera* variety, the pulp content is between 60 and 96% with shell thickness varies from 0.5 to 4mm. The kernel of *Tenera* fruits comprise about 3-15% of the fruit weight. *Pisifera* variety is not used for commercial purpose due to their high tendency of sterility. (Nwankwojike et al., 2011)

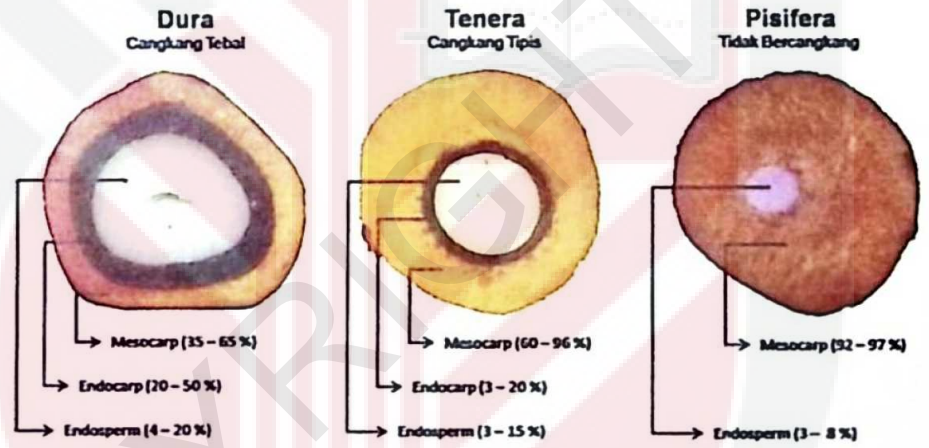


Figure 2.2: The three varieties of oil palm are Dura, Tenera and Pisifera. ("PKS (Palm Kernel Shell)," n.d.)

### 2.1.2 Length and width of oil palm single fruitlet

Malaysian Palm Oil Board (MPOB), an institution who focused on research relation to oil palm, had developed PORIM Series (PS) planting material to increase oil yield and oil quality. The PORIM Series consists of 13 planting material with different variations and each of them has their own special traits. In this research, Hazir & Shariff

(2011) used PS1 and PS2 oil palm because these planting materials are most commonly used in plantation. PS1 oil palm used in this study can be further divided into *virescens* type and *nigrescens* type. One hundred fruitlets from PS1 *virescens*, PS1 *nigrescens* and PS2 were collected and their linear dimensions (length, width and thickness) were measured by using Vernier caliper. A reading to 0.01mm was collected. This was shown in Table 2.1. Figure 2.3 showed the linear dimension (for measurement) for length and width of an oil palm fruilet.

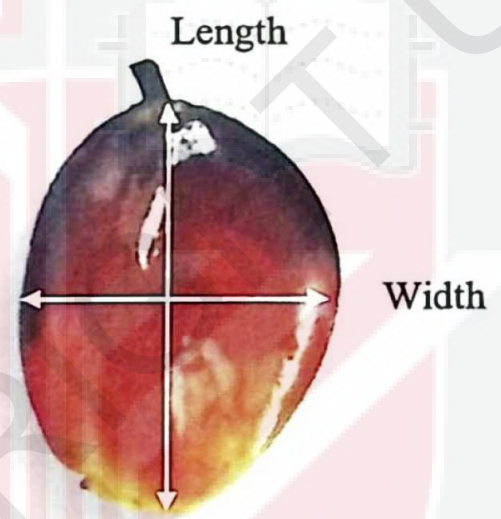


Figure 2.3: Linear dimensions (length and width) of an oil palm fruitlet. (Hazir & Shariff, 2011)

Table 2.1: Linear dimensions of oil palm fruit (*Tenera*) of different PORIM Series. (Hazir & Shariff, 2011)

| Category | Length (mm) | Width (mm) |
|---|---|---|
| PS 1 (*nigrescens*) | 34.57±3.54 | 23.65±2.73 |
| PS 1 (*virescens*) | 38.00±3.87 | 25.52±2.53 |
| PS 2 | 40.64±3.22 | 27.12±2.71 |

Owolarafe et al. (2007) studied the physical and mechanical properties of two varieties of oil palm fruit namely *Dura* and *Tenera*. 50 sample fruits were randomly selected to determine their physical properties. In this study, the linear dimensions (length, width and thickness) were measured by using Vernier caliper that capable to read to 0.01mm.The measurement for dimensions of each sample from *Dura* and *Tenera* varieties was replicated fifty times. It is concluded that the *Tenera* fruits had bigger size than *Dura* fruits because the values of length, width and thickness of *Tenera* fruits were greater than *Dura* fruits. Table 2.2 showed the linear dimensions of oil palm fruits obtained in this study.

Table 2.2: Linear dimensions of oil palm fruits of Dura and Tenera varieties. (Owolarafe et al., 2007)

| Variety | Length (mm) | Width (mm) |
|---|---|---|
| *Dura* | 30.25(+5.07) | 19.94(±2.64) |
| *Tenera* | 35.96(±4.08) | 20.15(±3.79) |

In a study conducted by Basyuni et al. (2017), Duncan's multiple range test (DMRT) was used to evaluate the oil palm fruits length and diameter. In contrast with the previous investigation by Owolarafe et al.(2007), this study found that *Dura* fruits were the largest among the three varieties of oil palm fruits. The linear dimensions of oil palm fruits were shown in Table 2.3. The author concluded that the *Dura* fruits are generally larger due to the presence of thick shell in *Dura* variety.

Table 2.3: Linear dimensions of oil palm fruits of *Dura*, *Pisifera* and *Tenera* varieties. (Basyuni et al., 2017)

| Variety | Length (mm) | Width (mm) |
|---|---|---|
| *Dura* | 39.30 | 25.20 |
| *Pisifera* | 35.00 | 20.40 |
| *Tenera* | 34.70 | 21.20 |

In another study, the three axial dimensions namely major, intermediate and minor diameters which also represent the length, width and thickness of an oil palm fruit were measured by using micrometer screw gauge. A reading to 0.01mm was collected. Samples of *Dura* variety and *Tenera* variety were collected from oil palm tree with different ages. Figure 2.4 depicted the typical linear dimensions of an oil palm fruitlet. The results were shown in Table 2.4. It is concluded that oil palm tree with larger age would have fruitlets with bigger size. (Afolabi & Adeleke, 2015)

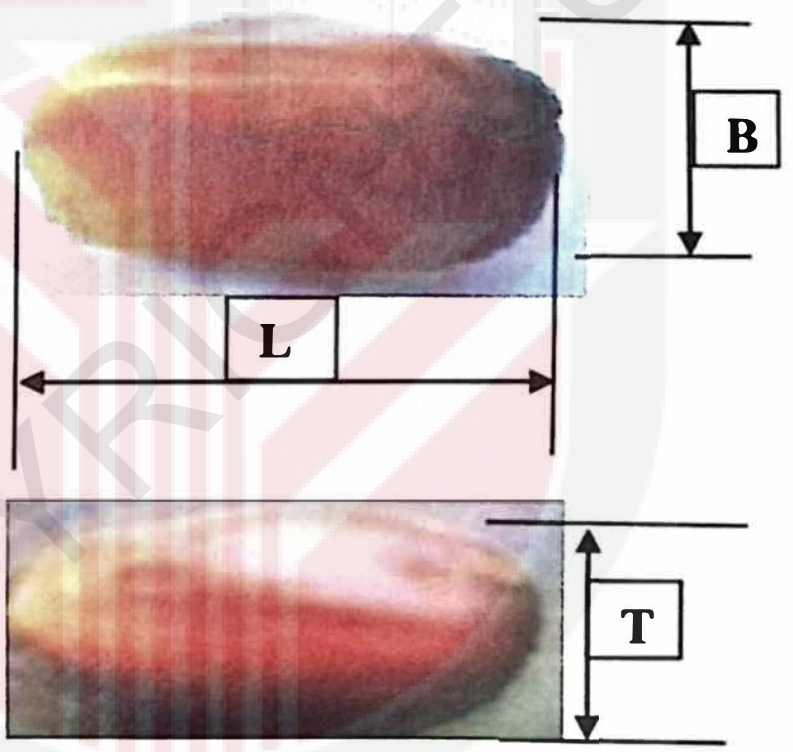


Figure 2.4: A typical oil palm fruitlet linear dimensions where L=length; B=breadth; T=thickness. (Afolabi & Adeleke, 2015)

Table 2.4: Linear dimensions of oil palm fruitlets (Dura and Tenera varieties) of different ages. (Afolabi & Adeleke, 2015)

| Age of oil palm tree (years) | *Dura* variety | | *Tenera* variety | |
|---|---|---|---|---|
| | Length (mm) | Width (mm) | Length (mm) | Width (mm) |
| 20 | 23.31±3.48 | 18.77±2.08 | 30.66±3.64 | 24.00±2.70 |
| 30 | 26.57±3.13 | 21.29±2.19 | 33.84±4.93 | 24.77±2.95 |
| 50 | 33.28±3.43 | 33.28±2.95 | 42.32±3.98 | 27.96±2.54 |

Rotimi (2012) carried out an investigation on the physical and mechanical properties of oil palm fruit, nut and kernel of *Dura* variety. In this research, 100 fruitlets of *Dura* variety were randomly selected to determine their length, width and thickness by using a micrometer screw gauge, having accuracy of 0.01mm. The linear dimensions obtained in this study were shown in Table 2.5.

A summary of linear dimensions of oil palm fruitlets is shown in Table 2.6.

Table 2.5: Linear dimensions of oil palm fruits (*Dura* variety). (Rotimi, 2012)

| Dimensions | Maximum | Minimum | Mean |
|---|---|---|---|
| Length (mm) | 42.32 | 28.04 | 34.99 |
| Width (mm) | 25.37 | 20.01 | 22.05 |

Table 2.6: Summary of linear dimensions of oil palm fruitlets.

| No. | Properties | *Dura* | *Pisifera* | *Tenera* | Remark | Source |
|---|---|---|---|---|---|---|
| 1 | Length (mm) | - | - | 34.57±3.54 | PS 1 (nigrescens) | (Hazir & Shariff, 2011) |
| | Width (mm) | - | - | 23.65±2.73 | | |
| | Length (mm) | - | - | 38.00±3.87 | PS 1 (virescens) | |
| | Width (mm) | - | - | 25.52±2.53 | | |
| | Length (mm) | - | - | 40.64±3.22 | PS 2 | |
| | Width (mm) | - | - | 27.12±2.71 | | |
| 2 | Length (mm) | 30.25±5.07 | - | 35.96±4.08 | - | (Owolarafe et al., 2007) |
| | Width (mm) | 19.94±2.64 | - | 20.15±3.79 | - | |
| 3 | Length (mm) | 39.30 | 35.00 | 34.70 | - | (Basyuni et al., 2017) |
| | Width (mm) | 25.20 | 20.40 | 21.20 | - | |
| 4 | Length (mm) | 23.31±3.48 | - | 30.66±3.64 | 20 years of age | (Afolabi & Adeleke, 2015) |
| | Width (mm) | 18.77±2.08 | - | 24.00±2.70 | | |
| | Length (mm) | 26.57±3.13 | - | 33.84±4.93 | 30 years of age | |
| | Width (mm) | 21.29±2.19 | - | 24.77±2.95 | | |
| | Length (mm) | 33.28±3.43 | - | 42.32±3.98 | 50 years of age | |
| | Width (mm) | 33.28±2.95 | - | 27.96±2.54 | | |
| 5 | Length (mm) | 34.99 | - | - | - | (Rotimi, 2012) |
| | Width (mm) | 22.05 | - | - | - | |

### 2.1.3 Diameter of kernel

Rotimi(2012) did a research on the physical and mechanical properties of oil palm fruit, nut and kernel of *Dura* variety. In this study, one hundred *Dura* fruits were selected randomly to evaluate the length, width and thickness of the fruit kernel. The results were shown in Table 2.7. Figure 2.5 showed the cross section image of an oil palm fruit kernel.

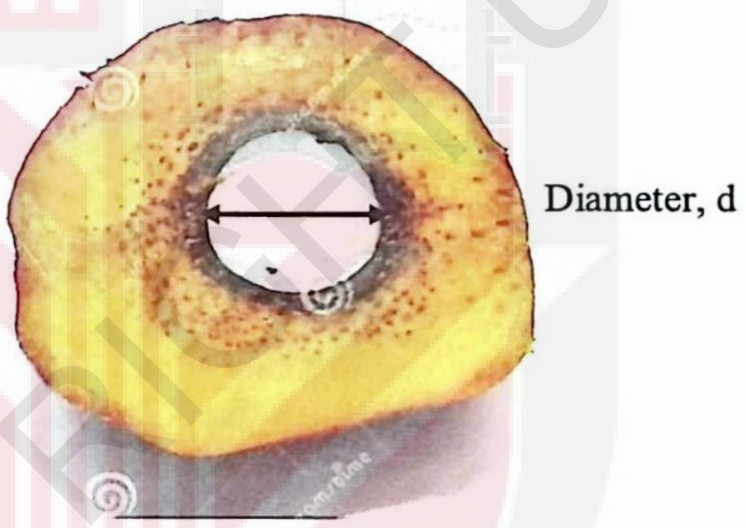


Figure 2.5: Cross section image of an oil palm fruit kernel. (*Cross Section Of Tenera Fruit Of Oil Palm Stock Photo - Image of Isolated, African: 115854784*, n.d.)

Table 2.7: Linear dimensions of kernel of oil palm fruit (*Dura* variety). (Rotimi, 2012)

| Dimensions | Maximum | Minimum | Mean |
|---|---|---|---|
| Length (mm) | 21.47 | 15.48 | 18.63 |
| Width (mm) | 17.90 | 11.80 | 15.20 |

In a study from Shehu et al.(2019), the dimensions such as fruit radius, endocarp radius and kernel radius were measured. The oil palm fruitlet was assumed to have

spherical shape for simulation. Figure 2.6 showed the cross section of oil palm fruitlet where the fruit radius, endocarp radius and kernel radius were measured. The result of this study was shown in Table 2.8.

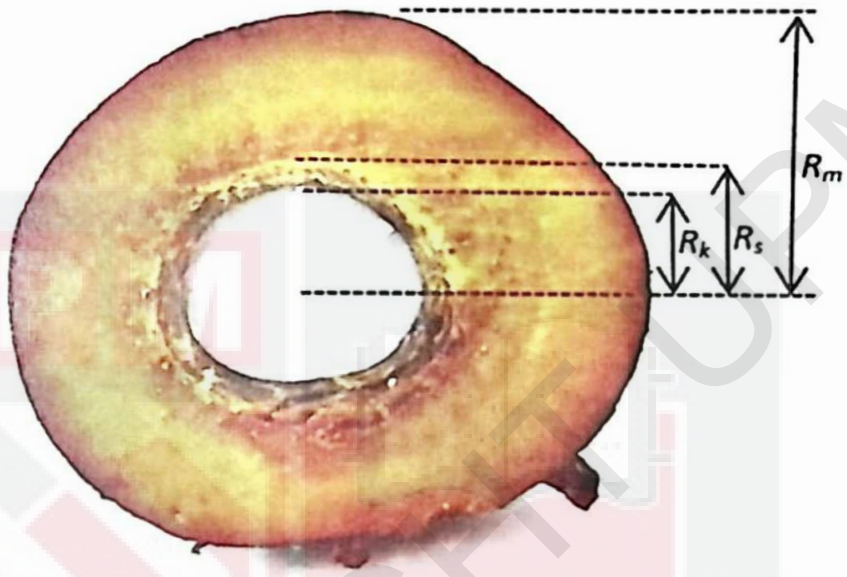


Figure 2.6: Section of the oil palm fruitlet to measure fruit radius, endocarp radius and kernel radius. (Shehu et al., 2019)

Table 2.8: Fruit radius, endocarp radius and kernel radius of an oil palm fruit var. *Tenera* were measured. (Shehu et al., 2019)

| Part | Dimenson (m) | Standard deviation |
|---|---|---|
| Fruit radius | $1.495 \times 10^{-2}$ | $\pm 4 \times 10^{-3}$ |
| Endocarp radius | $7.1 \times 10^{-3}$ | $\pm 2 \times 10^{-4}$ |
| Kernel radius | $6.1 \times 10^{-3}$ | $\pm 1 \times 10^{-4}$ |

Mohamed Halim et al. (2016) studied the nut and kernel size distribution because it is important for optimizing the process of kernel separation by using five-stage winnowing column system. Around 2.0 kg of nut and kernel sample were collected from the feeding to the nutcracker and the kernel discharge outlet. Perforated metal plates consisting of different sizes were used to measure the sizes of nut and kernel. The sizes

of nut and kernel were determined by measuring their horizontal cross-sectional diameter and consequently their size distribution was also determined.

The result in Figure 2.7 showed that the diameter of *Tenera* nuts was usually 16mm or less while the length for *Dura* nuts was between 16 and 18mm. The size distribution of kernel ranged from 7 to 15 mm with most of them having sizes between 10 to 12mm.

Table 2.9 showed a summary of diameter of oil palm fruit kernel.

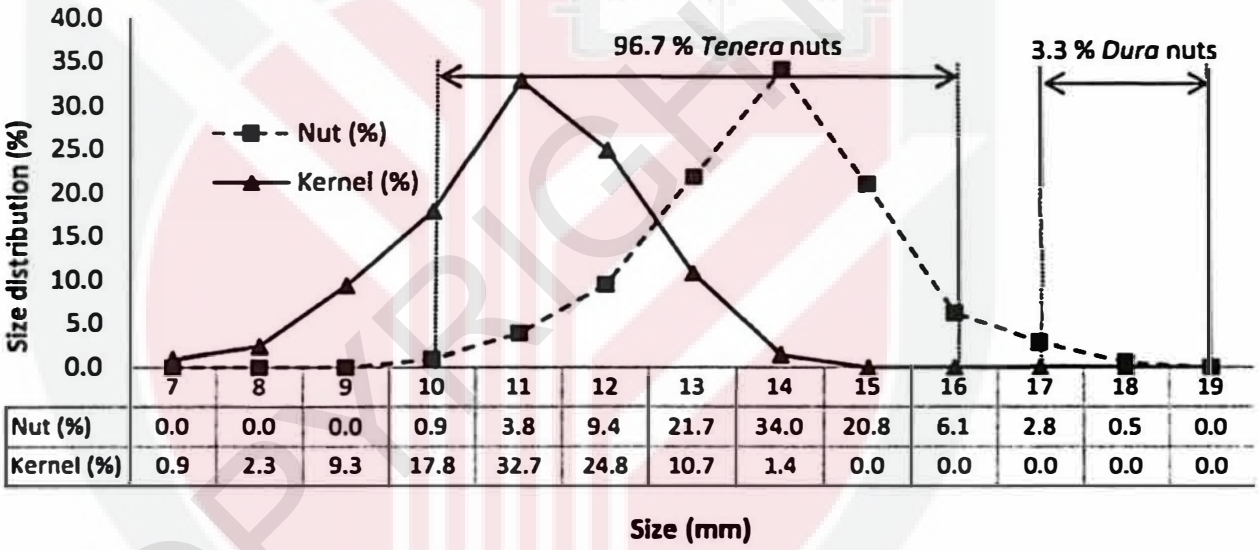


| | 7 | 8 | 9 | 10 | 11 | 12 | 13 | 14 | 15 | 16 | 17 | 18 | 19 |
|---|---|---|---|---|---|---|---|---|---|---|---|---|---|
| Nut (%) | 0.0 | 0.0 | 0.0 | 0.9 | 3.8 | 9.4 | 21.7 | 34.0 | 20.8 | 6.1 | 2.8 | 0.5 | 0.0 |
| Kernel (%) | 0.9 | 2.3 | 9.3 | 17.8 | 32.7 | 24.8 | 10.7 | 1.4 | 0.0 | 0.0 | 0.0 | 0.0 | 0.0 |

Figure 2.7: Size distribution of oil palm nut and kernel. (Mohamed Halim et al. , 2016)

Table 2.9: Summary of diameter of oil palm fruit kernel.

| No. | Properties | *Dura* | *Pisifera* | *Tenera* | Source |
|---|---|---|---|---|---|
| 1 | Length (mm) | 18.63 | - | - | (Rotimi, 2012) |
| | Width (mm) | 15.20 | - | - | |
| 2 | Diameter (mm) | - | - | 12.20 | (Shehu et al., 2019) |
| 3 | Diameter (mm) | - | - | 11.00 | (Mohamed Halim et al., 2016) |
| 4 | Diameter (mm) | 13.00 | - | - | (Bille Ngalle et al., 2014) |

## 2.2 Mechanical behaviour of oil palm mesocarp fibre (OPMF)

### 2.2.1 Theory

Hanipah et al.(2016) modeled the mechanical behaviour of OPMF by including a stress-softening function into a non-linear finite strain viscoelastic model. The model was used to carry out tensile tests, loading-unloading and relaxation tests. Oil palm mesocarp fibre was assumed to be isotropic and homogenous because there was no existing work on the anisotropic behaviour of OPMF.

The paper considered a van der Waals large strain model to simulate oil palm mesocarp fibre (OPMF) deformation. The van der Waals model can be expressed as (true stress under uniaxial tension):

$$\sigma_0(\lambda) = \mu\lambda\left(\lambda - \frac{1}{\lambda^2}\right)\left[\frac{\sqrt{\lambda_m^2 - 3}}{\sqrt{\lambda_m^2 - 3} - \sqrt{\lambda^2 + 2\lambda^{-1} - 3}} - a\sqrt{\frac{\lambda^2 + 2\lambda^{-1} - 3}{2}}\right]$$

where

$\mu$ = instantaneous initial shear modulus;

$\lambda_m$= locking stretch constant;

a = global interaction parameter

The locking stretch constant describes the finite extendability of material when the microstructure network unfolds and locks, whereas the global interaction parameter models the interaction within a chain network (interaction between cellulose–hemicellulose–lignin).

The viscoelastic model assumes a separable time and strain-dependent material behaviour. The relaxation stress under a step strain loading history is defined as a function of time, g(t) which is represented by the Prony series.

$$g(t) = g_\infty + \sum_{i=1}^{N} g_i exp\left(-\frac{t}{\xi_i}\right)$$

where t and $\xi_i$ are time and relaxation time constants respectively while $g_i$ and $g_\infty$ are dimensionless constants.

### 2.2.2 Results

The results proved that OPMF would behave like viscoelastic material because the stresses reduced during holding deformations. Besides, the loading-unloading test's result showed that plastic deformation occurred which was indicated by the value of strain after unloading (stress equal to zero). The results of loading-unloading tests and stress relaxation tensile tests (Figure 2.8 & Figure 2.9) obtained from experiment and model were compared and it showed a remarkable agreement between them.

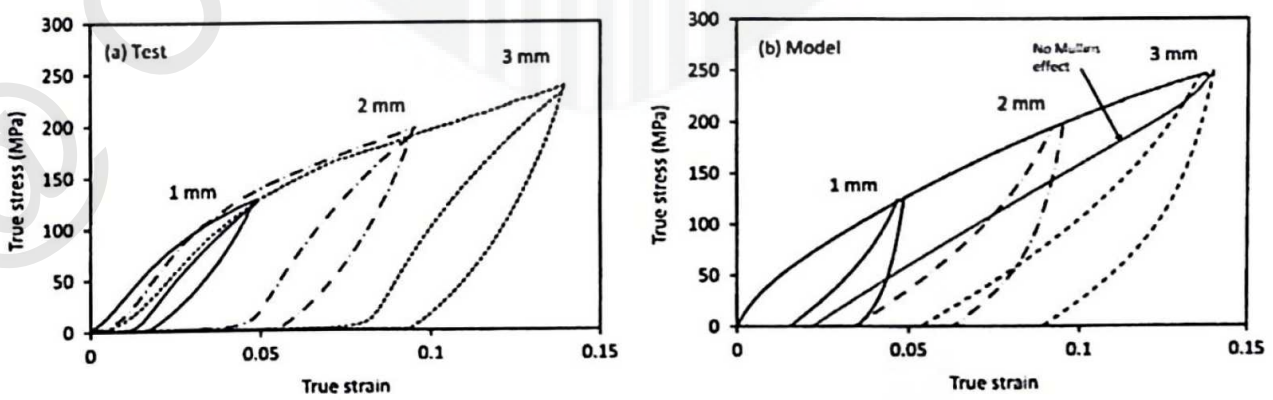


Figure 2.8 Loading-unloading tests: (a) experimental results and (b) modeling results. (Hanipah et al., 2016)

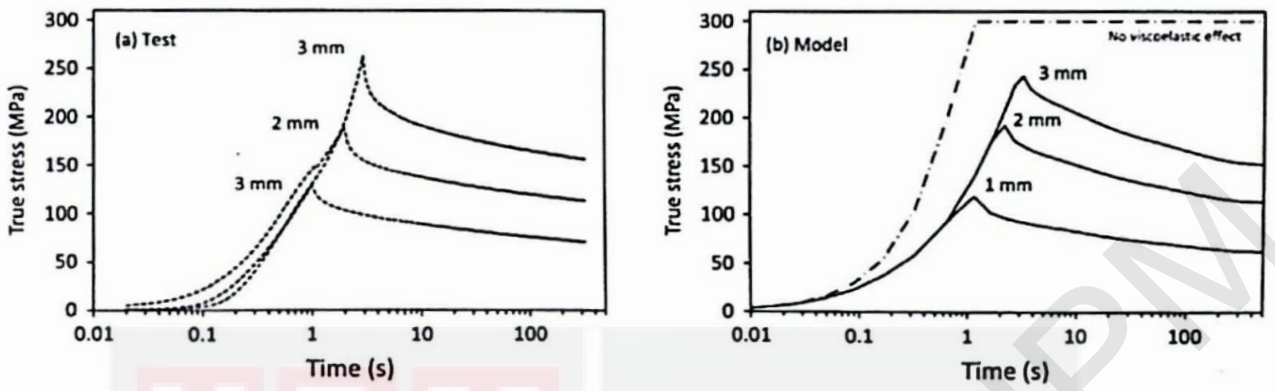


Figure 2.9: Relaxation tests: (a) experimental results and modeling results. (Hanipah et al., 2016)

Tensile tests, microstructure observation, and finite element models were used to investigate the non-linear mechanical behavior of oil palm mesocarp fibers (OPMF) (Hanipah et al., 2017). Mechanical testing such as cyclic loading and stress relaxation tests were carried out and the results were shown in Figure 2.10. The viscoelastic behaviour of the OPMF was indicated by the relaxation test results where the stress was found reduced over time at constant strain. The results from loading-unloading test showed that plastic deformation occurred which could be indicated by the permanent set when stress equal to zero. Whereas the tensile test result showed that the OPMF behaved as linear elastic material when strain is less than 0.04. Beyond this value of strain (>0.04), the fibre would have plastic behaviour which was probably caused by the microstructure damages in OPMF. Then, a finite viscoelastic model that included silica-bodies-fibre interface damage was developed to study the effect of silica bodies on the integrity of OPMF.

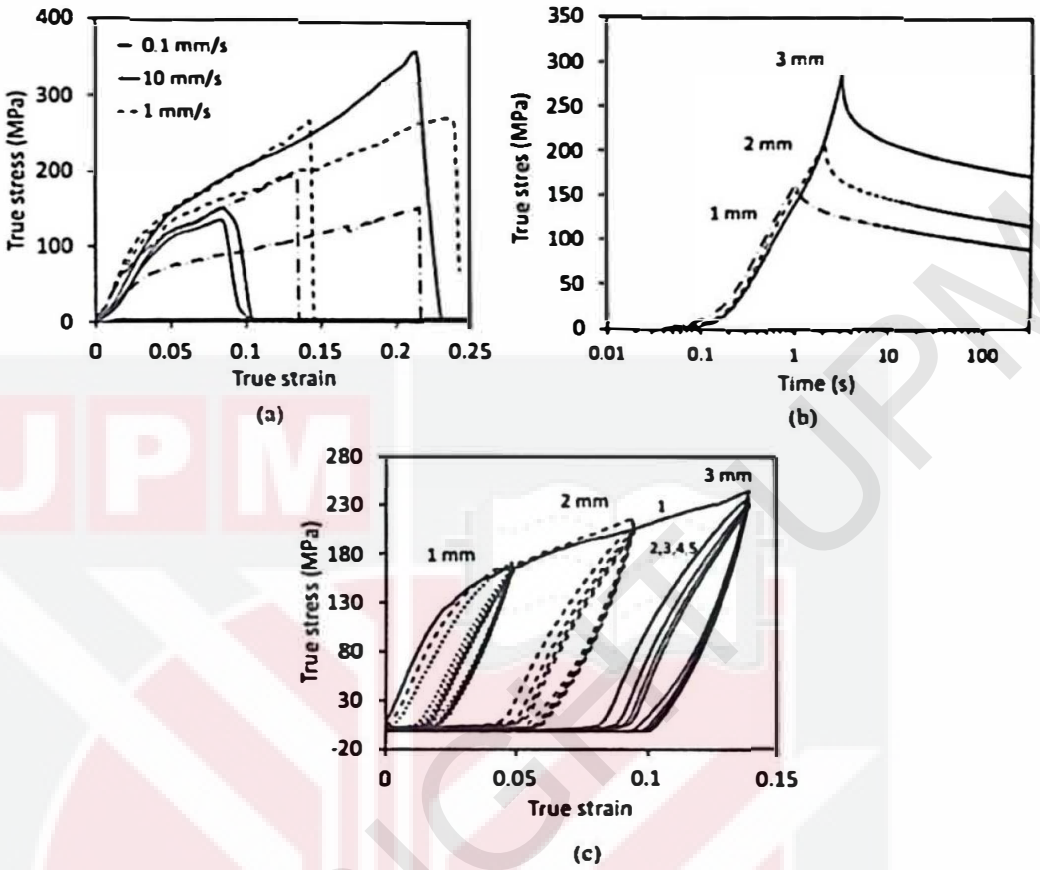


Figure 2.10: (a) Tensile tests results at different speed; (b)stress relaxation tests results; (c) cyclic tests results under different deformations.(Hanipah et al., 2017)

## 2.3 Cohesive zone modeling (CZM) of OPMF fibre-silica bodies interface

Hanipah et al.(2017) used the cohesive contact behaviour in Abaqus software to simulate the debonding of interface between the oil palm mesocarp fibre (OPMF) and silica bodies. In the study, traction-separation law was used to introduce cohesive zone modeling (CZM) into the model to simulate the damage between the interfaces. The three modes of failure in CZM consists of opening mode I (normal tension mode), mode II (shear mode), or mode III (out of plane shear mode). This study only considered mode 1 in order to simplify the model. From Figure 2.11, the failure of bond can be separate into two regions where the first region is linear elastic and can be described as: $t_n$ =

$K_{nn}\delta_n$ ($t_n$ = nominal traction stress; $K_{nn}$ = normal coefficient; $\delta_n$ = normal separation). Whereas the second region is the region where the damage is initiated by a critical normal stress which can be expressed by:

$$\max\left\{\frac{\langle t_n \rangle}{t_n^0}\right\} = 1$$

where the symbol $\langle t_n \rangle$ represents the Macaulay bracket, and is defined as $\langle t_n \rangle = \frac{1}{2}(|t_n| + t_n)$, implying that compression would not initiate the damage. Progressive damage in the interface occurs until complete failure/debonding. Cohesive energy, $G_C$ is the energy dissipated as a result of the damage process, is equal to the area under the traction–separation curve in Figure 2.11.

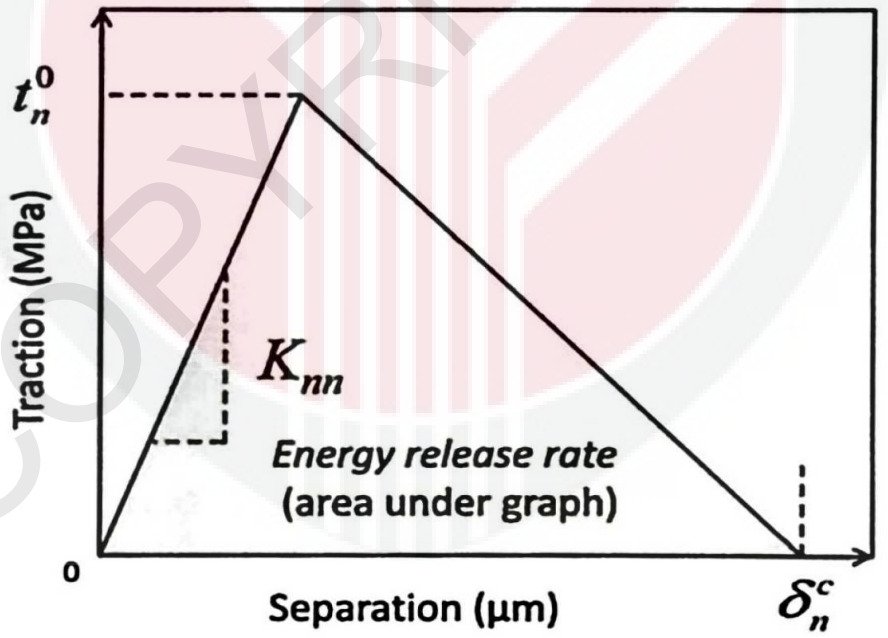


Figure 2.11: Traction versus separation law for cohesive zone modeling (CZM).(Hanipah et al., 2017)

A parametric study was used to investigate the sensitivity of CZM parameters to stress–strain curves. The control parameters used were shown in Table 2.10. The cohesive energy was varied at values of 1, 10 and 100 kN/m while keeping the critical stress constant at 100 MPa. Then, the value of critical stress was varied at 50, 100 and 200 MPa while keeping the cohesive energy constant at 1 kN/m. The results in Figure 2.12 showed that the stress-strain curve deviated from the 'no damage' model once the critical stress was activated. Also, the results showed that varying the cohesive energy did not caused noticeable difference to the stress-strain curves.

Table 2.10: Control parameters to simulate the debonding between the fibre-silica bodies interface. (Hanipah et al., 2017)

| | |
|---|---|
| $K_{nn}$ (GPa/m) | 1 x $10^8$ |
| $t_n^0$ (GPa) | 0.1 |
| $G_C$(kN/m) | 1.0 |

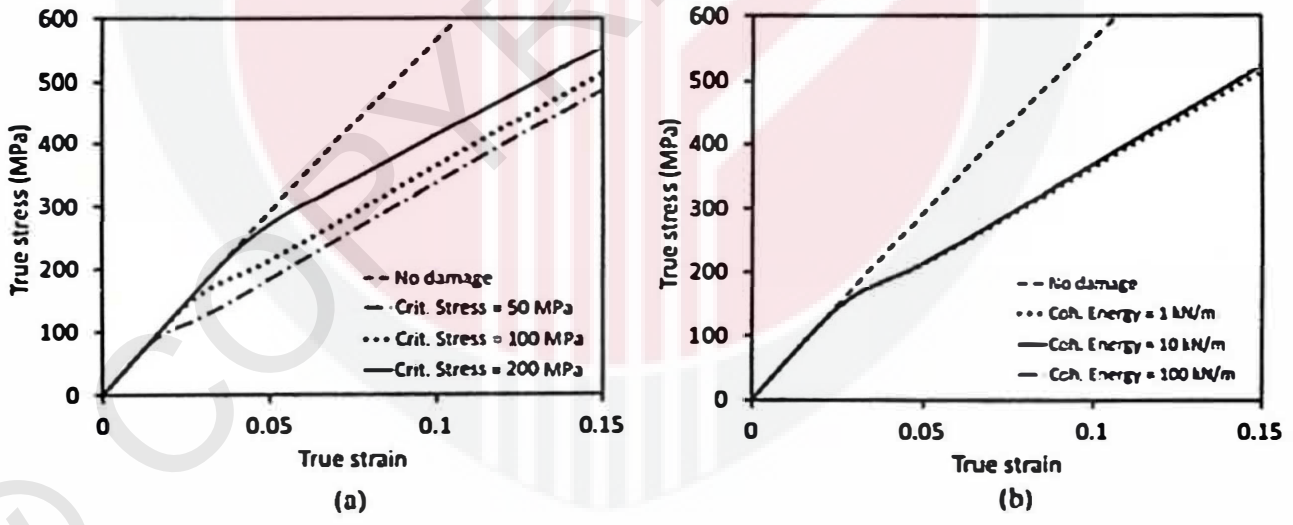


Figure 2.12: Results of parametric study of sensitivity of CZM parameters. (Hanipah et al., 2017)

## 2.4 Modeling the mechanical behaviour of fruits using other software

The mechanical behaviour of fruits plays an important role in developing oil palm grading system. Modeling the mechanical behaviour of a fruit provides better understanding on its physical and mechanical properties with high accuracy. (Dehkordi, 2016)

A finite element analysis of a tomato tissue cell was done by Dintwa et al. (2011). In this research, a liquid-filled sphere model was used to represent the tomato cell. The model had a membrane-like wall which allows the flowing of fluid under compression and was assumed to have linear elastic behaviour. The authors used MATLAB software to measure the deformation when a compression probe was used to load the cell. The simulation result from the finite element analysis of the model was compared with the experimental result in term of force-deformation data. This was shown in Figure 2.13. The model is valid because there was a remarkable agreement between the simulation result and experimental result.

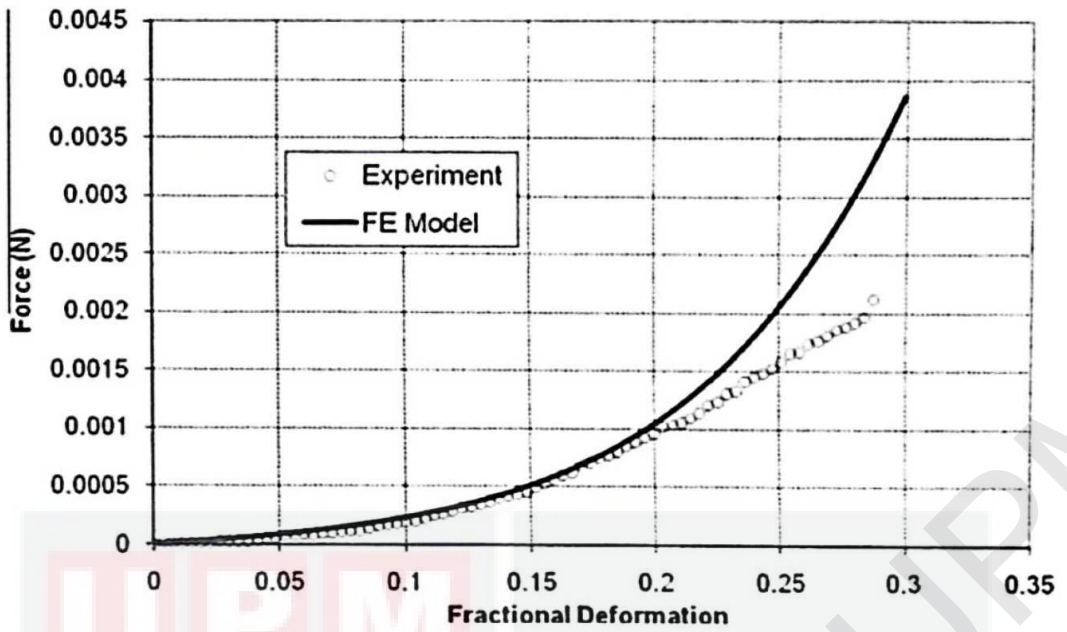


Figure 2.13: Comparison of force-deformation curve obtained from FE model and experimental method. Both curves agreed with each other in the lower deformation range, up to fractional deformation of 0.2.(E. Dintwa et al., 2011)

Another research was done by Lu et al. (2006) that measure the firmness of apple by using finite element method and empirical methods then the results from both methods were compared. FEA model was developed by using commercial software MARC to analyze the contact between the fruit and the probe. Assumption was made that the apple is axisymmetric with respect to the contact centre, thus the model can be simplified to 2-dimensional problem instead of 3-dimensional. Several factors such as fruit size or fruit skin properties may affect the distribution of stress/strain in the contact region. Thus, simulation of the model was performed to investigate their effects. The force/deformation (F/D) curve from the finite element model matched the experimental F/D curve obtained from compression test. The result in Figure 2.14 showed that there is an increasing in the difference between the simulation and experimental results when the load was further increased beyond a certain point. The increasing of non-linear

behaviour of the fruit might be a factor of this difference. However, the FE model was considered valid because the results from both methods have coefficient of correlation up to 0.828.

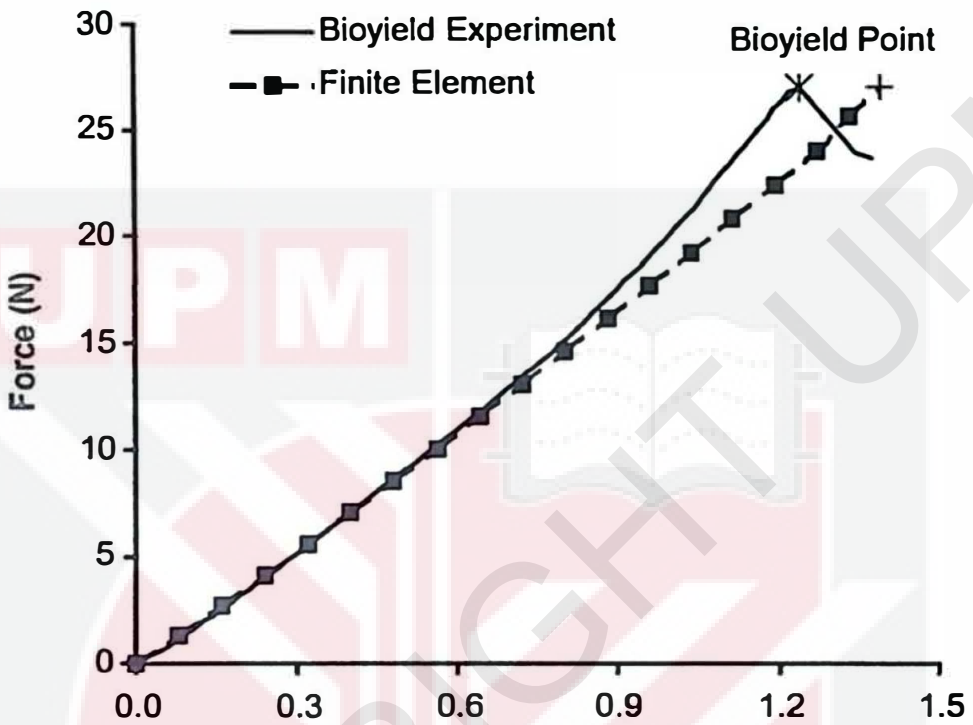


Figure 2.14: The force-deformation profiles obtained from FE model is compared with those obtained experimentally.(Lu et al., 2006)

Edward Dintwa et al. (2008) studied the finite element analysis of dynamic collision of apple against each other and with rigid walls. A 2D geometry of apple was introduced into the Mentat software and meshed. This apple model was assumed to be isotropic. The elastic properties of the apple such as elastic modulus and Poisson's ratio were also introduced into the software. The force-deformation curves were generated by using theoretical model and finite element model. Both curves were compared with each other and the result from the comparison showed that there is a closeness between both

model, thus it was concluded that the finite element method can be used to model of mechanical behaviour of fruits.

## 2.5 Correlation between fruit firmness and ripeness level of oil palm

A.R et al.(2009) did a research to find the correlation between injection force and ripeness level of FFB. The range of force that represented the ripeness level of FFB was also acquired in this literature. The force against the fleshy structure of the mesocarp was drastically depending on the ripeness level of FFB. The injection was applied to the fruitlet of FFB at different position (top, bottom, right and left). The injection process must be done gradually to prevent shock existence that may affect the accuracy of the result. Referring to Table 2.11, A.R et al.(2009) found that there were positive differences between ranges of forces for different ripeness levels. From Figure 2.15, the injection force was increasing in the order of ripe, underripe and unripe fruit. This indicated that the fruit firmness decreases with increasing ripeness level. Also, the research concluded that the position of the injection applied did not affect the injection forces too much (Figure 2.16).

Table 2.11: The range of injection forces for oil palm fruits from different field with various ripeness levels. (A.R et al., 2009)

| Fields | Fruit type | Mean | Std. Error | 95% Confidence Interval | |
|---|---|---|---|---|---|
| | | | | Lower Bound | Upper Bound |
| Sungai Buaya | Ripe | 58.061 | 1.856 | 54.392 | 61.731 |
| | Under ripe | 64.981 | 1.856 | 61.311 | 68.650 |
| | Unripe | 92.675 | 1.856 | 89.006 | 96.344 |
| Bukit Badung | Ripe | 55.403 | 1.856 | 51.733 | 59.072 |
| | Under ripe | 58.269 | 1.856 | 54.600 | 61.939 |
| | Unripe | 76.497 | 1.856 | 72.828 | 80.167 |

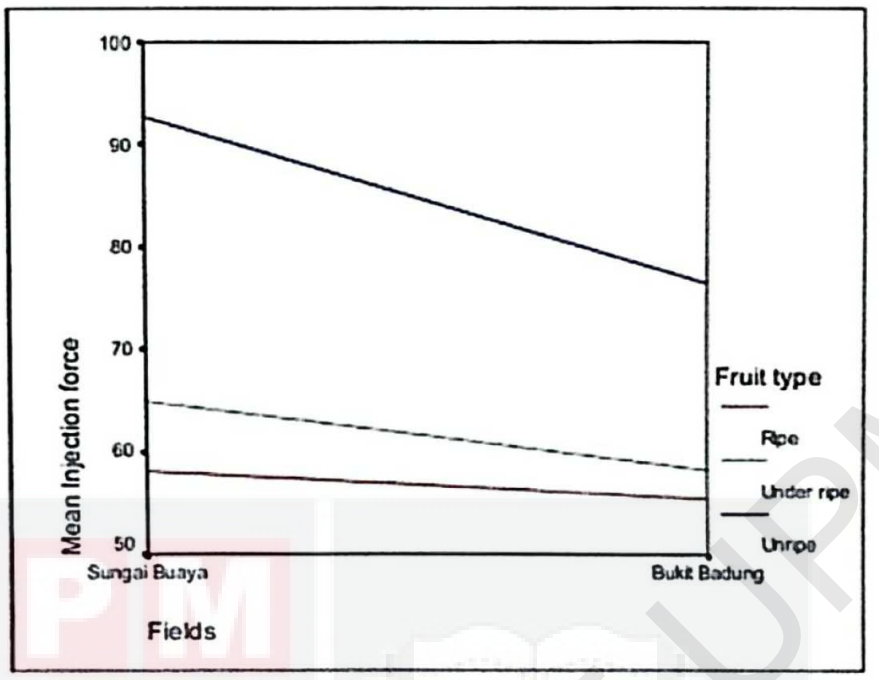


Figure 2.15: The graph indicated the positive difference between the injection force and the ripeness level. (A.R et al., 2009)

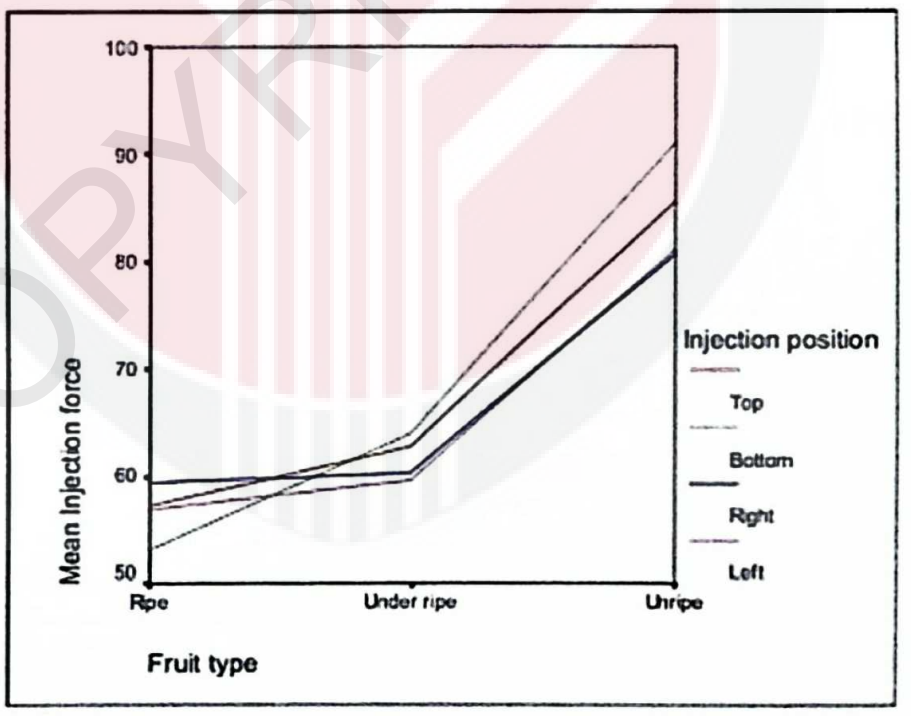


Figure 2.16: The graph showed that the effect of the injection position on the result is insignificant. (A.R et al., 2009)

Another research from Sari et al. (2019) also proved that there is a linear correlation between fruit firmness and the ripeness levels of FFB. In this research, the firmness levels of FFB were obtained by using a penetrometer. The unripe FFB has highest firmness value which is 9.39 kg/cm$^2$ while the overripe FFB has lowest firmness value which is 5.64 kg/cm$^2$. Again, this showed that the fruits tend to become softer when ripeness level increases.

## 2.6 Oil palm fresh fruit bunch (FFB) maturity detection technology

### 2.6.1 Optical sensor

It is known that the colour of FFB will change from purplish black to reddish orange during ripening process. These changes are because of the accumulation of carotene pigments.

The recently used technologies for estimation of ripeness of oil palm fresh fruit bunch (FFB) are eyesight, computer vision, hyperspectral imaging, light detection and ranging (LiDAR), near infrared (NIR) spectroscopy, and magnetic resonance imaging (Zulkifli et al., 2018). A light detection and ranging (LiDAR) scanning system was used in this study to detect the ripeness of oil palm fresh fruit bunch (FFB). LiDAR is considered as a promising solution for detection of oil palm FFB ripeness because it is non-destructive and independent of external light. This study verified that the oil palm FFB could be classified into underripe, ripe and overripe by using the intensity values from LiDAR sensors. The intensity values, ripeness level and the calculated reflected percentage using the concept of linearity were showed in Table 2.12. The low reflectance percentage in ripe oil palm fruits was due to their high lipid content.

Table 2.12: Technical specifications of LiDAR Lite V2. (Zulkifli et al., 2018)

| Intensity range | Reflectance percentage | Ripeness |
|---|---|---|
| 75-105 | 0%-50% | Over ripe |
| 105-126 | 51%-85% | Ripe |
| 112-135 | 86%-100% | Under ripe |

Although various technologies for oil palm maturity detection have been studied in previous research, there is no clear guideline related to which algorithm should be used to classify oil palm maturity under different conditions (Tuerxun et al., 2020). This study used a portable spectrometer, Oil Palm Ripeness Detector (OPRiD) to measure reflected energy from the surface of an oil palm FFB. A building classifier model was developed in Weka data mining tool to classify the oil palm FFB ripeness by using the data collected from the spectrometer. A comparative study of several machine learning algorithms was done. The result in Table 2.13 showed that Lazy KStar classifier algorithm was the most accurate with a 63% classifier model performance and 83.2% weighted average of receiver operating characteristics (ROC) curve.

Table 2.13: Comparative analysis of machine learning algorithms. (Tuerxun et al., 2020)

| Classifier Algorithm | All Attributes | | Selected Attributes | |
|---|---|---|---|---|
| | Performance (%) | ROC Weighted Average (%) | Performance (%) | ROC Weighted Average (%) |
| Naïve base | 54.74 | 74.9 | 51.58 | 77.1 |
| Logistic | 46.32 | 65.1 | 51.58 | 78.4 |
| Multilayer Perceptron | 54.74 | 76.7 | 60 | 79.3 |
| Simple Logistic | 56.84 | 80.7 | 54.74 | 76.3 |
| Supporting Vector Machine (SMO) | 52.58 | 73.3 | 51.58 | 76.5 |
| Lazy IBK | 60 | 73.5 | 54.74 | 69.4 |
| Lazy KStar | 63 | 83.2 | 55.79 | 80.2 |
| Cost sensitive | 58.95 | 78.9 | 57.89 | 79.1 |
| LMT | 56.84 | 80.7 | 54.74 | 76.3 |
| Random Forest | 58.95 | 82.8 | 54.74 | 80.5 |

Ishak & Hudzari (2010) published a paper that validates the relationship between the hue optical value of the oil palm fruits at different maturity stages and the oil content quantity of the fruits. For this study, Nikon Coolpix 4500 digital camera (Nikon, Japan) was used to capture the image of oil palm FFB and store it digitally. The relationship between the optical hue value and the mesocarp oil content of oil palm fruits were represented by using trendline analysis of polynomial second order method. Figure 2.17 showed that the mesocarp oil content of oil palm fruit increased with increasing optical hue value of fruit skin image. From Figure 2.18, a regression equation, having correlation coefficient of 0.8, was developed to represent this relationship, $y = -0.0116x^2 + 5.2376x - 514.88$ where y is the oil content of mesocarp and x is the hue value. The maximum mesocarp oil content from this study was found to be approximately 75% which is similar to previous findings.

| Exp. No. | Hue value | Mesocarp oil cont. |
|---|---|---|
| 1 | 158 | 24.44 |
| 2 | 157 | 35.15 |
| 3 | 160 | 36.01 |
| 4 | 160 | 46.33 |
| 5 | 166 | 65.77 |
| 6 | 177 | 68.87 |
| 7 | 185 | 70.66 |
| 8 | 187 | 72.73 |
| 7 | 210 | 73.01 |
| 10 | 210 | 73.47 |
| 11 | 212 | 73.75 |
| 12 | 224 | 74.22 |
| 13 | 225 | 74.33 |
| 14 | 225 | 74.5 |
| 15 | 227 | 74.67 |
| 16 | 230 | 74.76 |
| 17 | 230 | 74.83 |
| 18 | 243 | 75.46 |
| 17 | 245 | 75.67 |
| 20 | 250 | 76.75 |
| 21 | 255 | 77.76 |

Figure 2.17: The average optical value of fruit colour and the percentage of mesocarp oil content. (Ishak & Hudzari, 2010)

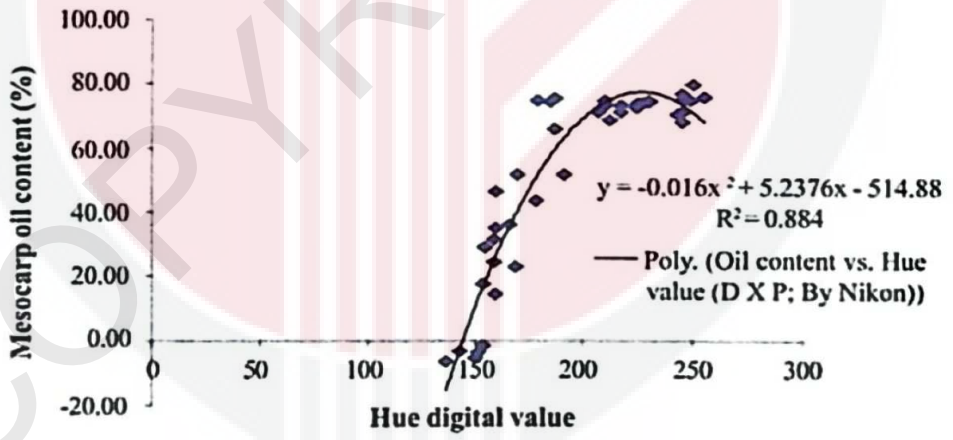


Figure 2.18: Graph that represents the relationship between the optical properties of fruit colour and the mesocarp oil content. (Ishak & Hudzari, 2010)

Alfatni et al. (2008) had successfully developed an automated oil palm grading system by using RGB color model. In this research, two cameras were used to acquire two different images simultaneously from opposite sides and MATLAB software was

used to analyze the RGB data of the images. The experimental setup of the oil palm fruit grading system was illustrated in Figure 2.19. First, the standard value of RGB intensity for each category (ripe, overripe, and underripe) were obtained. Then, the ripeness of a tested FFB was determined by comparing its mean RGB intensity (Table 2.15) with the standard RGB intensity (Table 2.14). Then, the final results which tell the ripeness level of the tested bunch would be shown (Figure 2.20). The system is able to determine and differentiate the colour properties of FFB at different ripeness level. However, the analysis of texture and shape of oil palm FFB were not involved in this study.

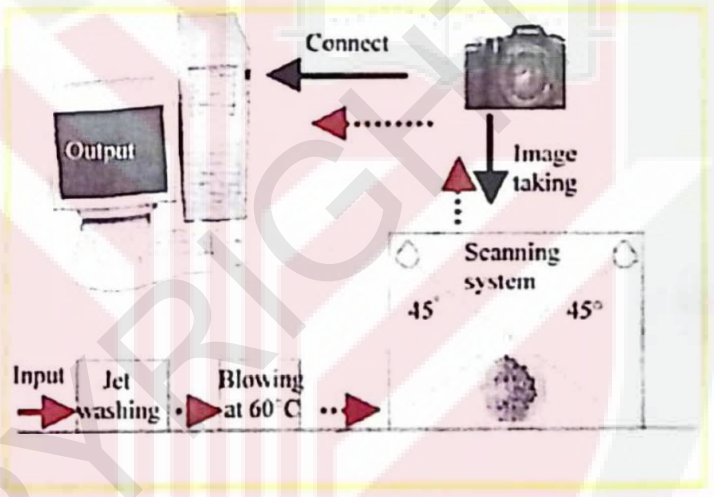


Figure 2.19: Setup of the oil palm fruit grading system. (Alfatni et al., 2008)

Table 2.14: The standard range of RGB intensity for each category. (Alfatni et al., 2008)

| | RGB intensity range | | | | | |
|---|---|---|---|---|---|---|
| | Red | | Green | | Blue | |
| Category | Min | Max | Min | Max | Min | Max |
| Ripe | 75 | 97 | 25 | 51 | 41 | 61 |
| Under ripe | 55 | 60 | 28 | 35 | 33 | 40 |
| Over ripe | 47 | 67 | 35 | 42 | 33 | 52 |

Table 2.15: The mean RGB intensity of a tested FFB. (Alfatni et al., 2008)

| | Mean of RGB | | |
|---|---|---|---|
| Tested image | Red | Green | Blue |
| Picture 1 | 88 | 36 | 50 |
| Picture 2 | 87 | 39 | 51 |
| Whole bunch | 88 | 38 | 50 |

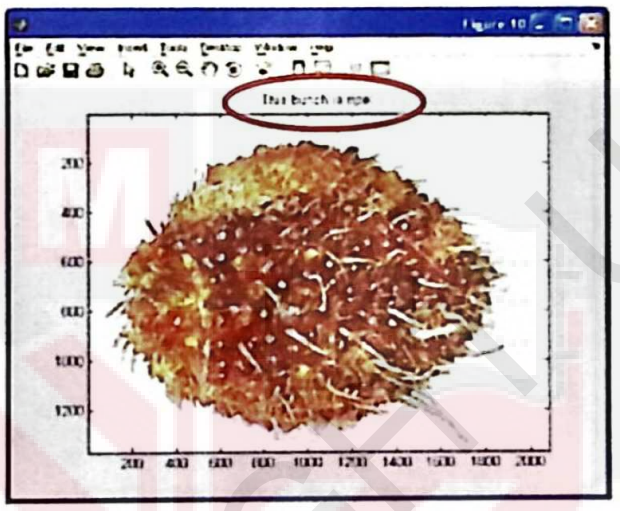

Figure 2.20: Final result that showed the ripeness level of the tested FFB. (Alfatni et al., 2008)

Bensaeed et al. (2014) successfully developed a hyperspectral-system to detect the ripeness of oil palm fresh fruit bunch (FFB). A hyperspectral device was used to scan the FFBs and reflectance was recorded at different wavelengths. After acquiring the reflectance data, the FFBs were classified into three ripeness categories (underripe, ripe and overripe) by using an artificial neural network (ANN). The ANN model successfully classified the FFBs according to their ripeness level and it could achieved an accuracy higher than 95% which was better than classifying the oil palm fruits by using human graders. The author concluded that using hyperspectral system has great potential and could provide technological advancement in oil palm fruits grading application.

Automated fruit grading methods such as computer vision is very commonly used for fruit grading operation because it eliminates human error and increases the speed of the task. However, the requirement of supporting equipment such as computer software, advanced digital camera and trained operator for this system make it not suitable for efficient on-site testing (Harun et al., 2013). Another grading method is spectral analysis which uses RGB colour feature to classify the fruit ripeness. This method depends on the different wavelength of red, green and blue colour of the fruit image. Jaffar et al. (2009) stated that this method has some disadvantages such as difficulty in differentiating the red component for unripe and underripe categories.

### 2.6.2 Electrochemical sensor

By using electrochemical ethylene sensor, a measurement system was successfully developed for monitoring ethylene gas concentrations to evaluate the fruit ripeness level (Ma et al., 2016). From this research, the process of measuring ethylene concentrations can be done rapidly by implementing a micropump and a novel signal conditioning circuit. Figure 2.21 showed the experimental setup for ethylene concentration measurement by using electrochemical sensor. Electrochemical sensor is simple-operated, small in size and portable, thus it is suitable for on-site monitoring. This sensor has availability to measure ethylene gas concentration in the range of 0-10 ppm, with constant gas flow rate at 0.4 L/min. The flow rate of ethylene gas is controlled by micopump.

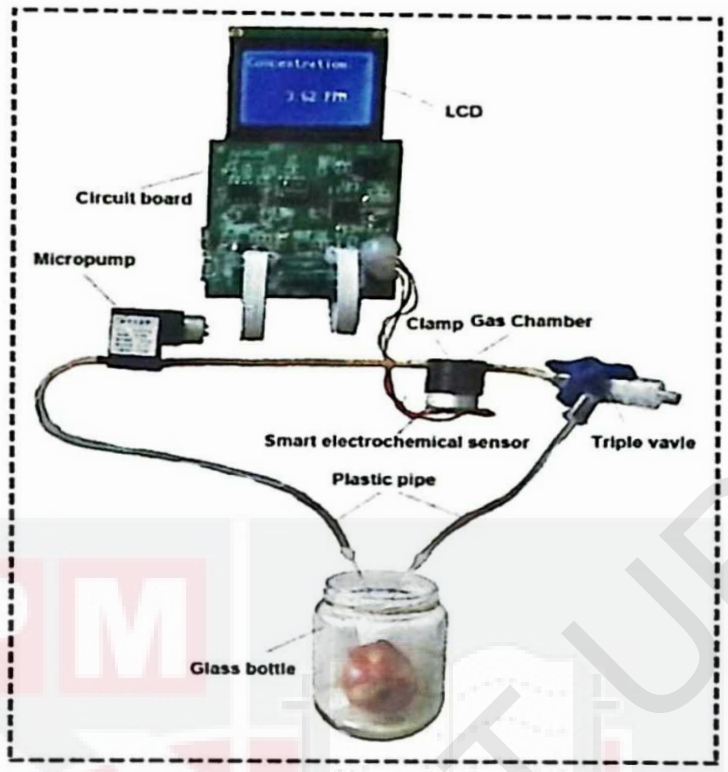


Figure 2.21: Experimental setup for ethylene concentration measurement by using electrochemical sensor. (Ma et al., 2016)

The results from the research showed that it is possible to evaluate the fruit ripeness level by measuring the ethylene gas concentration using a non-destructive electrochemical sensor. The electrochemical sensor can operate at room temperature, has high response value and is able to detect slight changes in ethylene concentration from fruits.

### 2.6.3 Inductive sensor

Sinambela et al. (2020) studied the using of inductive sensor to detect the oil palm maturity level and predict the harvesting time. The basic principle of the oil palm maturity detection system was shown in Figure 2.22. An inductive sensor was pasted on the oil palm FFB to measure its resonant frequency. Then, an intelligent algorithm, which embedded in the system, outputs a signal related to the oil palm maturity level. The intelligent algorithm used discriminant analysis and polynomial regression to

identify oil palm ripeness and to predict harvest time, respectively. The results of the oil palm ripeness evaluation would then be displayed on a mobile phone after connecting the system using Bluetooth. Field testing was also conducted in this study and the performance from the field testing proved that the inductive sensor system was able to identify the oil palm fruit ripeness with an accuracy of 100%. The author concluded that the system proposed is potential to be applied into oil palm ripeness identification operation because it is non-invasive, rapid and accurate.


Figure 2.22: (a) The inductive sensor was pasted to the FFB; (b) The resonant frequency was measured and analyzed; (c) The FFB evaluation results were shown on the mobile phone user interface. (Sinambela et al., 2020)

# CHAPTER 3

# METHODOLOGY

## 3.1 Creation of FEA Modeling

First, a geometric model of oil palm fruitlet was created in the FEA software. In this study, Abaqus/CAE Student Edition 2020 was used. The linear dimensions of oil palm mesocarp and kernel were obtained from online sources. The dimensions required were the diameter of kernel, length and width of the fruitlet. Various data were obtained from literature and the average values of those data were used as the representative geometry to create the FEA model. Table 3.1 showed the dimensions used to create the geometric model of the oil palm fruitlet. The mesocarp of the fruitlet was considered as ellipse shape while the kernel was considered as circle (Figure 3.1).

Table 3.1: Dimensions used to create the geometric model of oil palm fruitlet.

| | |
|---|---|
| Length of fruitlet (mm) | 36.34 |
| Width of fruitlet (mm) | 24.30 |
| Diameter of kernel (mm) | 11.60 |

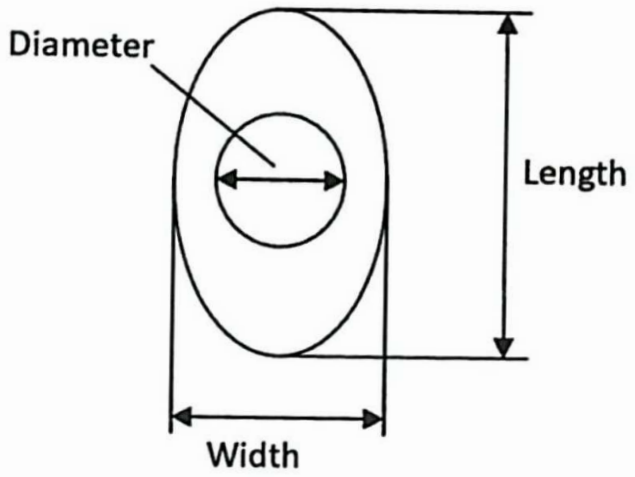


Figure 3.1: 2D geometry of the oil palm fruitlet.

### 3.1.1 Axisymmetric model

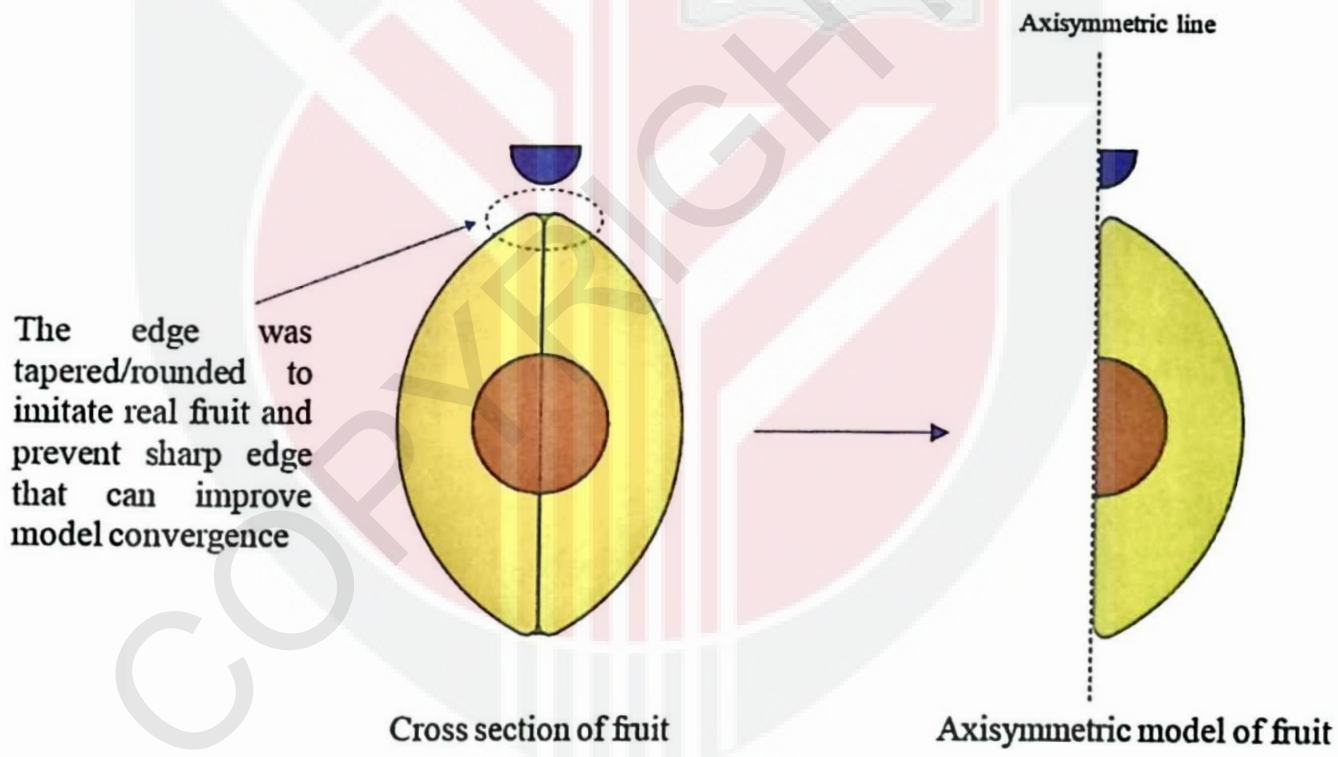


Figure 3.2: Axisymmetric model of oil palm fruitlet.

An axisymmetric model of the oil palm fruitlet was created (Figure 3.2). Axisymmetric model is suitable for analysis of non-linear structure where its geometry is axisymmetric but undergoes non-linear deformation ("Abaqus Analysis User's Guide," 2014). Axisymmetric modeling is able to analyze a 3D structure which is

rotationally symmetric about an axis. This modeling technique is suitable for symmetric loading problem. The 2D axisymmetric models represent a slice of the actual 3D model. When the 'slice' revolved around the Y-axis, it would become the original 3D structure. Using axisymmetric model reduced the number of elements thus generating a more accurate mesh. Therefore, it could minimize convergence error and ensure the model run smoothly thus resulting in a more accurate result.(P. Prabhakar, 2014)

Three models of oil palm fruitlet were created where the first model was used for pin puncture test, second model was for drop test and the third model was for compression test. This was illustrated in Figure 3.3. In the part module of ABAQUS, the geometrical axisymmetric models of mesocarp and kernel were created. In the first model, a puncture pin was placed above the oil palm fruitlet to apply the puncture force. In the second model, a rigid platen was placed below the oil palm fruitlet to allow drop test to be carried out. In the third model, compression force was applied in the direction perpendicular to the major axis of the fruitlet.

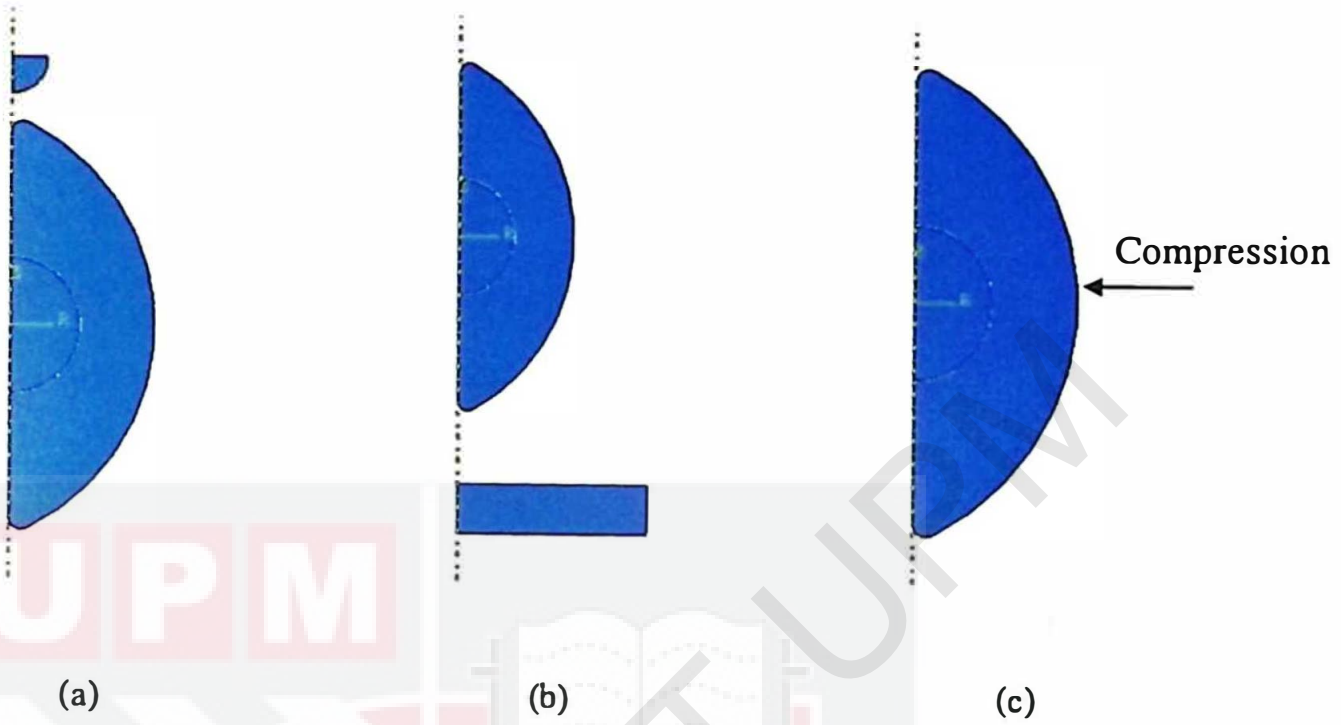


Figure 3.3: Axisymmetric model of (a) pin puncture test; (b) drop test and (c) compression test

## 3.2 Material Properties of Model

### 3.2.1 First material model – Linear elastic properties

The mesocarp and kernel of the oil palm fruitlet were first assumed as elastic materials. Linear elastic properties such as Modulus of elasticity (or Young's Modulus) and Poisson's ratio were included in the software Abaqus. The values of elastic modulus and Poisson's ratio were shown in Table 3.2.

Table 3.2: Material parameters used in linear elastic model.

| Material | Modulus of Elasticity (GPa) | Poisson's ratio |
|---|---|---|
| Mesocarp | 1.0 | 0.4 |
| Kernel | 1.2 | 0.4 |

### 3.2.2 Second material model – Combined Viscoelastic properties and Hyperelastic properties for mesocarp part

In Abaqus/CAE, to evaluate a viscoelastic material behaviour, it must be defined in time domain and coupled with hyperelastic or elastic material data. The software does not allow a viscoelastic material defined in frequency domain to be evaluated individually. (©ABAQUS, 2014)

Hanipah et al.(2020) reported the using of van der Waals hyperelastic and Prony series viscoelastic model for the oil palm mesocarp fibres (OPMF) to develop a finite element model to simulate the fibre pull-out. The mechanical properties shown in Table 3.3 were applied into the geometric model for this study.

Table 3.3: Material parameters used in visco-hyperelastic model.

| **Hyperelastic properties** | |
|---|---|
| Material constant | Value |
| Shear modulus, $\mu$ | 2.2GPa |
| Global interaction parameter, a | 1.6 |
| Locking stretch, $\lambda_m$ | 20 |
| **Viscoelastic properties (Prony series)** | |
| Modulus ratio, $g_i$ | Relaxation time, $\xi_i$ (s) |
| 0.6 | 0.1 |
| 0.08 | 1 |
| 0.06 | 10 |
| 0.05 | 100 |
| 0.005 | 1000 |
| 0.205 | ∞ |

### 3.2.3 Third material model – Combined Elastic properties and Viscoelastic properties for mesocarp

Hanipah et al. (2017) successfully developed a micromechanical finite element model to evaluate the contribution of silica bodies to the mechanical integrity of the surface of oil palm mesocarp fibre (OPMF). The research assumes the model to be incompressible material and no plasticity model was involved to combine with the viscoelastic model. Table 3.4 showed the material parameters used in this study.

Table 3.4: Material parameters used in viscoelastic model.

| **Elastic properties** | |
|---|---|
| Fibre elastic modulus, $E_f$ | 4.8GPa |
| **Viscoelastic properties (Prony series)** | |
| Modulus ratio, $g_i$ | Relaxation time, $\xi_i$ (s) |
| 0.3 | 0.1 |
| 0.15 | 1 |
| 0.1 | 10 |
| 0.05 | 100 |
| 0.005 | 1000 |
| 0.35 | ∞ |

## 3.3 Mesh Quality and Finite Element Modeling

One of the most crucial steps in FEA is to mesh the geometric model. In Mesh module, meshes are generated on the parts and assemblies created during previous steps. In this study, the element type selected was axisymmetric solid elements with non-linear asymmetric deformation. Linear quadrilateral element (CAX4RH) is a 4-node, reduced-integration, hybrid axisymmetric element with nonlinear asymmetric deformation while CAX3H is linear triangular element with hybrid. Figure 3.4 showed the definition of 3-

node and 4-node element in Abaqus software. The total number of nodes and elements generated in each model was shown in Table 3.5.

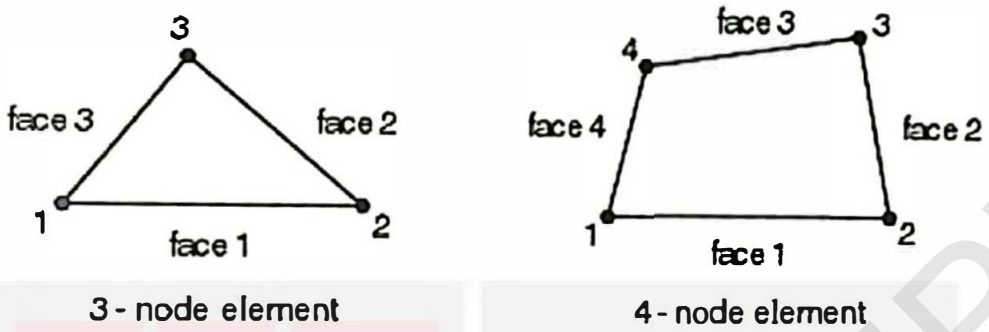


3 - node element  4 - node element

Figure 3.4: Definition of 3-node and 4-node element in Abaqus software.

Table 3.5: Summary of number of element and element type for each part of the model.

| Model | Part | Total number of nodes | Total number of elements | Element type | |
|---|---|---|---|---|---|
| | | | | 4-node | 3-node |
| 1 | Mesocarp | 461 | 414 | 408 | 6 |
| | Kernel | 102 | 86 | 83 | 3 |
| | Platen | 31 | 22 | 21 | 1 |
| 2 | Mesocarp | 461 | 414 | 408 | 6 |
| | Kernel | 102 | 86 | 83 | 3 |
| | Platen | 126 | 100 | 100 | 0 |
| 3 | Mesocarp | 576 | 525 | 514 | 11 |
| | Kernel | 121 | 103 | 100 | 3 |

## 3.4 Boundary Conditions and Load Definition

Defining the boundary conditions is another crucial step in FEA. The accuracy and reliability of the results could be increased if the boundary conditions were defined correctly. During the pin puncture test (Model 1), the nodes near the bottom of the fruitlet were applied with ENCASTRE (U1 = U2 = U3 = UR1 = UR2 = UR3 = 0). This

boundary condition constrains all active structural degrees of freedom which means that the nodes in this specified region cannot move in the three main directions (X, Y and Z). Only vertical indenter movements along Y-direction are allowed for the nodes near the top of the fruitlet. Displacement/rotation boundary condition was applied to the platen above the fruitlet so that it can move down in Y-direction to a specified deformation. Figure 3.5 illustrated the boundary condition defined in modeling of pin puncture test.

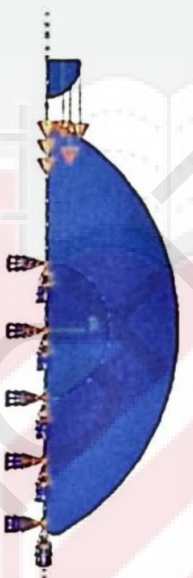

Figure 3.5: Boundary condition defined in pin puncture test.

For drop test, ENCASTRE boundary condition was applied to the platen below the fruitlet. The fruitlet was applied with displacement boundary condition so that it moves down in Y-direction. Figure 3.6 illustrated the boundary condition defined in drop test.

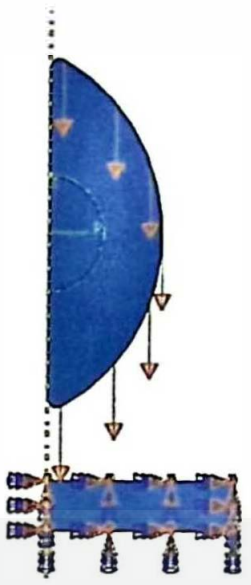

Figure 3.6: Boundary condition defined in drop test.

During the compression test, the longitudinal axis of the fruitlet was applied with ENCASTRE boundary condition. Displacement boundary condition was applied to the edge of the mesocarp so that it moves along the X-direction until a specified deformation. Figure 3.7 illustrated the boundary condition defined in compression test

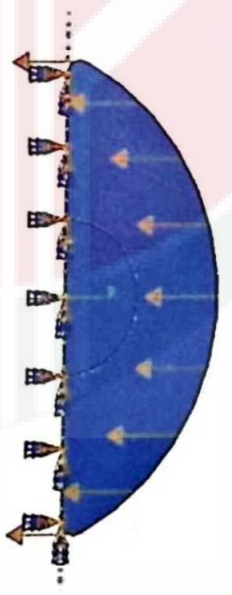

Figure 3.7: Boundary condition defined in compression test.

# CHAPTER 4

# RESULTS AND DISCUSSION

## 4.1 Simulation results of linear elastic model

### 4.1.1 Effect of varying material parameters (linear elastic model) on the stress-displacement curve

The simulation results of linear elastic model were shown in Figure 4.7 where (a) illustrated the pin puncture test, (b) drop test and (c) compression test. During this part, only linear elastic effect was considered.

The oil palm fruitlet was first assumed to have elastic mechanical behaviour. The effect of varying elastic modulus of mesocarp and displacement boundary condition on the stress-displacement curve was investigated. First, the elastic modulus of mesocarp was varied by using values of 0.5, 1.0 and 1.5GPa while keeping the displacement boundary condition constant at y = – 0.005m. Then, the elastic modulus of mesocarp was kept constant at 1.0GPa while varying the displacement boundary condition at – 0.005, – 0.006 and – 0.007m.

From Figure 4.2, it was found that increasing the elastic modulus of mesocarp will cause the stress-displacement curve to become stiffer. The gradient of a stress-strain

curve represent the elastic modulus. Referring to Figure 4.4, it can be seen that the elastic modulus can be estimated as the slope of a stress-strain curve. Thus, increasing the elastic modulus of mesocarp would increase the gradient which results in a stiffer curve.

The effect of varying displacement boundary condition on the stress-displacement curve was depicted in Figure 4.3. Changing the displacement boundary condition had no significant effect on the stress-displacement curve. The slope of the three curves was almost the same. However, the deformation showed small increment with increasing displacement boundary condition.

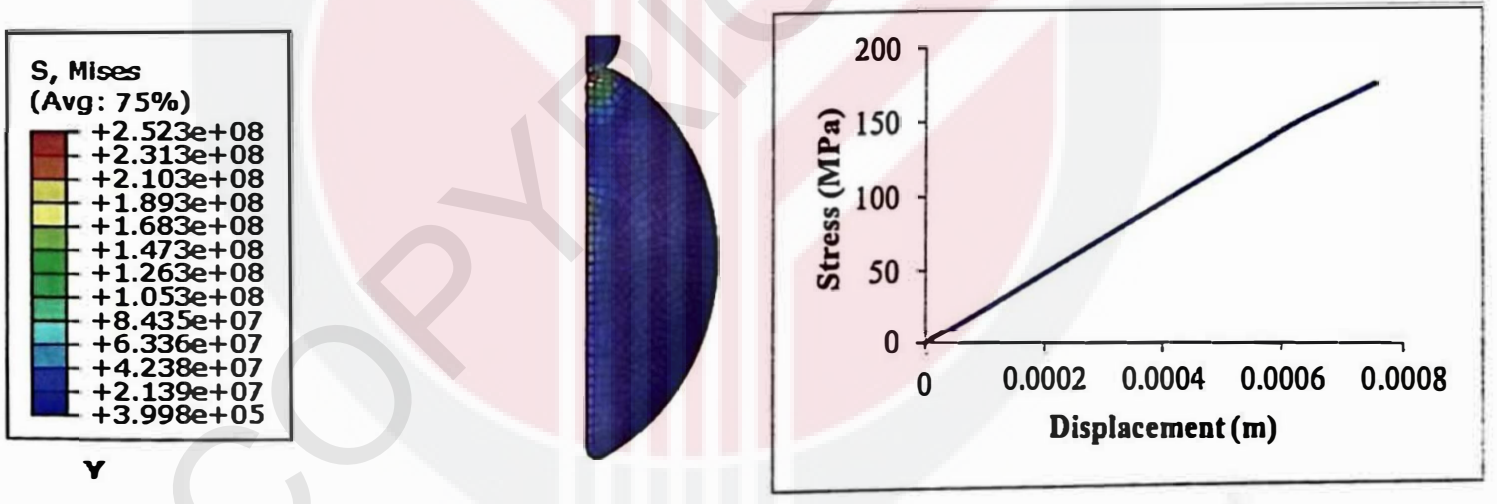


(a)

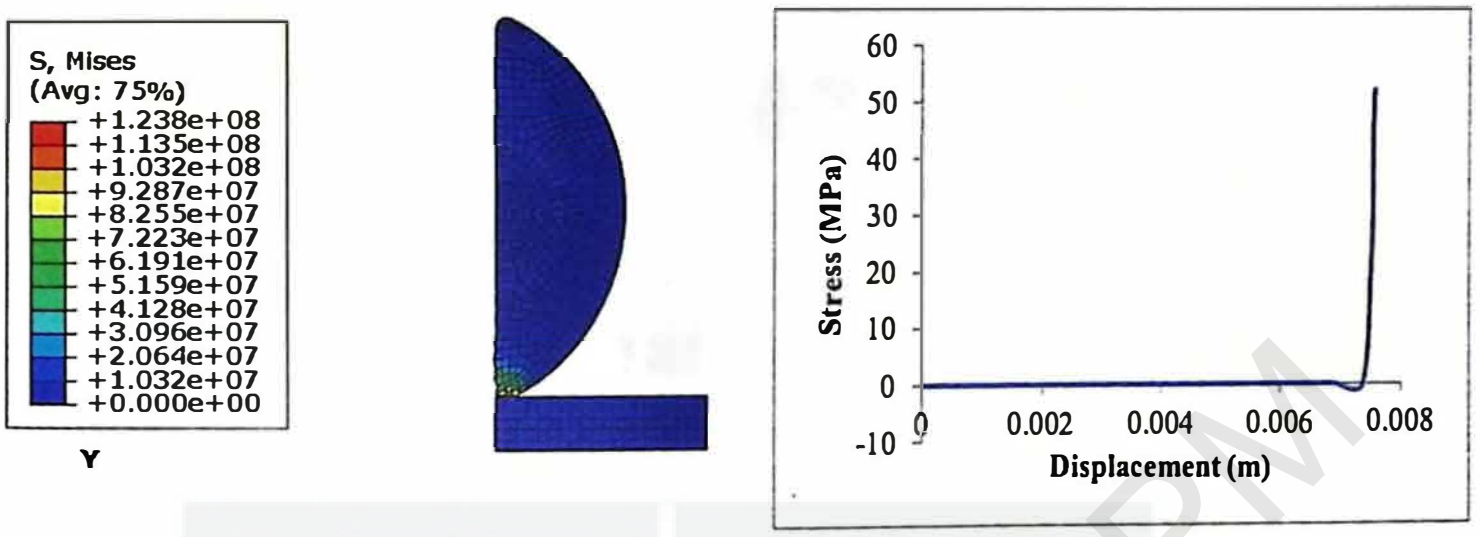


(b)

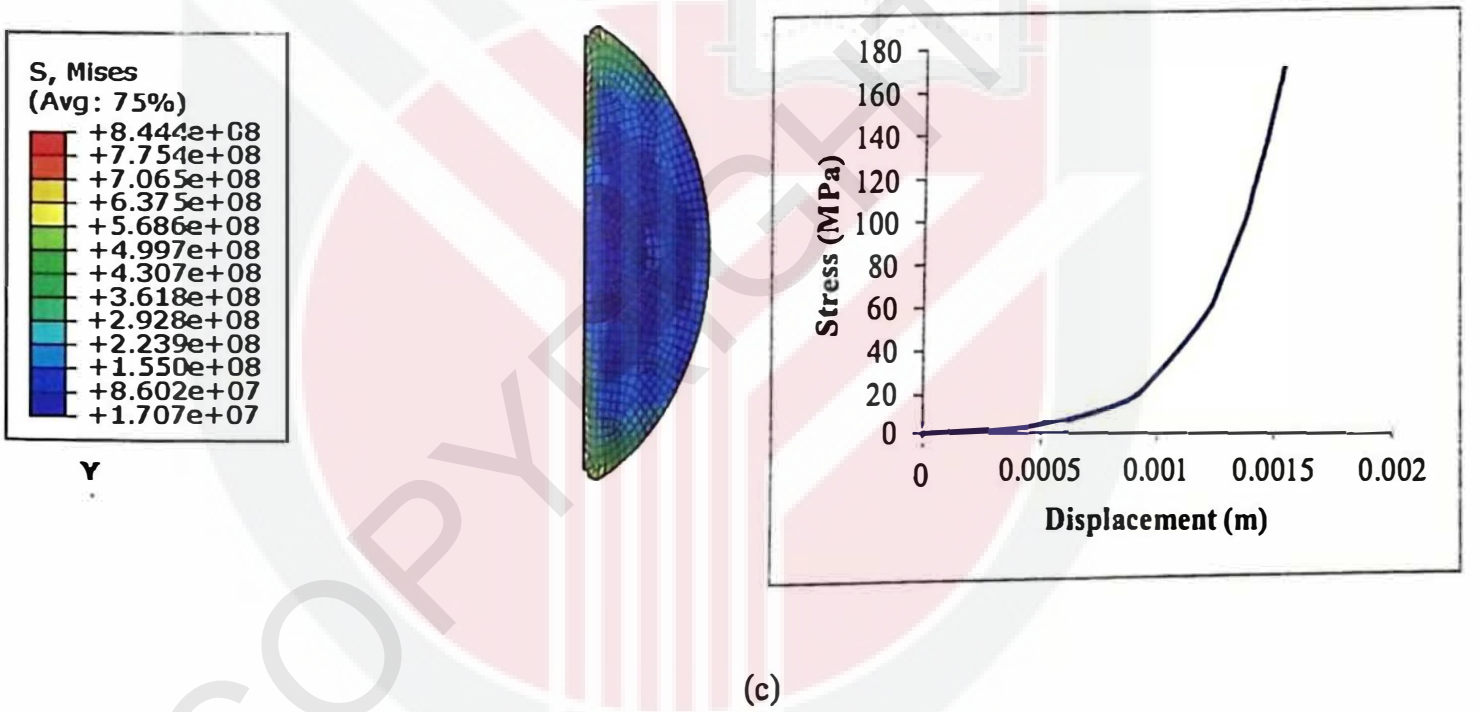


(c)

Figure 4.1: Results of linear elastic model (a) pin puncture test; (b) drop test; and (c) compression test.

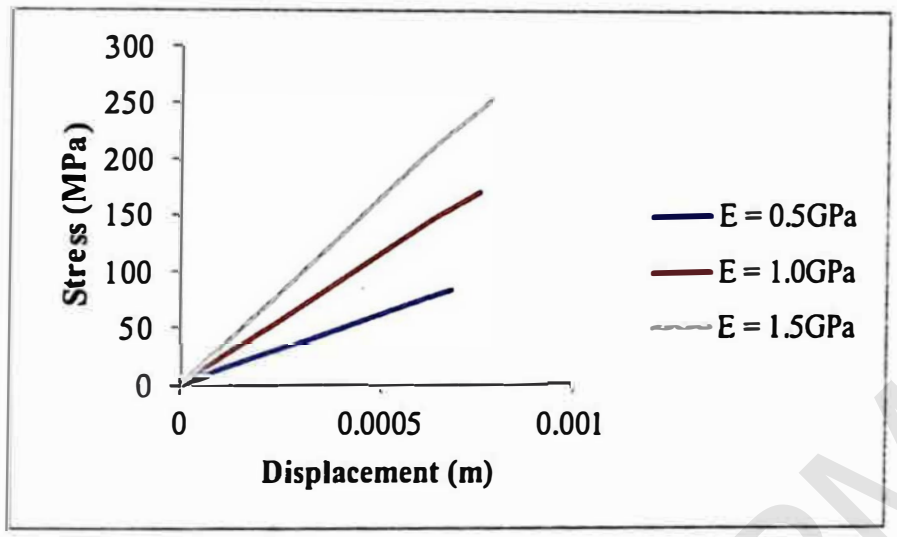


Figure 4.2: Results of pin puncture test (linear elastic model) when elastic modulus of mesocarp is varied.

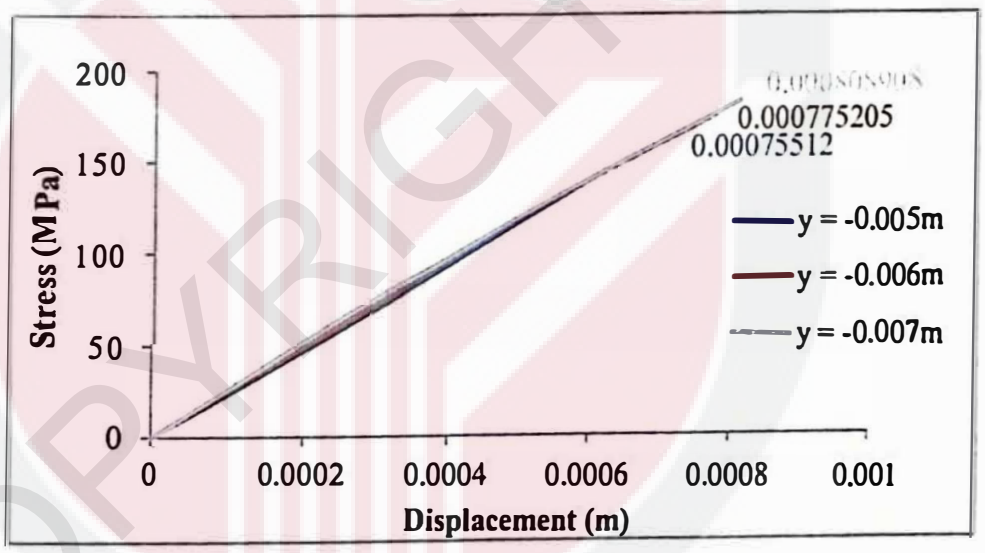


Figure 4.3: Results of pin puncture test (linear elastic model) when varying the value of displacement boundary condition.

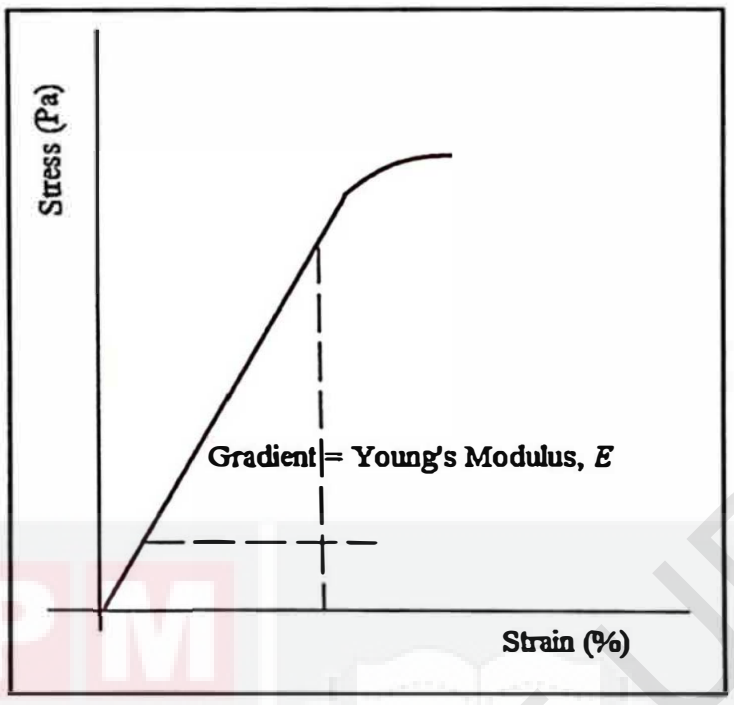


Figure 4.4: Stress-strain curve of a linear elastic material. (Figari, n.d.)

## 4.2 Simulation results of visco-hyperelastic model

### 4.2.1 Effect of varying material parameters (visco-hyperelastic model) on the stress-displacement curve

The simulation results of visco-hyperelastic model were shown in Figure 4.5 where (a) illustrated the pin puncture test, (b) drop test and (c) compression test. During this part, the viscoelastic and hyperelastic effect were considered.

The parameters of the van der Waals model such as $\mu$, $\lambda_m$ and $a$ were varied with different value to investigate their effect on the mechanical behaviour of the oil palm mesocarp. For case 1, the value of $\lambda_m$ and $a$ were kept constant at 20 and 1.6 respectively while varying the $\mu$ with values of 1, 2.2 and 3GPa. For case 2, the value of $\lambda_m$ was varied at 20, 30 and 50 while keeping the $\mu$ and $a$ constant at 2.2GPa and 1.6

respectively. For case 3, the values of $\mu$ and $\lambda_m$ were kept constant at 2.2GPa and 20 respectively while varying the $a$ with values of 1.6, 3 and 5.

Figure 4.6 showed that increasing the $\mu$ would increase the gradient of the stress-displacement curve which caused the curve to look stiffer. On the other hand, increasing $\lambda_m$ and $a$ did not have significant effect on the slope of the stress-displacement curve. However, the curve became lower with increasing $\lambda_m$ and $a$. The results obtained here were same as those studied by Hanipah et al.(2016).

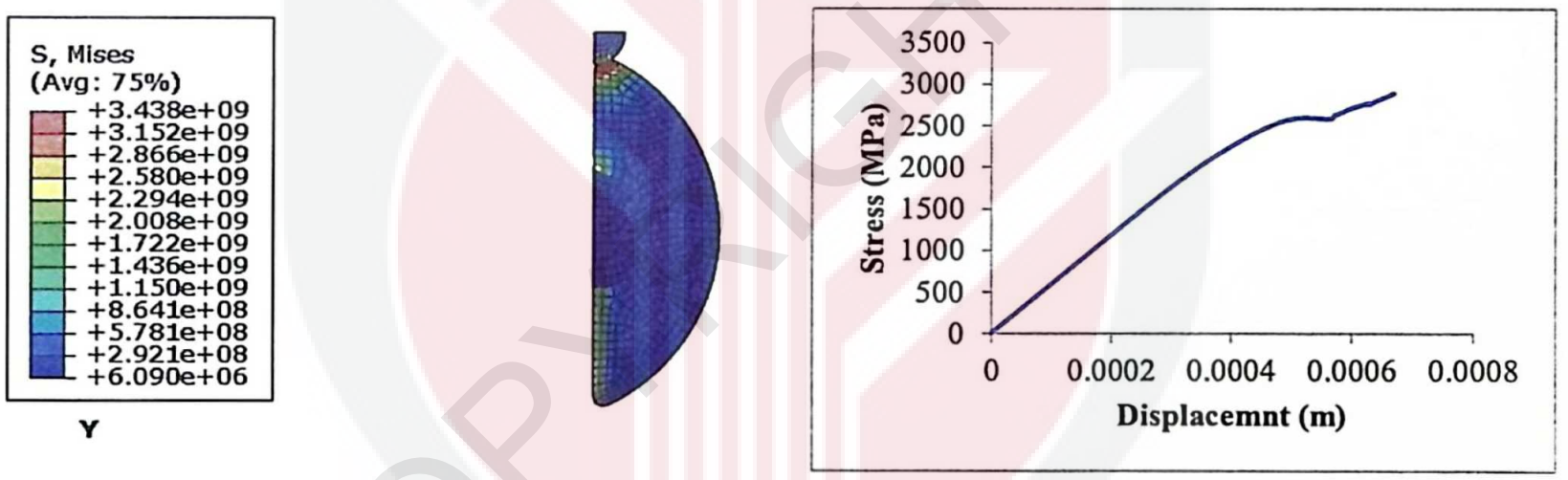


(a)

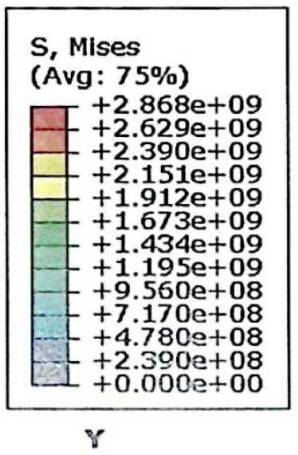


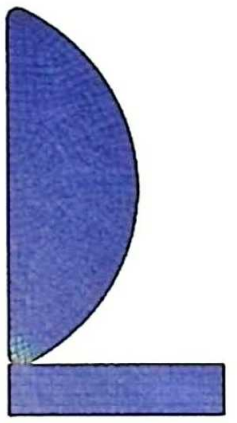

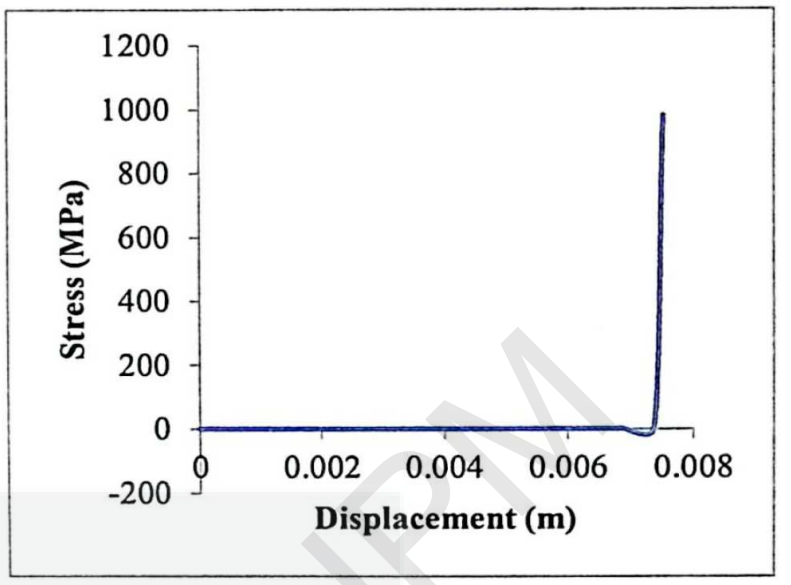


(b)

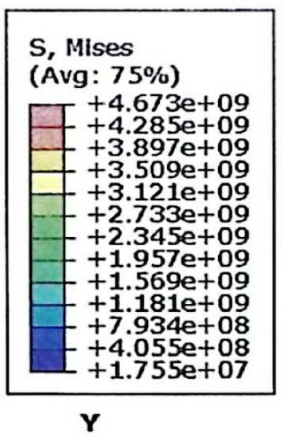


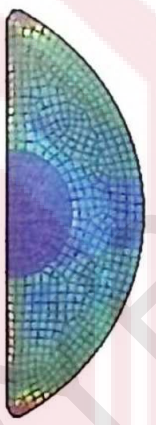

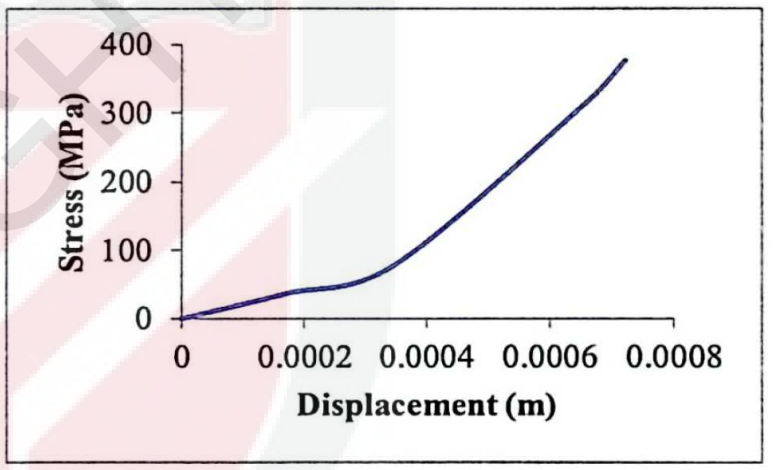


(c)

Figure 4.5: Results of visco-hyperelastic model (a) pin puncture test; (b) drop test; and (c) compression test.

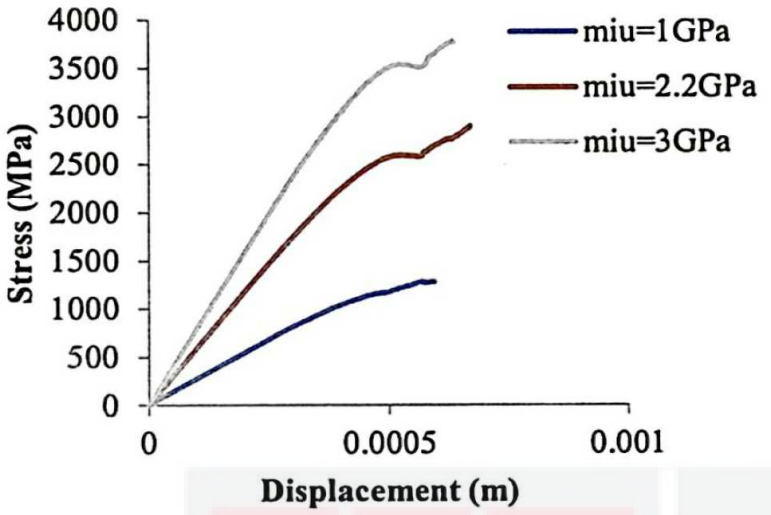


(a)

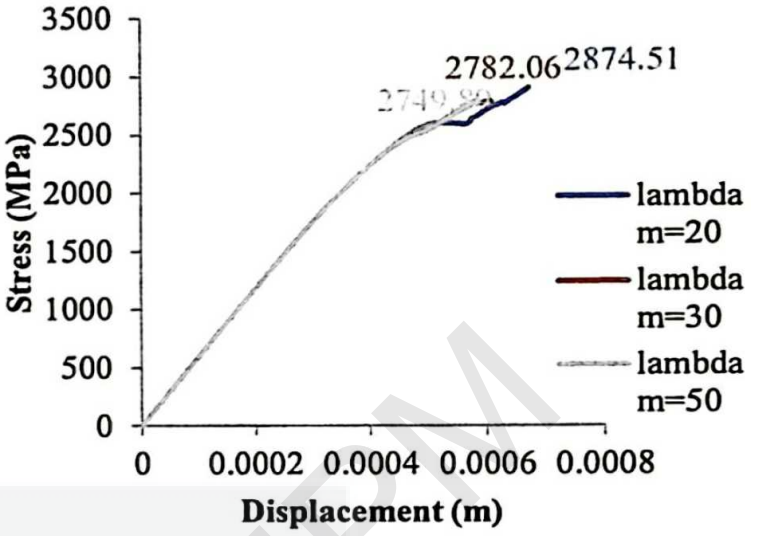


(b)

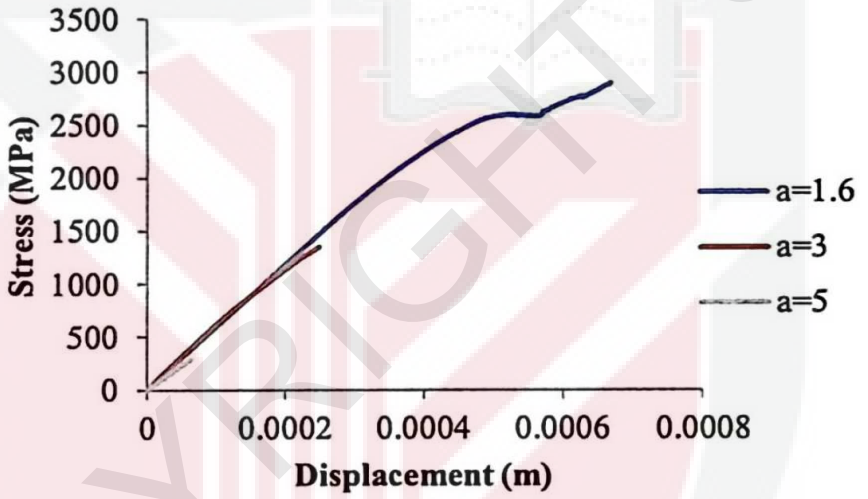


(c)

Figure 4.6: Results of pin puncture test (visco-hyperelastic model) when varying (a) instantaneous initial shear stress, $\mu$; (b) locking stretch constant, $\lambda_m$; and (c) global interaction parameter, a.

## 4.3 Simulation results of viscoelastic model

The simulation results of viscoelastic model were shown in Figure 4.7 where (a) illustrated the pin puncture test, (b) drop test and (c) compression test. During this part, only viscoelastic effect was considered.


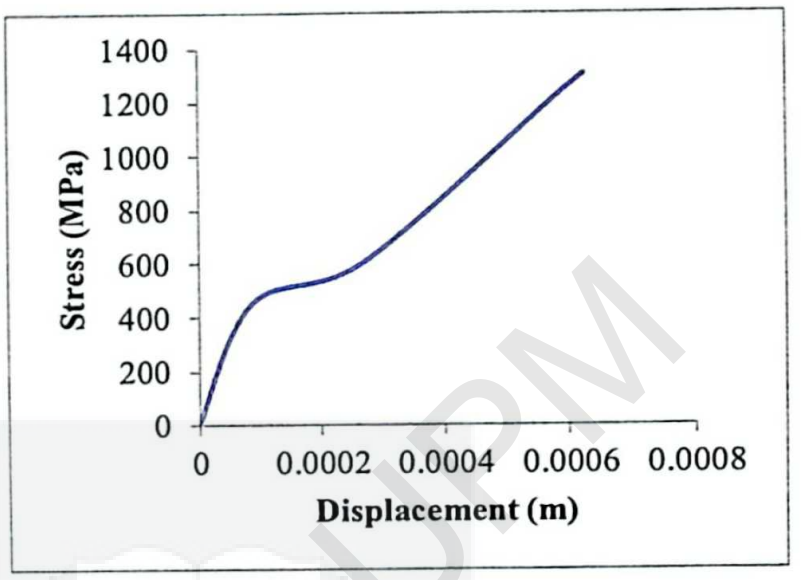


(a)

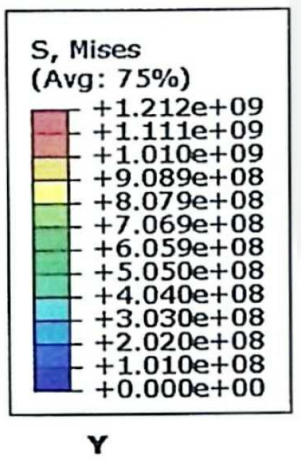


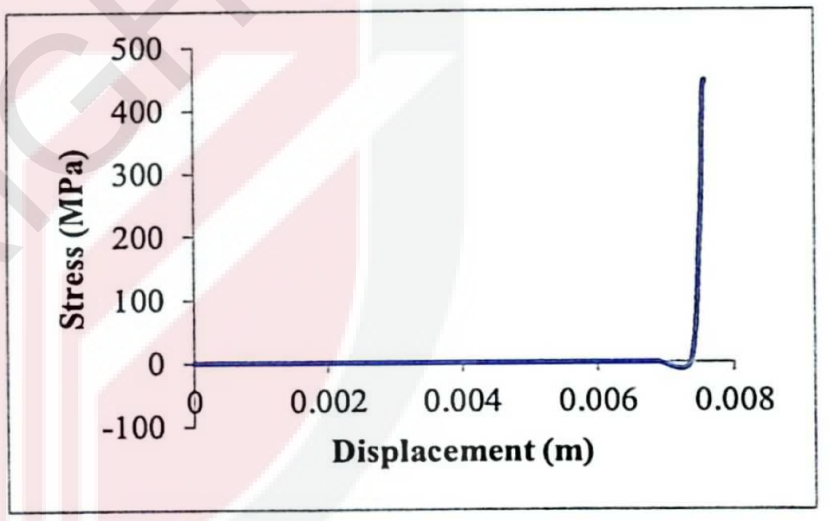


(b)

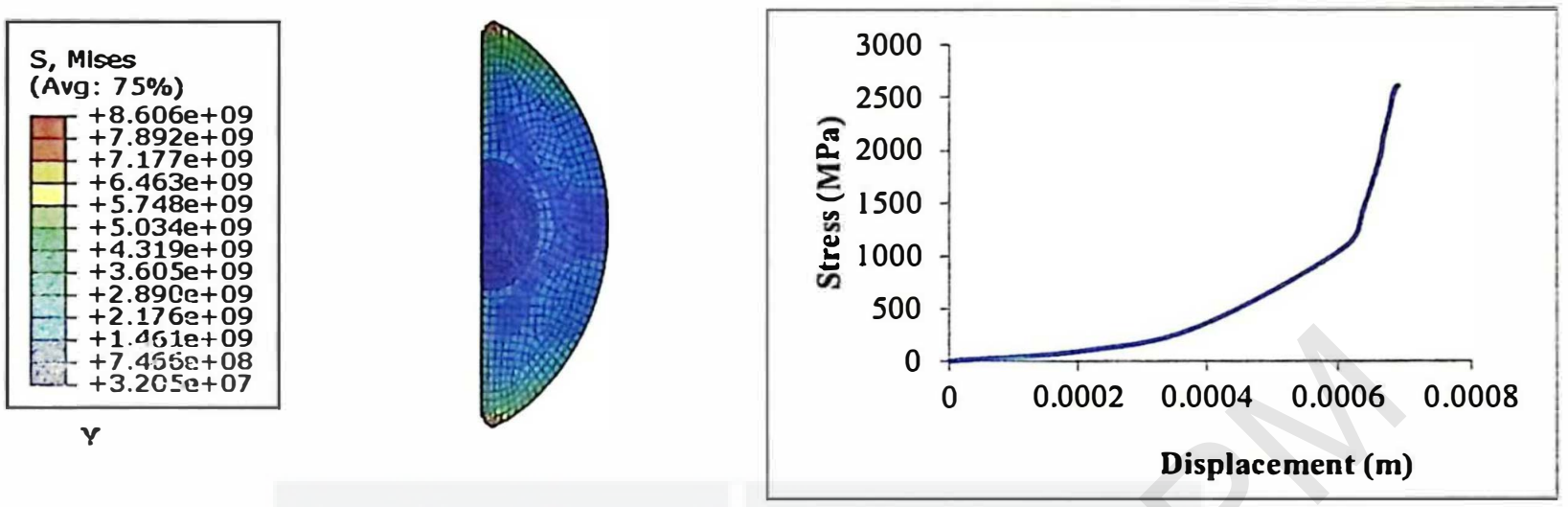


(c)

Figure 4.7: Results of viscoelastic model (a) pin puncture test; (b) drop test; and (c) compression test.

## 4.4 Comparison between results of different material properties

In this study, three different models (elastic model, viscoelastic combined with hyperelastic model and elastic combined with viscoelastic model) were applied to the material properties of the oil palm mesocarp to investigate its mechanical behaviour. From Figure 4.8(a), it can be seen that the stress-displacement curves for the three type of material were noticeably different. The differences could be probably due to the varying parameters used in the previous research which made it difficult to be compared.

Since the stress-displacement curves could not showed the differences between the models obviously, stress relaxation test was carried out to check the difference between the linear elastic behaviour and viscoelastic behaviour. Stress relaxation test was conducted by compressing the oil palm fruitlet to a specified deformation and the deformation was held fixed for a period of time to measure the stress decay.

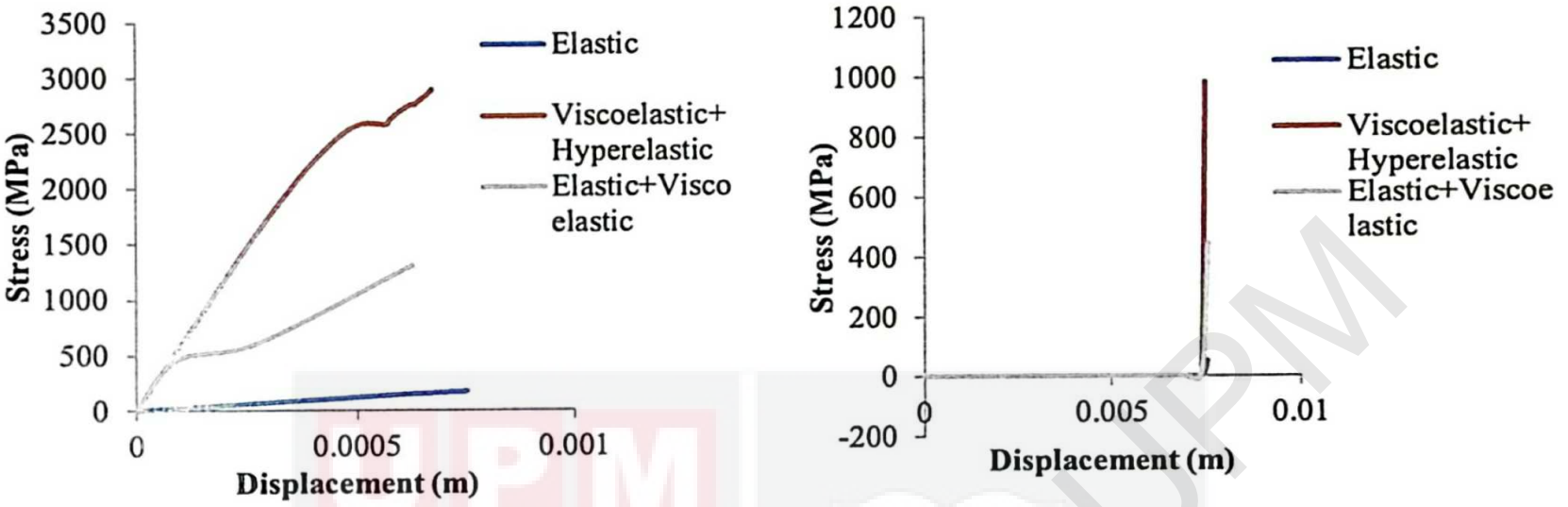


Figure 4.8: Comparison between the results of different material properties (a) pin puncture test; (b) drop test; and (c) compression test.

## 4.5 Results of stress relaxation test

Figure 4.9 showed the results of stress relaxation test obtained by using pin puncture test and compression test. Comparison was made between the linear elastic model and viscoelastic model. It clearly showed the viscoelastic behaviour of oil palm mesocarp because the stress gradually reduced over time at holding deformation. The viscoelastic behaviour of oil palm mesocarp observed in this study was similar with the typical viscoelastic time-dependence behaviour as shown in Figure 4.10.

Referring to Figure 4.11, similar results were observed by using viscoelastic combined with hyperelastic model. At holding deformation, the stress reduced steadily over time. Figure 4.12 showed the comparison between the stress-time curve of the visco-hyperleastic model and viscoelastic model. Both curve showed the viscoelastic behaviour but it was observed that the reduction of stress for visco-hyperelastic model is greater than the viscoelastic model. For visco-hyperelastic model, the stress reduced from 731MPa to 433MPa (298MPa difference) while the stress for elastic-viscoelastic model reduced from 397MPa to 288MPa (109MPa difference).This is probably due to the hyperelastic behaviour which is rubberlike and can undergo large elastic deformation. A rubberlike material could show complete recovery after being subjected to large deformations. (Mohammed, 2020)

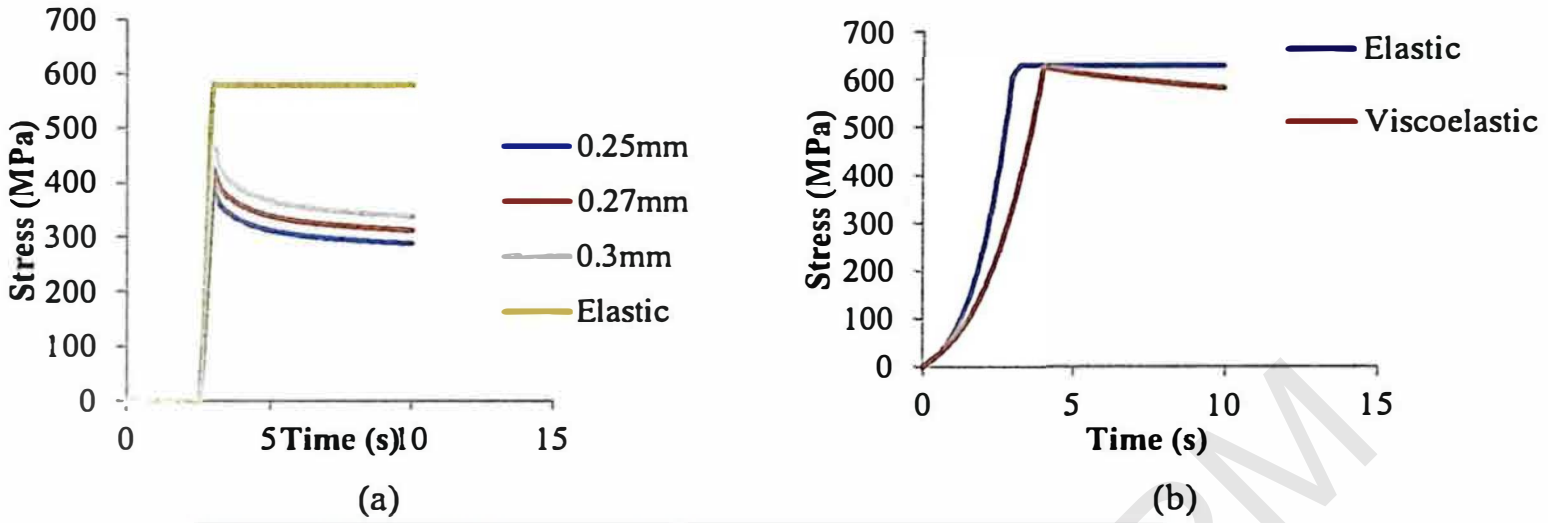


Figure 4.9: Stress relaxation test results of (a) pin puncture test under different deformation; (b) compression test.

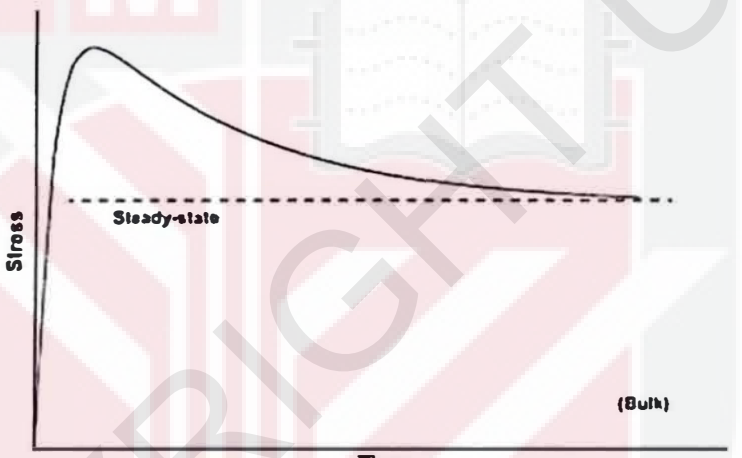


Figure 4.10: Typical time-dependence behaviour of viscoelastic fluids under relaxation after a step increase in strain rate. (Sochi, 2010)

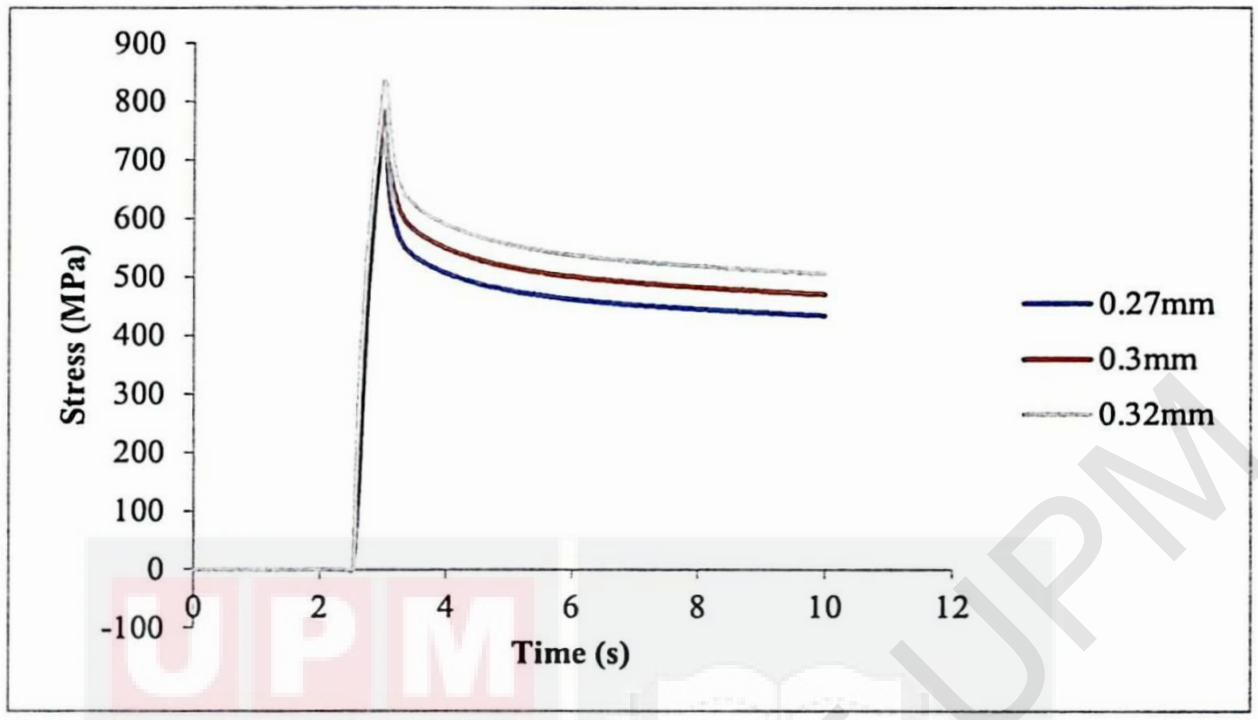


Figure 4.11: Stress relaxation test results obtained by using visco-hyperelastic model.

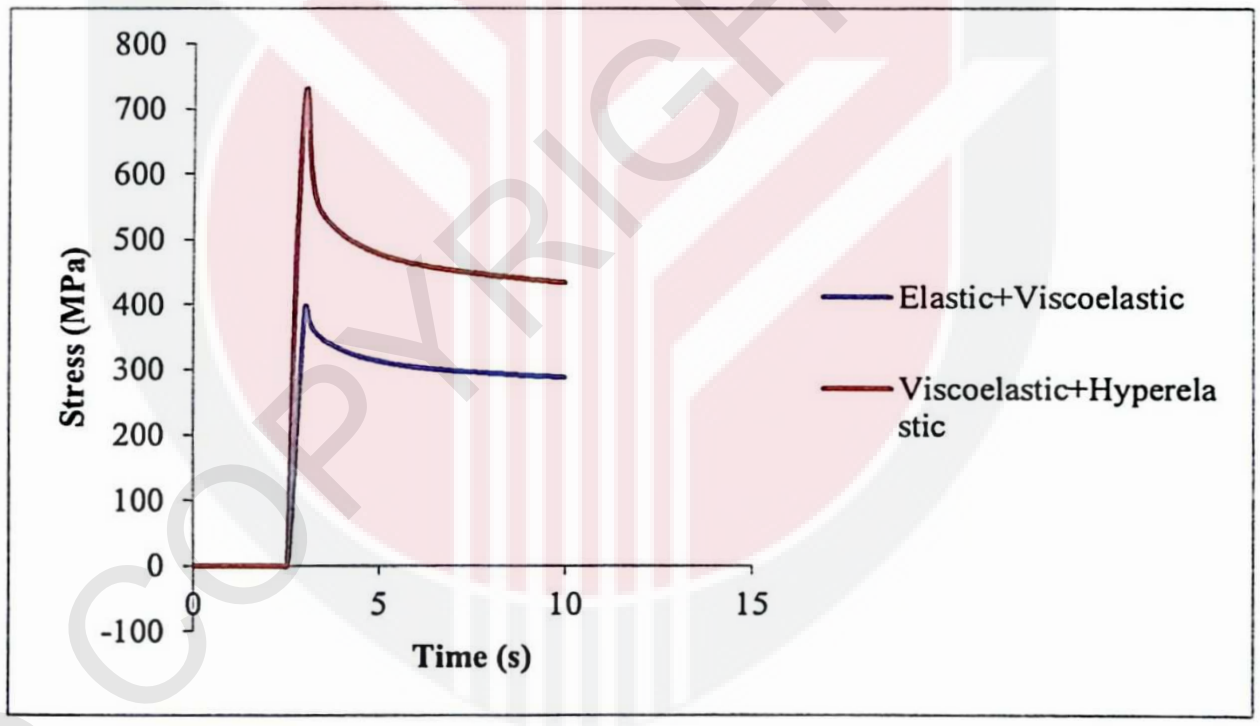


Figure 4.12: Comparison of stress relaxation test results between viscoelastic model and visco-hyperelastic model.

## 4.6 Study on the mesocarp-kernel interface properties

The parameters of the mesocarp-kernel interface properties such as critical stress and cohesive energy were varied with different values to investigate their sensitivity. First, the critical stress was varied at values of 10, 50 and 100MPa while keeping the cohesive energy constant at 1kN/m. Then, the critical stress was kept constant while varying the cohesive energy at values of 1, 10 and 100kN/m.

From Figure 4.13, it was observed that varying the critical stress and cohesive energy did not affect the mechanical behaviour of the oil palm fruitlet because all of the stress-displacement curves obtained from different simulations were same. The reason of this situation might be due to the boundary condition defined in the previous step which limited the movement of the fruitlet.

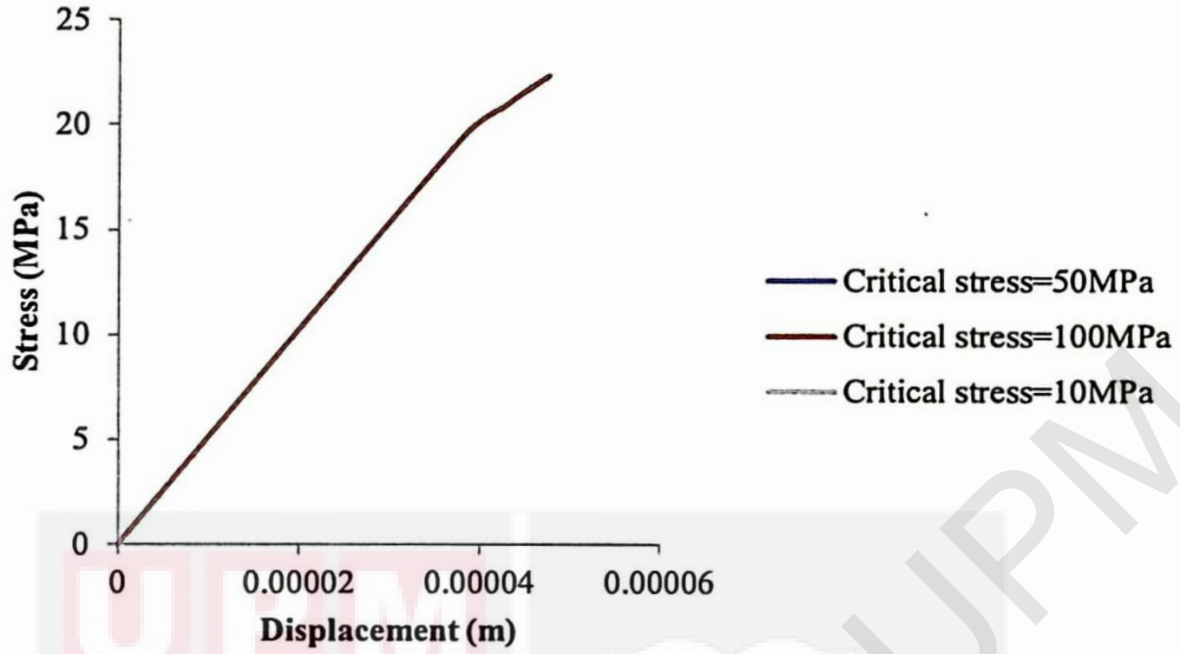


(a)

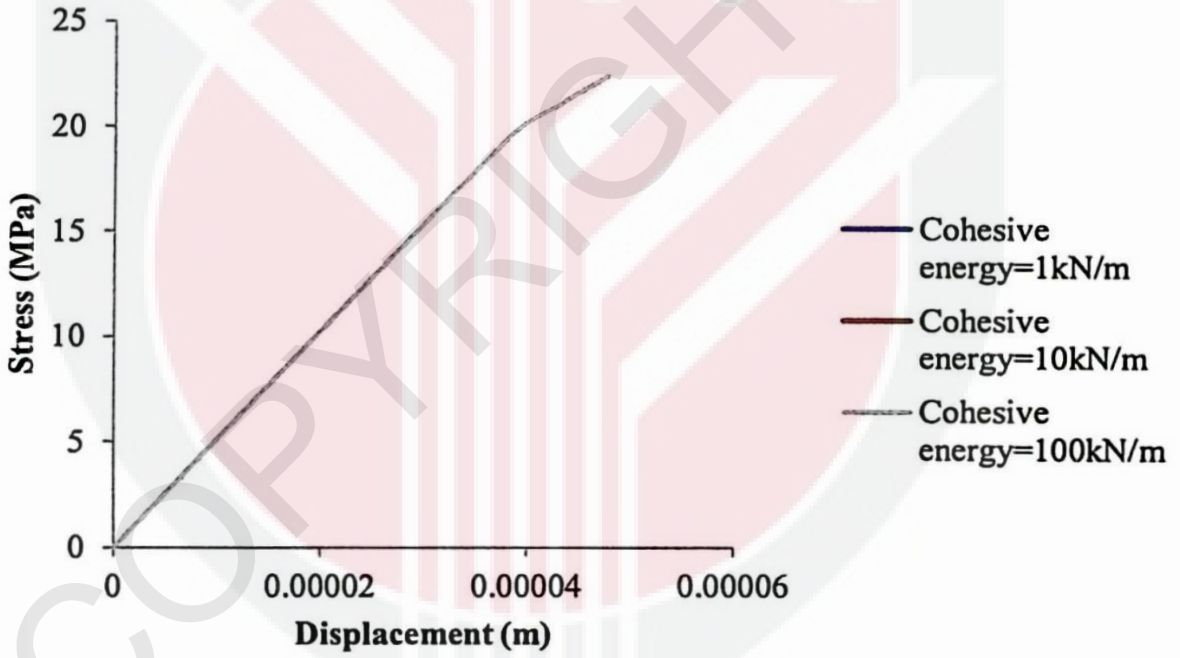


(b)

Figure 4.13: Results of parametric study of the mesocarp-kernel interface properties (a) varying critical stress; (b) varying cohesive energy.

## 4.7 Discussion from previous results

This work studied the mechanical behaviour of a single oil palm fruitlet through different constitutive material models namely linear elastic, viscoelastic and hyperelastic model. Most of fruits have typical viscoelastic behaviour. The viscoelastic behaviour of oil palm fruitlets can be indicated through the stress relaxation test where the stress reduced steadily over time at constant deformation. From the results of compression test (Figure 4.1(c)), it clearly showed that the stress increased with the displacement, indicating the strain hardening (hyperelastic) behaviour of the fruitlet. Thus, it is believed that the mesocarp of an oil palm fruit would behave like visco-hyperelastic material.

Mesocarp-kernel interface properties might be important in evaluating the mechanical properties of oil palm fruitlet. Since the model in this study has limitation in obtaining a reasonable result, a more complex model might be needed to investigate the effect of mesocarp-kernel interface properties on the mechanical behaviour of the fruitlet.

Firmness is an essential characteristic to evaluate the maturity of oil palm fruits. It can be characterized by the force-deformation or stress-strain curve (Fekete, 1997). The firmness of a fruit is closely related to its elastic modulus. A firmer fruit would have higher elastic modulus (stiffer stress-strain curve) than a softer one.

The model has potential to be applied into oil palm maturity detection system but experimental work is required to validate the model and also to provide a better understanding on the mechanical behaviour of the fruitlet. For the experimental work, it

is suggested to use a custom-made probe connected to miniature load cell to 'map' the force/stress distribution of the fruitlet. A simplified model could then be used to translate this stress (elasticity) 'map' into the virtual fruitlet created in this study. A correlation could be made to relate the mechanical properties (e.g. firmness or texture) to the maturity level of the fruitlet. For example, when a load sensor is used to touch the fruitlet, it will show the maturity level based on the firmness of the fruitlet.

# CHAPTER 5

# CONCLUSION AND RECOMMENDATIONS

A geometric model of a single oil palm fruitlet was developed to simulate the pin puncture test, drop test and compression test to study its mechanical behaviour. The parameters were varied to investigate their effect on the stress-displacement curve. Results showed that increasing the elastic moduli of mesocarp will caused the curve to become stiffer while increasing the displacement boundary condition will slightly increase the deformation of the fruitlet. For the visco-hyperelastic model, increasing $\mu$ would resulted a stiffer stress-strain curve while increasing $\lambda_m$ and $a$ would lower the stress-strain curve. The stress relaxation test results showed the evidence of the viscoelastic behaviour of the oil palm mesocarp. A parametric study of the mesocarp-kernel interface properties was also carried out. The results showed that the model is not sensitive to the varying parameters due to the boundary conditions that limited the movement of the fruitlet.

Future experimental work could be carry out to study more detailed on the mechanical properties (e.g texture or softness) of the oil palm fruitlets and to decide which model best describe the mechanical behaviour of the fruitlets.

## REFERENCES


A.R, A., K, S., S, N. H., & C.A, S. (2009). Novel Method of Grading Fresh Fruit Bunches ( FFB ) of Oil Palm Fruit Novel Method of Grading Fresh Fruit Bunches ( FFB ) of Oil. *Conference on Scientific & Social Research 14*, *November 2016*.

ABAQUS. (2014). Abaqus 6.14. *Abaqus 6.14 Analysis User's Guide*, 14.

Abaqus Analysis User's Guide. (2014). In *Dassault Systemes: Vol. IV*.

Afolabi, M. T., & Adeleke, B. I. (2015). Effects of age on some physical properties of oil palm fruitlets. *Agricultural Engineering International: The CIGR Journal*, *17*, 342–352.

Alfatni, M. S. M., Shariff, A. R. M., Shafri, H. Z. M., Saaed, O. M. B., & Eshanta, O. M. (2008). Oil palm fruit bunch grading system using red, green and blue digital number. *Journal of Applied Sciences*, *8*(8), 1444–1452. https://doi.org/10.3923/jas.2008.1444.1452

Basyuni, M., Amri, N., Putri, L. A. P., Syahputra, I., & Arifiyanto, D. (2017). Characteristics of fresh fruit bunch yield and the physicochemical qualities of palm oil during storage in north sumatra, Indonesia. *Indonesian Journal of Chemistry*, *17*(2), 182–190. https://doi.org/10.22146/ijc.24910

Bensaeed, O. M., Shariff, A. M., Mahmud, A. B., Shafri, H., & Alfatni, M. (2014). Oil palm fruit grading using a hyperspectral device and machine learning algorithm. *IOP Conference Series: Earth and Environmental Science*, *20*(1). https://doi.org/10.1088/1755-1315/20/1/012017

Bille Ngalle, H., Bell, J. M., Ngando-Ebongue, G. F., Eman-Evina, H., Ntsomboh Ntsefong, G., & Nsimi-Mva, A. (2014). Morphogenesis of Oil Palm (Elaeis guineensis Jacq.) Fruit in Seed Development. *Journal of Life Sciences*, *8*, 946–954. https://doi.org/10.17265/1934-7391/2014.12.004

*Cross Section Of Tenera Fruit Of Oil Palm Stock Photo - Image of isolated, african: 115854784*. (n.d.). Retrieved August 12, 2021, from https://www.dreamstime.com/cross-section-tenera-fruit-oil-palm-closeup-tenera-fruit-cutting-oil-palm-isolated-white-background-image115854784

Dehkordi, A. L. (2016). Modeling the Mechanical Behavior of Fruits : A Review. *20th Nordic Seminar on Computational Mechanics*, *8*(2), 60–64.

Dintwa, E., Jancsók, P., Mebatsion, H. K., Verlinden, B., Verboven, P., Wang, C. X., Thomas, C. R., Tijskens, E., Ramon, H., & Nicolaï, B. (2011). A finite element

model for mechanical deformation of single tomato suspension cells. *Journal of Food Engineering*, *103*(3), 265–272. https://doi.org/10.1016/j.jfoodeng.2010.10.023

Dintwa, Edward, Van Zeebroeck, M., Ramon, H., & Tijskens, E. (2008). Finite element analysis of the dynamic collision of apple fruit. *Postharvest Biology and Technology*, *49*(2), 260–276. https://doi.org/10.1016/j.postharvbio.2008.01.012

Fekete, A. (1997). Modeling the compression test process of fruits. *IFAC Proceedings Volumes*, *30*(5), 323–328. https://doi.org/10.1016/s1474-6670(17)44452-1

Figari, P. (n.d.). *Steps to Analyzing a Material's Properties From Its Stress/Strain Curve : 9 Steps - Instructables*. Retrieved August 3, 2021, from https://www.instructables.com/Steps-to-Analyzing-a-Materials-Properties-from-its/

Hanipah, S. H., Mohammed, M. A. P., & Baharuddin, A. S. (2016). Non-linear mechanical behaviour and bio-composite modelling of oil palm mesocarp fibres. *Composite Interfaces*, *23*(1), 37–49. https://doi.org/10.1080/09276440.2016.1091681

Hanipah, S. H., Omar, F. N., Talib, A. T., Mohammed, M. A. P., Baharuddin, A. S., & Wakisaka, M. (2020). Effect of silica bodies on oil palm fibre-polyethylene composites. *BioResources*, *15*(1), 360–367. https://doi.org/10.15376/biores.15.1.360-367

Hanipah, S. H., Yu Xiang, L., Mohammed, M. A. P., & Samsu Baharuddin, A. (2017). Study of Non-linear Mechanical Behavior of Oil Palm Mesocarp Fibers. *Journal of Natural Fibers*, *14*(2), 153–165. https://doi.org/10.1080/15440478.2015.1093575

Harun, N. H., Misron, N., Sidek, R. M., Aris, I., Ahmad, D., Wakiwaka, H., & Tashiro, K. (2013). Investigations on a Novel Inductive Concept Frequency Technique for the Grading of Oil Palm Fresh Fruit Bunches. *Sensors*, *13*(2), 2254–2266. https://doi.org/10.3390/s130202254

Hazir, M. H. M., & Shariff, A. R. M. (2011). Oil palm physical and optical characteristics from two different: Planting materials. *Research Journal of Applied Sciences, Engineering and Technology*, *3*(9), 953–962.

Ishak, W. I. W., & Hudzari, R. M. (2010). Image based modeling for oil palm fruit maturity prediction. *Journal of Food, Agriculture and Environment*, *8*(2), 469–476.

Jaffar, A., Jaafar, R., Jamil, N., Low, C. Y., & Abdullah, B. (2009). Photogrammetric grading of oil palm fresh fruit bunches. *International Journal of Mechanical and Mechatronics Engineering*, *9*(10), 18–24.

Lu, R., Srivastava, A. K., & Ababneh, H. A. A. (2006). *FINITE ELEMENT ANALYSIS AND EXPERIMENTAL EVALUATION OF BIOYIELD PROBES FOR MEASURING APPLE FRUIT FIRMNESS*. *49*(1), 123–132.

Ma, L., Wang, L., Chen, R., Chang, K., Wang, S., Hu, X., Sun, X., Lu, Z., Sun, H., Guo, Q., Jiang, M., & Hu, J. (2016). A low cost compact measurement system constructed using a smart electrochemical sensor for the real-time discrimination of fruit ripening. *Sensors (Switzerland)*, *16*(4). https://doi.org/10.3390/s16040501

*Malaysian palm oil's worldwide significance*. (n.d.). Palm Oil Health. Retrieved January 29, 2021, from https://www.excelvite.com/malaysian-palm-oil-worldwide-significance/

*Malaysian Palm Oil Industry – MPOC*. (n.d.). http://mpoc.org.my/malaysian-palm-oil-industry/

Misron, N., Azhar, N. S. K., Hamidon, M. N., Aris, I., Tashiro, K., & Nagata, H. (2020). Fruit battery with charging concept for oil palm maturity sensor. *Sensors (Switzerland)*, *20*(1). https://doi.org/10.3390/s20010226

Mohamed Halim, R., Ramli, R., Che Mat, C., Yuen May, C., Abu Bakar, N., & Abdul Hadi, N. (2016). Dry Separation of Palm Kernel and Palm Shell Using a Novel Five-Stage Winnowing Column System. *Technologies*, *4*(2), 13. https://doi.org/10.3390/technologies4020013

Mohammed, M. A. P. (2020). *Visco-Hyperelastic Model for Soft Rubber-like Materials Visco-Hyperelastic Model for Soft Rubber-like Materials. March 2014*.

Murah, A. J. (n.d.). *Grading of FFB for Palm Oil Mills in Malaysia*.

Nwankwojike, B. N., Odukwe, A. O., & Agunwamba, J. C. (2011). Modification of sequence of unit operations in mechanized palm fruit. *Nigerian Journal of Technology*, *30*(3), 41–49.

Owolarafe, O. K., Olabige, M. T., & Faborode, M. O. (2007). Physical and mechanical properties of two varieties of fresh oil palm fruit. *Journal of Food Engineering*, *78*(4), 1228–1232. https://doi.org/10.1016/j.jfoodeng.2005.12.049

P. Prabhakar. (2014). *What is the benefits of 3D finite element simulation of axisymmetric problems over 2D simulation?* https://www.researchgate.net/post/What_is_the_benefits_of_3D_finite_element_simulation_of_axisymmetric_problems_over_2D_simulation

PKS (Palm Kernel Shell). (n.d.). In *Pax Union Resources Malaysia-Thailand-Indonesia*. https://paxunion.wordpress.com/biomass/pks/

Rotimi, D. (2012). Physical and mechanical properties of palm fruit, kernel and nut. *Journal of Agricultural Technology*, *8*(7), 2147–2156.

Sari, N., Shiddiq, M., Fitra, R. H., & Yasmin, N. Z. (2019). Ripeness Classification of Oil Palm Fresh Fruit Bunch Using an Optical Probe. *Journal of Aceh Physics Society*, *8*(3), 72–77. https://doi.org/10.24815/jacps.v8i3.14122

Shabdin, M. K., Shariff, A. R. M., Johari, M. N. A., Saat, N. K., & Abbas, Z. (2016). A study on the oil palm fresh fruit bunch (FFB) ripeness detection by using Hue, Saturation and Intensity (HSI) approach. *IOP Conference Series: Earth and Environmental Science*, *37*(1). https://doi.org/10.1088/1755-1315/37/1/012039

Shehu, U. E., Mokhtar, M. N., Nor, M. Z. M., Baharuddin, A. S., & Nawi, N. M. (2019). A study on the use of water as a medium for the thermal inactivation of endogenous lipase in oil of palm fruit. In *Energies* (Vol. 12, Issue 20). https://doi.org/10.3390/en12203981

Sinambela, R., Mandang, T., Subrata, I. D. M., & Hermawan, W. (2020). Application of an inductive sensor system for identifying ripeness and forecasting harvest time of oil palm. *Scientia Horticulturae*, *265*(January), 109231. https://doi.org/10.1016/j.scienta.2020.109231

Sochi, T. (2010). Non-Newtonian flow in porous media. *Polymer*, *51*(22), 5007–5023. https://doi.org/10.1016/j.polymer.2010.07.047

Tuerxun, A., Mohamed Shariff, A. R., Janius, R., Abbas, Z., & Mahdiraji, G. A. (2020). Oil Palm Fresh Fruit Bunches Maturity Prediction by Using Optical Spectrometer. *IOP Conference Series: Earth and Environmental Science*, *540*(1). https://doi.org/10.1088/1755-1315/540/1/012085

Utom, S. L., Mohamad, E. J., Ameran, H. L. M., Kadir, H. A., Muji, S. Z. M., Rahim, R. A., & Pusppanathan, J. (2018). Non-Destructive Oil Palm Fresh Fruit Bunch (FFB) grading technique using optical sensor. *International Journal of Integrated Engineering*, *10*(1), 35–39. https://doi.org/10.30880/ijie.2018.10.01.006

Zulkifli, Z. M., Hashim, F. H., Raj, T., & Huddin, A. B. (2018). A Rapid and Non-Destructive Technique in Determining The Ripeness of Oil Palm Fresh Fruit Bunch (FFB). *Jurnal Kejuruteraan*, *30*(1), 93–101. https://doi.org/10.17576/jkukm-2018-30(1)-12

# APPENDICES

Raw data of Figure 4.2

| Avg (+ve) 0.5gpa | |
|---|---|
| Displace | Stress (Mpa) |
| 0 | 0 |
| 4.01E-20 | 2.34E-17 |
| 1.4E-19 | 6.24E-17 |
| 0.000596 | 75.02887 |
| 0.00063 | 78.74655 |
| 0.000648 | 80.63909 |
| 0.000656 | 81.59964 |
| 0.000663 | 82.33539 |
| 0.00067 | 83.07166 |
| 0.000677 | 83.81349 |
| 0.000683 | 84.55243 |
| 0.000683 | 84.55243 |

| 1.0gpa | |
|---|---|
| Displace | Stress (Mpa) |
| 0 | 0 |
| -3.8E-20 | -3.7E-17 |
| -1.7E-19 | 4.42E-17 |
| 0.00061 | 142.8387 |
| 0.000679 | 156.7023 |
| 0.000714 | 163.8038 |
| 0.000717 | 164.261 |
| 0.000718 | 164.6017 |
| 0.00072 | 164.8634 |
| 0.000721 | 165.056 |
| 0.000721 | 165.2136 |
| 0.000722 | 165.3713 |
| 0.000723 | 165.5295 |
| 0.000724 | 165.7646 |
| 0.000726 | 166.1186 |
| 0.000728 | 166.4765 |
| 0.000729 | 166.8316 |
| 0.000731 | 167.1842 |
| 0.000733 | 167.5424 |
| 0.000734 | 167.8066 |
| 0.000735 | 168.0087 |
| 0.000736 | 168.1655 |
| 0.000737 | 168.3251 |
| 0.000738 | 168.4834 |
| 0.000738 | 168.6417 |
| 0.000739 | 168.7994 |
| 0.00074 | 169.0364 |
| 0.000742 | 169.3929 |
| 0.000744 | 169.7528 |
| 0.000746 | 170.1075 |
| 0.000747 | 170.3761 |
| 0.000748 | 170.5791 |
| 0.000749 | 170.779 |
| 0.00075 | 170.9383 |
| 0.000751 | 171.0984 |
| 0.000751 | 171.2577 |
| 0.000752 | 171.4168 |
| 0.000753 | 171.5749 |
| 0.000754 | 171.8132 |
| 0.000755 | 171.9937 |
| 0.000755 | 171.9937 |

| 1.5gpa | |
|---|---|
| Displace | Stress (Mp |
| 0 | 0 |
| 3.61E-20 | 4.55E-17 |
| 1.52E-19 | 4E-17 |
| 0.000619 | 207.1028 |
| 0.000688 | 227.0387 |
| 0.00076 | 247.2973 |
| 0.000761 | 247.5565 |
| 0.000762 | 247.7976 |
| 0.000762 | 248.041 |
| 0.000763 | 248.2916 |
| 0.000764 | 248.5378 |
| 0.000765 | 248.7864 |
| 0.000766 | 249.0368 |
| 0.000767 | 249.2857 |
| 0.000768 | 249.5325 |
| 0.000769 | 249.7831 |
| 0.000769 | 250.0321 |
| 0.00077 | 250.2791 |
| 0.000771 | 250.5298 |
| 0.000772 | 250.7768 |
| 0.000773 | 251.0259 |
| 0.000774 | 251.277 |
| 0.000775 | 251.5244 |
| 0.000776 | 251.7737 |
| 0.000776 | 252.0249 |
| 0.000777 | 252.2726 |
| 0.000778 | 252.5221 |
| 0.000779 | 252.7736 |
| 0.00078 | 253.0214 |
| 0.000781 | 253.2733 |
| 0.000781 | 253.5025 |

Raw data of Figure 4.3

| y= -0.007 | |
|---|---|
| Displace | Stress(Mpa) |
| 0 | 0 |
| 0.000238312 | 61.85812 |
| 0.000381961 | 94.05565 |
| 0.000586797 | 138.7811 |
| 0.000690238 | 159.7812 |
| 0.000717192 | 165.184 |
| 0.000744591 | 170.6727 |
| 0.000748109 | 171.3885 |
| 0.000750733 | 171.9201 |
| 0.000753359 | 172.4518 |
| 0.000757303 | 173.25 |
| 0.000763217 | 174.444 |
| 0.000772137 | 176.246 |
| 0.000781059 | 178.042 |
| 0.000783482 | 178.5326 |
| 0.000785912 | 179.0246 |
| 0.000788327 | 179.5108 |
| 0.000790755 | 180.001 |
| 0.000793185 | 180.492 |
| 0.000795619 | 180.9839 |
| 0.000799286 | 181.7272 |
| 0.000804788 | 182.8417 |
| 0.000808908 | 183.6731 |
| 0.000808908 | 183.6731 |

| y=-0.005 | |
|---|---|
| Displace | Stress (Mpa) |
| 0 | 0 |
| -3.8039E-20 | -3.7E-17 |
| -1.71525E-19 | 4.42E-17 |
| 0.000609789 | 142.8387 |
| 0.000678687 | 156.7023 |
| 0.000714365 | 163.8038 |
| 0.000716648 | 164.261 |
| 0.000718349 | 164.6017 |
| 0.000719643 | 164.8634 |
| 0.000720602 | 165.056 |
| 0.000721384 | 165.2136 |
| 0.000722167 | 165.3713 |
| 0.000722951 | 165.5295 |
| 0.000724121 | 165.7646 |
| 0.00072588 | 166.1186 |
| 0.000727653 | 166.4765 |
| 0.000729418 | 166.8316 |
| 0.000731176 | 167.1842 |
| 0.000732952 | 167.5424 |
| 0.000734271 | 167.8066 |
| 0.000735273 | 168.0087 |
| 0.000736056 | 168.1655 |
| 0.000736847 | 168.3251 |
| 0.000737635 | 168.4834 |
| 0.000738423 | 168.6417 |
| 0.000739209 | 168.7994 |
| 0.00074039 | 169.0364 |
| 0.000742166 | 169.3929 |
| 0.000743952 | 169.7528 |
| 0.000745723 | 170.1075 |
| 0.00074706 | 170.3761 |
| 0.000748068 | 170.5791 |
| 0.000749066 | 170.779 |
| 0.00074986 | 170.9383 |
| 0.000750655 | 171.0984 |
| 0.000751449 | 171.2577 |
| 0.000752242 | 171.4168 |
| 0.000753033 | 171.5749 |
| 0.000754222 | 171.8132 |
| 0.00075512 | 171.9937 |
| 0.00075512 | 171.9937 |

| y=-0.006 | |
|---|---|
| Displace | Stress (Mp |
| 0 | 0 |
| 3.8039E-20 | 3.67E-17 |
| 1.28723E-19 | 3.34E-17 |
| 0.000428119 | 104.0783 |
| 0.00070222 | 161.766 |
| 0.000729281 | 167.1613 |
| 0.00073189 | 167.6878 |
| 0.000733836 | 168.0807 |
| 0.000735405 | 168.3966 |
| 0.000736982 | 168.7153 |
| 0.00073857 | 169.0371 |
| 0.000740152 | 169.3564 |
| 0.000741727 | 169.6736 |
| 0.000743309 | 169.9931 |
| 0.000744902 | 170.3156 |
| 0.000746489 | 170.636 |
| 0.000748069 | 170.954 |
| 0.000749664 | 171.2769 |
| 0.000751246 | 171.5951 |
| 0.000752836 | 171.9158 |
| 0.000754434 | 172.2387 |
| 0.000756019 | 172.5571 |
| 0.000757619 | 172.8803 |
| 0.000759206 | 173.1988 |
| 0.0007608 | 173.5198 |
| 0.000762402 | 173.8431 |
| 0.000763992 | 174.1621 |
| 0.000765597 | 174.4858 |
| 0.000767189 | 174.805 |
| 0.000768795 | 175.1291 |
| 0.000770396 | 175.451 |
| 0.000771992 | 175.771 |
| 0.000773595 | 176.0932 |
| 0.000775205 | 176.418 |
| 0.000775205 | 176.418 |

Raw data of Figure 4.6

| Avg-miu-1e9 | | Avg-miu-2.2e9 | | Avg-miu=3e9 | |
|---|---|---|---|---|---|
| Displace | Stress (Mpa) | Displace | Stress (Mpa) | Displace | Stress (Mpa) |
| 0 | 0 | 0 | 0 | 0 | 0 |
| 2.85576E-20 | 7.85E-16 | 2.14E-20 | 1.29E-15 | 1.83E-20 | 1.51E-15 |
| 4.07864E-20 | 1.99E-14 | 2.65E-20 | 3.18E-14 | 2.9E-20 | 3.69E-14 |
| 7.91866E-20 | 1.08E-14 | 8.29E-20 | 4.31E-14 | 6.64E-20 | 5.33E-14 |
| 0.000233103 | 637.6144 | 0.000235 | 1384.245 | 0.000235 | 1880.682 |
| 0.000309236 | 835.4908 | 0.000311 | 1808.585 | 0.000311 | 2456.455 |
| 0.000384228 | 1006.159 | 0.000387 | 2185.042 | 0.000388 | 2969.876 |
| 0.000449886 | 1125.746 | 0.000454 | 2454.142 | 0.000455 | 3338.609 |
| 0.000499765 | 1177.153 | 0.000508 | 2589 | 0.00051 | 3528.902 |
| 0.000517938 | 1202.383 | 0.000568 | 2585.957 | 0.000568 | 3509.725 |
| 0.000546713 | 1245.872 | 0.000574 | 2622.464 | 0.000585 | 3607.799 |
| 0.00056783 | 1273.592 | 0.000581 | 2642.893 | 0.000595 | 3645.192 |
| 0.000570473 | 1275.825 | 0.000587 | 2661.542 | 0.000602 | 3675.976 |
| 0.000571648 | 1276.24 | 0.000593 | 2681.51 | 0.00061 | 3708.024 |
| 0.000572598 | 1275.566 | 0.000598 | 2698.242 | 0.000617 | 3733.036 |
| 0.000573348 | 1273.697 | 0.000607 | 2721.577 | 0.000624 | 3753.457 |
| 0.00057408 | 1271.701 | 0.000615 | 2742.693 | 0.000628 | 3762.585 |
| 0.000575127 | 1271.449 | 0.000623 | 2757.381 | 0.000631 | 3770.399 |
| 0.000575991 | 1271.814 | 0.000627 | 2763.605 | 0.000632 | 3772.162 |
| 0.000576849 | 1272.229 | 0.000629 | 2766.438 | 0.000633 | 3773.237 |
| 0.000577664 | 1272.385 | 0.00063 | 2768.597 | 0.000634 | 3772.738 |
| 0.000578828 | 1272.328 | 0.000631 | 2768.656 | 0.000634 | 3770.667 |
| 0.000580545 | 1272.06 | 0.000631 | 2767.114 | 0.000635 | 3766.979 |
| 0.000583208 | 1272.143 | 0.000631 | 2763.765 | 0.000635 | 3766.979 |
| 0.000587725 | 1274.855 | 0.000632 | 2761.372 | | |
| 0.000592181 | 1277.29 | 0.000633 | 2764.146 | | |
| 0.000594355 | 1277.992 | 0.000633 | 2765.991 | | |
| 0.000595815 | 1277.673 | 0.000634 | 2768.508 | | |
| 0.000596412 | 1276.573 | 0.000635 | 2772.053 | | |
| 0.000596412 | 1276.573 | 0.000637 | 2777.592 | | |
| | | 0.00064 | 2785.832 | | |
| | | 0.000644 | 2798.266 | | |
| | | 0.000649 | 2817.029 | | |
| | | 0.000658 | 2845.868 | | |
| | | 0.000672 | 2897.243 | | |
| | | 0.000668 | 2874.512 | | |
| | | 0.000668 | 2874.512 | | |

| Avg-lamda-30 | | Avg-lamda-20 | | Avg-lamda-50 | |
|---|---|---|---|---|---|
| Displace | Stress | Displace | Stress (Mpa) | Displace | Stress (Mpa) |
| 0 | 0 | 0 | 0 | 0 | 0 |
| 2.13821E-20 | 1.29E-15 | 2.14E-20 | 1.29E-15 | -2.1E-20 | 1.29E-15 |
| 2.65287E-20 | 3.18E-14 | 2.65E-20 | 3.18E-14 | -2.7E-20 | 3.18E-14 |
| 8.29299E-20 | 4.31E-14 | -8.3E-20 | 4.31E-14 | -8.3E-20 | 4.31E-14 |
| 0.000234495 | 1381.96 | 0.000235 | 1384.245 | 0.000234 | 1380.217 |
| 0.000310556 | 1805.271 | 0.000311 | 1808.585 | 0.00031 | 1802.622 |
| 0.000386504 | 2178.671 | 0.000387 | 2185.042 | 0.000386 | 2173.56 |
| 0.000453268 | 2442.173 | 0.000454 | 2454.142 | 0.000452 | 2432.455 |
| 0.000504542 | 2560.148 | 0.000508 | 2589 | 0.000502 | 2534.96 |
| 0.000520382 | 2597.992 | 0.000568 | 2585.957 | 0.000529 | 2618.353 |
| 0.000539772 | 2660.448 | 0.000574 | 2622.464 | 0.000559 | 2710.222 |
| 0.000568725 | 2751.224 | 0.000581 | 2642.893 | 0.000573 | 2753.087 |
| 0.000579289 | 2777.359 | 0.000587 | 2661.542 | 0.000578 | 2763.511 |
| 0.000581799 | 2780.754 | 0.000593 | 2681.51 | 0.00058 | 2766.034 |
| 0.000582802 | 2779.656 | 0.000598 | 2698.242 | 0.000583 | 2764.943 |
| 0.000583751 | 2777.966 | 0.000607 | 2721.577 | 0.000583 | 2763.116 |
| 0.000584633 | 2775.443 | 0.000615 | 2742.693 | 0.000584 | 2760.416 |
| 0.000585854 | 2770.695 | 0.000623 | 2757.381 | 0.000585 | 2753.851 |
| 0.00058789 | 2766.033 | 0.000627 | 2763.605 | 0.000585 | 2749.885 |
| 0.000590212 | 2764.862 | 0.000629 | 2766.438 | | |
| 0.000592896 | 2767.999 | 0.00063 | 2768.597 | | |
| 0.000595657 | 2772.142 | 0.000631 | 2768.656 | | |
| 0.00059842 | 2776.345 | 0.000631 | 2767.114 | | |
| 0.000602456 | 2781.681 | 0.000631 | 2763.765 | | |
| 0.000608035 | 2783.878 | 0.000632 | 2761.372 | | |
| 0.000609063 | 2782.064 | 0.000633 | 2764.146 | | |
| 0.000609063 | 2782.064 | 0.000633 | 2765.991 | | |
| | | 0.000634 | 2768.508 | | |
| | | 0.000635 | 2772.053 | | |
| | | 0.000637 | 2777.592 | | |
| | | 0.00064 | 2785.832 | | |
| | | 0.000644 | 2798.266 | | |
| | | 0.000649 | 2817.029 | | |
| | | 0.000658 | 2845.868 | | |
| | | 0.000672 | 2897.243 | | |
| | | 0.000668 | 2874.512 | | |
| | | 0.000668 | 2874.512 | | |

| Avg-a-3 | |
|---|---|
| Displace | Stress (Mpa) |
| 0 | 0 |
| 2.1382E-20 | 1.2924E-15 |
| 2.6529E-20 | 3.17942E-14 |
| 8.293E-20 | 4.30585E-14 |
| 1.896E-19 | 4.44073E-14 |
| 4.1546E-19 | 2.60338E-14 |
| 4.5185E-05 | 286.7883413 |
| 0.00012091 | 732.8750933 |
| 0.00021988 | 1232.004352 |
| 0.0002495 | 1349.538304 |
| 0.0002495 | 1349.538304 |

| Avg-a-5 | |
|---|---|
| Displace | Stress (Mpa) |
| 0 | 0 |
| 2.14E-20 | 1.29E-15 |
| 2.65E-20 | 3.18E-14 |
| 8.29E-20 | 4.31E-14 |
| 1.9E-19 | 4.44E-14 |
| 6.28E-05 | 288.2067 |
| 6.28E-05 | 288.2067 |

| Avg-a-1.6 | |
|---|---|
| Displace | Stress (Mpa) |
| 0 | 0 |
| -2.1E-20 | 1.29E-15 |
| -2.7E-20 | 3.18E-14 |
| -8.3E-20 | 4.31E-14 |
| 0.000235 | 1384.245 |
| 0.000311 | 1808.585 |
| 0.000387 | 2185.042 |
| 0.000454 | 2454.142 |
| 0.000508 | 2589 |
| 0.000568 | 2585.957 |
| 0.000574 | 2622.464 |
| 0.000581 | 2642.893 |
| 0.000587 | 2661.542 |
| 0.000593 | 2681.51 |
| 0.000598 | 2698.242 |
| 0.000607 | 2721.577 |
| 0.000615 | 2742.693 |
| 0.000623 | 2757.381 |
| 0.000627 | 2763.605 |
| 0.000629 | 2766.438 |
| 0.00063 | 2768.597 |
| 0.000631 | 2768.656 |
| 0.000631 | 2767.114 |
| 0.000631 | 2763.765 |
| 0.000632 | 2761.372 |
| 0.000633 | 2764.146 |
| 0.000633 | 2765.991 |
| 0.000634 | 2768.508 |
| 0.000635 | 2772.053 |
| 0.000637 | 2777.592 |
| 0.00064 | 2785.832 |
| 0.000644 | 2798.266 |
| 0.000649 | 2817.029 |
| 0.000658 | 2845.868 |
| 0.000672 | 2897.243 |
| 0.000668 | 2874.512 |
| 0.000668 | 2874.512 |

Raw data of Figure 4.8

Comaprison model 1

| Elastic | | Visco+Hyper | | Elastic+Visco | |
|---|---|---|---|---|---|
| Avg | | Avg | | Avg | |
| Displace | Stress (Mpa) | Displace | Stress (Mpa) | Displace | Stress (Mpa) |
| 0 | 0 | 0 | 0 | 0 | 0 |
| -3.8E-20 | -3.7E-17 | -2.1E-20 | 1.79E-15 | 1.74E-20 | 7.49E-17 |
| -1.7E-19 | 4.42E-17 | -2.7E-20 | 3.18E-14 | 5.24E-20 | 1.15E-16 |
| 0.00061 | 142.8387 | -8.3E-20 | 4.31E-14 | 8.86E-05 | 455.1156 |
| 0.000679 | 156.7023 | 0.000235 | 1384.245 | 0.000272 | 607.7486 |
| 0.000714 | 163.8038 | 0.000311 | 1808.585 | 0.000594 | 1244.898 |
| 0.000717 | 164.261 | 0.000387 | 2185.042 | 0.000613 | 1282.02 |
| 0.000718 | 164.6017 | 0.000454 | 2454.142 | 0.000623 | 1300.464 |
| 0.00072 | 164.8634 | 0.000508 | 2589 | 0.000624 | 1302.832 |
| 0.000721 | 165.056 | 0.000568 | 2585.957 | 0.000626 | 1306.275 |
| 0.000721 | 165.2136 | 0.000574 | 2622.464 | 0.000626 | 1306.275 |
| 0.000722 | 165.3713 | 0.000581 | 2642.893 | | |
| 0.000723 | 165.5295 | 0.000587 | 2661.542 | | |
| 0.000724 | 165.7646 | 0.000593 | 2681.51 | | |
| 0.000726 | 166.1186 | 0.000598 | 2698.242 | | |
| 0.000728 | 166.4765 | 0.000607 | 2721.577 | | |
| 0.000729 | 166.8316 | 0.000615 | 2742.693 | | |
| 0.000731 | 167.1842 | 0.000623 | 2757.381 | | |
| 0.000733 | 167.5424 | 0.000627 | 2763.605 | | |
| 0.000734 | 167.8066 | 0.000629 | 2766.438 | | |
| 0.000735 | 168.0087 | 0.00063 | 2768.597 | | |
| 0.000736 | 168.1655 | 0.000631 | 2768.656 | | |
| 0.000737 | 168.3251 | 0.000631 | 2767.114 | | |
| 0.000738 | 168.4834 | 0.000631 | 2763.765 | | |
| 0.000738 | 168.6417 | 0.000632 | 2761.372 | | |
| 0.000739 | 168.7994 | 0.000633 | 2764.146 | | |
| 0.00074 | 169.0364 | 0.000633 | 2765.991 | | |
| 0.000742 | 169.3929 | 0.000634 | 2768.508 | | |
| 0.000744 | 169.7528 | 0.000635 | 2772.053 | | |
| 0.000746 | 170.1075 | 0.000637 | 2777.592 | | |
| 0.000747 | 170.3761 | 0.00064 | 2785.832 | | |
| 0.000748 | 170.5791 | 0.000644 | 2798.266 | | |
| 0.000749 | 170.779 | 0.000649 | 2817.029 | | |
| 0.00075 | 170.9383 | 0.000658 | 2845.868 | | |
| 0.000751 | 171.0984 | 0.000672 | 2897.243 | | |
| 0.000751 | 171.2577 | 0.000668 | 2874.512 | | |
| 0.000752 | 171.4168 | 0.000668 | 2874.512 | | |
| 0.000753 | 171.5749 | | | | |
| 0.000754 | 171.8132 | | | | |
| 0.000755 | 171.9937 | | | | |
| 0.000755 | 171.9937 | | | | |

Comaprison model 2

Elastic

| Avg Displace | Stress (Mpa) |
|---|---|
| 0 | 0 |
| 0.001 | -2.9E-13 |
| 0.002 | 1.56E-13 |
| 0.0035 | -4.8E-14 |
| 0.00575 | 7.52E-14 |
| 0.006594 | 1.4E-13 |
| 0.00691 | 9.26E-14 |
| 0.007385 | 2.9E-14 |
| 0.007522 | 23.94488 |
| 0.007545 | 45.36235 |
| 0.007553 | 50.25464 |
| 0.007567 | 51.89903 |
| 0.007569 | 51.57737 |
| 0.007569 | 51.25156 |

Visco+Hyper

| Avg Displace | Stress(Mpa) |
|---|---|
| 0 | 0 |
| 0.001 | 6.97E-09 |
| 0.002 | 6.17E-12 |
| 0.0035 | 1.69E-12 |
| 0.00575 | -8.9E-12 |
| 0.006594 | -2.8E-12 |
| 0.00691 | -5.7E-12 |
| 0.007385 | -9.9E-12 |
| 0.007512 | 886.7864 |
| 0.007524 | 963.4807 |
| 0.007526 | 976.6842 |
| 0.007527 | 981.5121 |
| 0.007527 | 981.5121 |

Elastic+Visco

| Avg Displace | Stress (Mpa) |
|---|---|
| 0 | 0 |
| 0.001 | 9.22E-13 |
| 0.002 | 8.44E-13 |
| 0.0035 | 4.72E-15 |
| 0.00575 | 6.01E-13 |
| 0.006594 | 1.44E-12 |
| 0.00691 | 8.2E-13 |
| 0.007385 | 6.85E-13 |
| 0.007526 | 227.8009 |
| 0.007561 | 376.3333 |
| 0.00757 | 410.5575 |
| 0.007581 | 436.9177 |
| 0.007596 | 444.7613 |
| 0.007601 | 439.0289 |
| 0.007601 | 439.0289 |

Comaprison model 3

Elastic

Avg (+ve)

| Displace | Stress (Mpa) |
|---|---|
| 0 | 0 |
| 0.000433 | 2.836497 |
| 0.000858 | 14.73392 |
| 0.001002 | 27.05591 |
| 0.001211 | 54.37653 |
| 0.00128 | 70.83934 |
| 0.001383 | 99.83051 |
| 0.001418 | 113.4411 |
| 0.001472 | 135.0637 |
| 0.001491 | 144.0197 |
| 0.001522 | 158.1239 |
| 0.001535 | 163.9076 |
| 0.00154 | 166.2504 |
| 0.001542 | 167.1896 |
| 0.001546 | 168.7712 |
| 0.00155 | 169.5952 |
| 0.001549 | 169.5813 |
| 0.001549 | 169.5651 |
| 0.001549 | 169.5394 |
| 0.001549 | 169.5186 |
| 0.001549 | 169.5186 |

Visco+Hyper

Avg (+ve)

| Displace | Stress (Mpa) |
|---|---|
| 0 | 0 |
| 0.00017 | 36.28676 |
| 0.000349 | 78.56891 |
| 0.000659 | 311.9367 |
| 0.000725 | 376.9544 |

Elastic+Visco

| Displace | Stress (Mpa) |
|---|---|
| 0 | 0 |
| 0.000204 | 92.44997 |
| 0.000385 | 322.4649 |
| 0.000609 | 1070.108 |
| 0.000639 | 1452.532 |
| 0.000663 | 1914.783 |
| 0.00067 | 2114.019 |
| 0.00068 | 2429.793 |
| 0.000686 | 2561.706 |
| 0.000687 | 2575.578 |
| 0.000687 | 2581.03 |
| 0.000688 | 2589.685 |
| 0.000691 | 2601.942 |
| 0.000691 | 2602.457 |
| 0.00069 | 2602.045 |
| 0.00069 | 2601.835 |
| 0.00069 | 2601.559 |
| 0.00069 | 2601.289 |

Raw data of Figure 4.9

| 0.25mm time | stress | stress (mpa) |
|---|---|---|
| 0 | 0 | 0 |
| 0.01 | 6.31E-11 | 6.31E-17 |
| 0.02 | 1.04E-10 | 1.04E-16 |
| 0.03 | 3.59E-10 | 3.59E-16 |
| 0.045 | 2.74E-10 | 2.74E-16 |
| 0.0675 | -4.7E-11 | 4.66E-17 |
| 0.10125 | -4.7E-10 | 4.73E-16 |
| 0.151875 | 3.04E-10 | 3.04E-16 |
| 0.227812 | 1.9E-10 | 1.9E-16 |
| 0.327812 | -3.4E-10 | 3.38E-16 |
| 0.427812 | -2.9E-10 | 2.91E-16 |
| 0.527812 | -4.7E-10 | 4.72E-16 |
| 0.627813 | -4.6E-11 | 4.59E-17 |
| 0.727813 | -4.9E-10 | 4.85E-16 |
| 0.827812 | -2.5E-10 | 2.46E-16 |
| 0.927813 | 1.18E-10 | 1.18E-16 |
| 1.027812 | -3.8E-10 | 3.77E-16 |
| 1.127813 | 5.17E-10 | 5.17E-16 |
| 1.227813 | 1.63E-10 | 1.63E-16 |
| 1.327813 | -2.9E-10 | 2.86E-16 |
| 1.427812 | -3.3E-10 | 3.3E-16 |
| 1.527812 | -2.3E-10 | 2.32E-16 |
| 1.627813 | -3.8E-10 | 3.8E-16 |
| 1.727813 | -6.5E-10 | 6.52E-16 |
| 1.827813 | -2.3E-10 | 2.34E-16 |
| 1.927812 | 2.09E-10 | 2.09E-16 |
| 2.027812 | 4E-10 | 4E-16 |
| 2.127812 | 4.04E-10 | 4.04E-16 |
| 2.227813 | 5.88E-10 | 5.88E-16 |
| 2.327812 | 1.16E-10 | 1.16E-16 |
| 2.427813 | 7.46E-12 | 7.46E-18 |
| 2.527812 | 3.61E-10 | 3.61E-16 |
| 2.627812 | -4.7E+07 | 47.3901 |
| 2.727813 | -1.4E+08 | 141.8042 |
| 2.827812 | -2.3E+08 | 232.7053 |
| 2.927813 | -3.3E+08 | 327.3327 |
| 3.027812 | -4E+08 | 396.6156 |
| 3.127812 | -3.7E+08 | 373.9059 |
| 3.227813 | -3.6E+08 | 362.0898 |
| 3.327812 | -3.5E+08 | 354.7769 |
| 3.427813 | -3.5E+08 | 349.4374 |
| 3.527812 | -3.5E+08 | 345.0747 |
| 3.627812 | -3.4E+08 | 341.2812 |
| 3.727813 | -3.4E+08 | 337.8803 |
| 3.827812 | -3.3E+08 | 334.7872 |

| 0.27mm time | stress | stress (mpa) |
|---|---|---|
| 0 | 0 | 0 |
| 0.01 | 6.31E-11 | 6.31E-17 |
| 0.02 | 1.04E-10 | 1.04E-16 |
| 0.03 | 3.59E-10 | 3.59E-16 |
| 0.045 | 2.74E-10 | 2.74E-16 |
| 0.0675 | -4.7E-11 | 4.66E-17 |
| 0.10125 | -4.7E-10 | 4.73E-16 |
| 0.151875 | 3.04E-10 | 3.04E-16 |
| 0.227812 | 1.9E-10 | 1.9E-16 |
| 0.327812 | -3.4E-10 | 3.38E-16 |
| 0.427812 | -2.9E-10 | 2.91E-16 |
| 0.527812 | -4.7E-10 | 4.72E-16 |
| 0.627813 | -4.6E-11 | 4.59E-17 |
| 0.727813 | -4.9E-10 | 4.85E-16 |
| 0.827812 | -2.5E-10 | 2.46E-16 |
| 0.927813 | 1.18E-10 | 1.18E-16 |
| 1.027812 | -3.8E-10 | 3.77E-16 |
| 1.127813 | 5.17E-10 | 5.17E-16 |
| 1.227813 | 1.63E-10 | 1.63E-16 |
| 1.327813 | -2.9E-10 | 2.86E-16 |
| 1.427812 | -3.3E-10 | 3.3E-16 |
| 1.527812 | -2.3E-10 | 2.32E-16 |
| 1.627813 | -3.8E-10 | 3.8E-16 |
| 1.727813 | -6.5E-10 | 6.52E-16 |
| 1.827813 | -2.3E-10 | 2.34E-16 |
| 1.927812 | 2.09E-10 | 2.09E-16 |
| 2.027812 | 4E-10 | 4E-16 |
| 2.127812 | 4.04E-10 | 4.04E-16 |
| 2.227813 | 5.88E-10 | 5.88E-16 |
| 2.327812 | 1.16E-10 | 1.16E-16 |
| 2.427813 | 7.46E-12 | 7.46E-18 |
| 2.527812 | 3.61E-10 | 3.61E-16 |
| 2.627812 | -7.3E+07 | 73.37462 |
| 2.727813 | -1.7E+08 | 166.3895 |
| 2.827812 | -2.6E+08 | 261.0245 |
| 2.927813 | -3.6E+08 | 355.2602 |
| 3.027812 | -4.3E+08 | 429.9899 |
| 3.127812 | -4.1E+08 | 405.8169 |
| 3.227813 | -3.9E+08 | 393.1835 |
| 3.327812 | -3.9E+08 | 385.3362 |
| 3.427813 | -3.8E+08 | 379.5861 |
| 3.527812 | -3.7E+08 | 374.8773 |
| 3.627812 | -3.7E+08 | 370.7778 |
| 3.727813 | -3.7E+08 | 367.1004 |
| 3.827812 | -3.6E+08 | 363.7549 |

| 0.30mm time | stress |
|---|---|
| 0 | 0 |
| 0.01 | 6.31E-11 |
| 0.02 | 1.04E-10 |
| 0.03 | 3.59E-10 |
| 0.045 | 2.74E-10 |
| 0.0675 | -4.7E-11 |
| 0.10125 | -4.7E-10 |
| 0.151875 | 3.04E-10 |
| 0.227812 | 1.9E-10 |
| 0.327812 | -3.4E-10 |
| 0.427812 | -2.9E-10 |
| 0.527812 | -4.7E-10 |
| 0.627813 | -4.6E-11 |
| 0.727813 | -4.9E-10 |
| 0.827812 | -2.5E-10 |
| 0.927813 | 1.18E-10 |
| 1.027812 | -3.8E-10 |
| 1.127813 | 5.17E-10 |
| 1.227813 | 1.63E-10 |
| 1.327813 | -2.9E-10 |
| 1.427812 | -3.3E-10 |
| 1.527812 | -2.3E-10 |
| 1.627813 | -3.8E-10 |
| 1.727813 | -6.5E-10 |
| 1.827813 | -2.3E-10 |
| 1.927812 | 2.09E-10 |
| 2.027812 | 4E-10 |
| 2.127812 | 4.04E-10 |
| 2.227813 | 5.88E-10 |
| 2.327812 | 1.16E-10 |
| 2.427813 | 7.46E-12 |
| 2.527812 | 3.61E-10 |
| 2.627812 | -1E+08 |
| 2.727813 | -1.9E+08 |
| 2.827812 | -2.9E+08 |
| 2.927813 | -3.9E+08 |
| 3.027812 | -4.6E+08 |
| 3.127812 | -4.4E+08 |
| 3.227813 | -4.2E+08 |
| 3.327812 | -4.2E+08 |
| 3.427813 | -4.1E+08 |
| 3.527812 | -4E+08 |
| 3.627812 | -4E+08 |
| 3.727813 | -4E+08 |
| 3.827812 | -3.9E+08 |

| | | | | | | | | |
|---|---|---|---|---|---|---|---|---|
| 3.927813 | -3.3E+08 | 331.9546 | 3.927813 | -3.6E+08 | 360.6906 | 3.927813 | -3.9E+08 | |
| 4.027812 | -3.3E+08 | 329.3512 | 4.027812 | -3.6E+08 | 357.874 | 4.027812 | -3.9E+08 | |
| 4.127812 | -3.3E+08 | 326.9531 | 4.127812 | -3.6E+08 | 355.2792 | 4.127812 | -3.8E+08 | |
| 4.227812 | -3.2E+08 | 324.7404 | 4.227812 | -3.5E+08 | 352.8849 | 4.227812 | -3.8E+08 | |
| 4.327813 | -3.2E+08 | 322.6958 | 4.327813 | -3.5E+08 | 350.6723 | 4.327813 | -3.8E+08 | |
| 4.427813 | -3.2E+08 | 320.8038 | 4.427813 | -3.5E+08 | 348.6246 | 4.427813 | -3.8E+08 | |
| 4.527812 | -3.2E+08 | 319.0507 | 4.527812 | -3.5E+08 | 346.7272 | 4.527812 | -3.7E+08 | |
| 4.627812 | -3.2E+08 | 317.4237 | 4.627812 | -3.4E+08 | 344.9662 | 4.627812 | -3.7E+08 | |
| 4.727812 | -3.2E+08 | 315.9117 | 4.727812 | -3.4E+08 | 343.3294 | 4.727812 | -3.7E+08 | |
| 4.827813 | -3.1E+08 | 314.5043 | 4.827813 | -3.4E+08 | 341.8056 | 4.827813 | -3.7E+08 | |
| 4.927813 | -3.1E+08 | 313.1921 | 4.927813 | -3.4E+08 | 340.3849 | 4.927813 | -3.7E+08 | |
| 5.027812 | -3.1E+08 | 311.9667 | 5.027812 | -3.4E+08 | 339.0579 | 5.027812 | -3.7E+08 | |
| 5.127812 | -3.1E+08 | 310.8178 | 5.127812 | -3.4E+08 | 337.8137 | 5.127812 | -3.6E+08 | |
| 5.227812 | -3.1E+08 | 309.7436 | 5.227812 | -3.4E+08 | 336.6502 | 5.227812 | -3.6E+08 | |
| 5.327813 | -3.1E+08 | 308.7354 | 5.327813 | -3.4E+08 | 335.5579 | 5.327813 | -3.6E+08 | |
| 5.427813 | -3.1E+08 | 307.787 | 5.427813 | -3.3E+08 | 334.5304 | 5.427813 | -3.6E+08 | |
| 5.527812 | -3.1E+08 | 306.8933 | 5.527812 | -3.3E+08 | 333.5621 | 5.527812 | -3.6E+08 | |
| 5.627812 | -3.1E+08 | 306.0496 | 5.627812 | -3.3E+08 | 332.6478 | 5.627812 | -3.6E+08 | |
| 5.727812 | -3.1E+08 | 305.2515 | 5.727812 | -3.3E+08 | 331.7828 | 5.727812 | -3.6E+08 | |
| 5.827813 | -3E+08 | 304.4952 | 5.827813 | -3.3E+08 | 330.963 | 5.827813 | -3.6E+08 | |
| 5.927813 | -3E+08 | 303.7771 | 5.927813 | -3.3E+08 | 330.1844 | 5.927813 | -3.6E+08 | |
| 6.027812 | -3E+08 | 303.094 | 6.027812 | -3.3E+08 | 329.4437 | 6.027812 | -3.6E+08 | |
| 6.127812 | -3E+08 | 302.4429 | 6.127812 | -3.3E+08 | 328.7376 | 6.127812 | -3.5E+08 | |
| 6.227812 | -3E+08 | 301.8212 | 6.227812 | -3.3E+08 | 328.0632 | 6.227812 | -3.5E+08 | |
| 6.327813 | -3E+08 | 301.2263 | 6.327813 | -3.3E+08 | 327.4179 | 6.327813 | -3.5E+08 | |
| 6.427813 | -3E+08 | 300.6562 | 6.427813 | -3.3E+08 | 326.7994 | 6.427813 | -3.5E+08 | |
| 6.527812 | -3E+08 | 300.1088 | 6.527812 | -3.3E+08 | 326.2055 | 6.527812 | -3.5E+08 | |
| 6.627812 | -3E+08 | 299.5824 | 6.627812 | -3.3E+08 | 325.6341 | 6.627812 | -3.5E+08 | |
| 6.727812 | -3E+08 | 299.0752 | 6.727812 | -3.3E+08 | 325.0836 | 6.727812 | -3.5E+08 | |
| 6.827813 | -3E+08 | 298.5857 | 6.827813 | -3.2E+08 | 324.5523 | 6.827813 | -3.5E+08 | |
| 6.927813 | -3E+08 | 298.1126 | 6.927813 | -3.2E+08 | 324.0387 | 6.927813 | -3.5E+08 | |
| 7.027812 | -3E+08 | 297.6547 | 7.027812 | -3.2E+08 | 323.5414 | 7.027812 | -3.5E+08 | |
| 7.127812 | -3E+08 | 297.2107 | 7.127812 | -3.2E+08 | 323.0593 | 7.127812 | -3.5E+08 | |
| 7.227812 | -3E+08 | 296.7797 | 7.227812 | -3.2E+08 | 322.5912 | 7.227812 | -3.5E+08 | |
| 7.327813 | -3E+08 | 296.3608 | 7.327813 | -3.2E+08 | 322.1362 | 7.327813 | -3.5E+08 | |
| 7.427813 | -3E+08 | 295.9529 | 7.427813 | -3.2E+08 | 321.6932 | 7.427813 | -3.5E+08 | |
| 7.527812 | -3E+08 | 295.5555 | 7.527812 | -3.2E+08 | 321.2614 | 7.527812 | -3.5E+08 | |
| 7.627812 | -3E+08 | 295.1678 | 7.627812 | -3.2E+08 | 320.8402 | 7.627812 | -3.5E+08 | |
| 7.727812 | -2.9E+08 | 294.7891 | 7.727812 | -3.2E+08 | 320.4287 | 7.727812 | -3.5E+08 | |
| 7.827813 | -2.9E+08 | 294.4188 | 7.827813 | -3.2E+08 | 320.0263 | 7.827813 | -3.5E+08 | |
| 7.927813 | -2.9E+08 | 294.0565 | 7.927813 | -3.2E+08 | 319.6325 | 7.927813 | -3.5E+08 | |
| 8.027813 | -2.9E+08 | 293.7016 | 8.027813 | -3.2E+08 | 319.2468 | 8.027813 | -3.4E+08 | |
| 8.127812 | -2.9E+08 | 293.3536 | 8.127812 | -3.2E+08 | 318.8685 | 8.127812 | -3.4E+08 | |
| 8.227813 | -2.9E+08 | 293.0122 | 8.227813 | -3.2E+08 | 318.4975 | 8.227813 | -3.4E+08 | |
| 8.327812 | -2.9E+08 | 292.677 | 8.327812 | -3.2E+08 | 318.1331 | 8.327812 | -3.4E+08 | |
| 8.427813 | -2.9E+08 | 292.3476 | 8.427813 | -3.2E+08 | 317.775 | 8.427813 | -3.4E+08 | |
| 8.527813 | -2.9E+08 | 292.0237 | 8.527813 | -3.2E+08 | 317.4229 | 8.527813 | -3.4E+08 | |

| | | |
|---|---|---|
| 8.627812 | -2.9E+08 | 291.7052 |
| 8.727813 | -2.9E+08 | 291.3916 |
| 8.827812 | -2.9E+08 | 291.0827 |
| 8.927813 | -2.9E+08 | 290.7783 |
| 9.027813 | -2.9E+08 | 290.4783 |
| 9.127812 | -2.9E+08 | 290.1824 |
| 9.227813 | -2.9E+08 | 289.8905 |
| 9.327812 | -2.9E+08 | 289.6024 |
| 9.427813 | -2.9E+08 | 289.3179 |
| 9.527813 | -2.9E+08 | 289.037 |
| 9.627812 | -2.9E+08 | 288.7595 |
| 9.727813 | -2.9E+08 | 288.4853 |
| 9.827812 | -2.9E+08 | 288.2142 |
| 9.927813 | -2.9E+08 | 287.9463 |
| 10 | -2.9E+08 | 287.7548 |

| | | |
|---|---|---|
| 8.627812 | -3.2E+08 | 317.0765 |
| 8.727813 | -3.2E+08 | 316.7355 |
| 8.827812 | -3.2E+08 | 316.3996 |
| 8.927813 | -3.2E+08 | 316.0687 |
| 9.027813 | -3.2E+08 | 315.7424 |
| 9.127812 | -3.2E+08 | 315.4207 |
| 9.227813 | -3.2E+08 | 315.1032 |
| 9.327812 | -3.1E+08 | 314.7899 |
| 9.427813 | -3.1E+08 | 314.4805 |
| 9.527813 | -3.1E+08 | 314.175 |
| 9.627812 | -3.1E+08 | 313.8732 |
| 9.727813 | -3.1E+08 | 313.5749 |
| 9.827812 | -3.1E+08 | 313.2802 |
| 9.927813 | -3.1E+08 | 312.9887 |
| 10 | -3.1E+08 | 312.7804 |

| | |
|---|---|
| 8.627812 | -3.4E+08 |
| 8.727813 | -3.4E+08 |
| 8.827812 | -3.4E+08 |
| 8.927813 | -3.4E+08 |
| 9.027813 | -3.4E+08 |
| 9.127812 | -3.4E+08 |
| 9.227813 | -3.4E+08 |
| 9.327812 | -3.4E+08 |
| 9.427813 | -3.4E+08 |
| 9.527813 | -3.4E+08 |
| 9.627812 | -3.4E+08 |
| 9.727813 | -3.4E+08 |
| 9.827812 | -3.4E+08 |
| 9.927813 | -3.4E+08 |
| 10 | -3.4E+08 |

Elastic

| Time | Stress | Stress (Mpa) |
|---|---|---|
| 0 | 0 | 0 |
| 0.01 | -368622.2188 | 0.368622 |
| 0.02 | -741303.625 | 0.741304 |
| 0.03 | -1118091.75 | 1.118092 |
| 0.05 | -1882155.5 | 1.882156 |
| 0.09 | -3453223 | 3.453223 |
| 0.17 | -6775152.5 | 6.775153 |
| 0.27 | -11337212 | 11.33721 |
| 0.37 | -16429204 | 16.4292 |
| 0.47 | -22110540 | 22.11054 |
| 0.57 | -28446462 | 28.44646 |
| 0.67 | -35507036 | 35.50704 |
| 0.77 | -43366932 | 43.36693 |
| 0.87 | -52105096 | 52.1051 |
| 0.97 | -61804376 | 61.80438 |
| 1.07 | -72551112 | 72.55111 |
| 1.17 | -84434576 | 84.43458 |
| 1.27 | -97546448 | 97.54645 |
| 1.37 | -111980184 | 111.9802 |
| 1.47 | -127830416 | 127.8304 |
| 1.57 | -145192416 | 145.1924 |
| 1.67 | -164161536 | 164.1615 |
| 1.77 | -184832928 | 184.8329 |
| 1.87 | -207301344 | 207.3013 |
| 1.97 | -231661120 | 231.6611 |
| 2.07 | -258006480 | 258.0065 |
| 2.17 | -286431168 | 286.4312 |
| 2.27 | -317029440 | 317.0294 |
| 2.37 | -349899136 | 349.8991 |
| 2.47 | -385142816 | 385.1428 |
| 2.57 | -422864832 | 422.8648 |
| 2.67 | -463174400 | 463.1744 |
| 2.77 | -506185344 | 506.1853 |
| 2.87 | -552018496 | 552.0185 |
| 2.97 | -600799744 | 600.7997 |
| 3.07 | -616148608 | 616.1486 |
| 3.17 | -623080832 | 623.0808 |
| 3.27 | -629326712 | 629.3267 |
| 3.37 | -629326712 | 629.3267 |
| 3.47 | -629326712 | 629.3267 |
| 3.57 | -629326712 | 629.3267 |
| 3.67 | -629326712 | 629.3267 |
| 3.77 | -629326712 | 629.3267 |
| 3.87 | -629326712 | 629.3267 |
| 3.97 | -629326712 | 629.3267 |

Viscoelastic

| Time | Stress | Stress (Mpa) |
|---|---|---|
| 0 | 0 | 0 |
| 0.01 | -652614 | 0.652614 |
| 0.02 | -1283552.75 | 1.283553 |
| 0.03 | -1895008.625 | 1.895009 |
| 0.05 | -3065732.5 | 3.065733 |
| 0.09 | -5243902.5 | 5.243903 |
| 0.17 | -9204279 | 9.204279 |
| 0.27 | -13881448 | 13.88145 |
| 0.37 | -18588570 | 18.58857 |
| 0.47 | -23490292 | 23.49029 |
| 0.57 | -28669268 | 28.66927 |
| 0.67 | -34179336 | 34.17934 |
| 0.77 | -40064380 | 40.06438 |
| 0.87 | -46364576 | 46.36458 |
| 0.97 | -53118576 | 53.11858 |
| 1.07 | -60364020 | 60.36402 |
| 1.17 | -68137536 | 68.13754 |
| 1.27 | -76474528 | 76.47453 |
| 1.37 | -85408968 | 85.40897 |
| 1.47 | -94973176 | 94.97318 |
| 1.57 | -105197640 | 105.1976 |
| 1.67 | -116111096 | 116.1111 |
| 1.77 | -127740416 | 127.7404 |
| 1.87 | -140110880 | 140.1109 |
| 1.97 | -153246432 | 153.2464 |
| 2.07 | -167169984 | 167.17 |
| 2.17 | -181903856 | 181.9039 |
| 2.27 | -197470384 | 197.4704 |
| 2.37 | -213891760 | 213.8918 |
| 2.47 | -231188528 | 231.1885 |
| 2.57 | -249385504 | 249.3855 |
| 2.67 | -268511712 | 268.5117 |
| 2.77 | -288597600 | 288.5976 |
| 2.87 | -309674432 | 309.6744 |
| 2.97 | -331774016 | 331.774 |
| 3.07 | -354930752 | 354.9308 |
| 3.17 | -379185408 | 379.1854 |
| 3.27 | -404578240 | 404.5782 |
| 3.37 | -431150144 | 431.1501 |
| 3.47 | -458942976 | 458.943 |
| 3.57 | -487999040 | 487.999 |
| 3.67 | -518261344 | 518.2613 |
| 3.77 | -549960128 | 549.9601 |
| 3.87 | -583076352 | 583.0764 |
| 3.97 | -617972224 | 617.9722 |

| | | | | | |
|---|---|---|---|---|---|
| 4.07 | -629326712 | 629.3267 | 4.07 | -627299520 | 627.2995 |
| 4.17 | -629326712 | 629.3267 | 4.17 | -625596032 | 625.596 |
| 4.27 | -629326712 | 629.3267 | 4.195 | -625249280 | 625.2493 |
| 4.37 | -629326712 | 629.3267 | 4.2325 | -624858560 | 624.8586 |
| 4.47 | -629326712 | 629.3267 | 4.246562 | -624731584 | 624.7316 |
| 4.57 | -629326712 | 629.3267 | 4.251836 | -624687488 | 624.6875 |
| 4.67 | -629326712 | 629.3267 | 4.259746 | -624629376 | 624.6294 |
| 4.77 | -629326712 | 629.3267 | 4.262712 | -624612800 | 624.6128 |
| 4.87 | -629326712 | 629.3267 | 4.267162 | -624607296 | 624.6073 |
| 4.97 | -629326712 | 629.3267 | 4.271611 | -624809408 | 624.8094 |
| 5.07 | -629326712 | 629.3267 | 4.276061 | -624775616 | 624.7756 |
| 5.17 | -629326712 | 629.3267 | 4.282735 | -624723648 | 624.7236 |
| 5.27 | -629326712 | 629.3267 | 4.292746 | -624644032 | 624.644 |
| 5.37 | -629326712 | 629.3267 | 4.307763 | -624520896 | 624.5209 |
| 5.47 | -629326712 | 629.3267 | 4.330288 | -624326912 | 624.3269 |
| 5.57 | -629326712 | 629.3267 | 4.364077 | -624006272 | 624.0063 |
| 5.67 | -629326712 | 629.3267 | 4.414759 | -623479936 | 623.4799 |
| 5.77 | -629326712 | 629.3267 | 4.490782 | -622626432 | 622.6264 |
| 5.87 | -629326712 | 629.3267 | 4.590782 | -621439680 | 621.4397 |
| 5.97 | -629326712 | 629.3267 | 4.690782 | -620238016 | 620.238 |
| 6.07 | -629326712 | 629.3267 | 4.790782 | -619055424 | 619.0554 |
| 6.17 | -629326712 | 629.3267 | 4.890782 | -617910208 | 617.9102 |
| 6.27 | -629326712 | 629.3267 | 4.990782 | -616802368 | 616.8024 |
| 6.37 | -629326712 | 629.3267 | 5.090782 | -615732672 | 615.7327 |
| 6.47 | -629326712 | 629.3267 | 5.190782 | -614710464 | 614.7105 |
| 6.57 | -629326712 | 629.3267 | 5.290782 | -613733376 | 613.7334 |
| 6.67 | -629326712 | 629.3267 | 5.390782 | -612797696 | 612.7977 |
| 6.77 | -629326712 | 629.3267 | 5.490782 | -611899584 | 611.8996 |
| 6.87 | -629326712 | 629.3267 | 5.590782 | -611035072 | 611.0351 |
| 6.97 | -629326712 | 629.3267 | 5.690782 | -610200576 | 610.2006 |
| 7.07 | -629326712 | 629.3267 | 5.790782 | -609392640 | 609.3926 |
| 7.17 | -629326712 | 629.3267 | 5.890782 | -608608192 | 608.6082 |
| 7.27 | -629326712 | 629.3267 | 5.990782 | -607844480 | 607.8445 |
| 7.37 | -629326712 | 629.3267 | 6.090782 | -607099072 | 607.0991 |
| 7.47 | -629326712 | 629.3267 | 6.190782 | -606369728 | 606.3697 |
| 7.57 | -629326712 | 629.3267 | 6.290782 | -605654656 | 605.6547 |
| 7.67 | -629326712 | 629.3267 | 6.390782 | -604952064 | 604.9521 |
| 7.77 | -629326712 | 629.3267 | 6.490782 | -604260480 | 604.2605 |
| 7.87 | -629326712 | 629.3267 | 6.590782 | -603579072 | 603.5791 |
| 7.97 | -629326712 | 629.3267 | 6.690782 | -602905216 | 602.9052 |
| 8.07 | -629326712 | 629.3267 | 6.790782 | -602240000 | 602.24 |
| 8.17 | -629326712 | 629.3267 | 6.890782 | -601580864 | 601.5809 |
| 8.27 | -629326712 | 629.3267 | 6.990782 | -600927808 | 600.9278 |
| 8.37 | -629326712 | 629.3267 | 7.090782 | -600280256 | 600.2803 |
| 8.47 | -629326712 | 629.3267 | 7.190782 | -599637504 | 599.6375 |
| 8.57 | -629326712 | 629.3267 | 7.290782 | -598999168 | 598.9992 |
| 8.67 | -629326712 | 629.3267 | 7.390782 | -598364864 | 598.3649 |

| | | |
|---|---|---|
| 8.77 | -629326712 | 629.3267 |
| 8.87 | -629326712 | 629.3267 |
| 8.97 | -629326712 | 629.3267 |
| 9.07 | -629326712 | 629.3267 |
| 9.17 | -629326712 | 629.3267 |
| 9.27 | -629326712 | 629.3267 |
| 9.37 | -629326712 | 629.3267 |
| 9.47 | -629326712 | 629.3267 |
| 9.57 | -629326712 | 629.3267 |
| 9.67 | -629326712 | 629.3267 |
| 9.77 | -629326712 | 629.3267 |
| 9.87 | -629326712 | 629.3267 |
| 9.97 | -629326712 | 629.3267 |
| 10 | -629326712 | 629.3267 |

| | | |
|---|---|---|
| 7.490782 | -597734336 | 597.7343 |
| 7.590782 | -597107264 | 597.1073 |
| 7.690782 | -596483520 | 596.4835 |
| 7.790782 | -595862976 | 595.863 |
| 7.890782 | -595245376 | 595.2454 |
| 7.990782 | -594630848 | 594.6308 |
| 8.090782 | -594019008 | 594.019 |
| 8.190783 | -593410112 | 593.4101 |
| 8.290782 | -592804032 | 592.804 |
| 8.390782 | -592200768 | 592.2008 |
| 8.490782 | -591600320 | 591.6003 |
| 8.590782 | -591002688 | 591.0027 |
| 8.690783 | -590407872 | 590.4079 |
| 8.790782 | -589816128 | 589.8161 |
| 8.890782 | -589227200 | 589.2272 |
| 8.990782 | -588641408 | 588.6414 |
| 9.090782 | -588058560 | 588.0586 |
| 9.190783 | -587478784 | 587.4788 |
| 9.290782 | -586902208 | 586.9022 |
| 9.390782 | -586328960 | 586.329 |
| 9.490782 | -585758848 | 585.7588 |
| 9.590782 | -585192064 | 585.1921 |
| 9.690783 | -584628672 | 584.6287 |
| 9.790782 | -584068608 | 584.0686 |
| 9.890782 | -583512192 | 583.5122 |
| 9.990782 | -582959104 | 582.9591 |
| 10 | -582908352 | 582.9084 |

Raw data of Figure 4.11

| 0.00027m | | | 0.0003m | | 0.00032 | |
|---|---|---|---|---|---|---|
| Time | stress | Stress (Mpa) | Time | Stress (mpa) | Time | Stress (mpa) |
| 0 | 0 | 0 | 0 | 0 | 0 | 0 |
| 0.01 | -3.7E-10 | 3.71E-16 | 0.01 | 3.71E-16 | 0.01 | 3.71E-16 |
| 0.02 | -7E-09 | 6.99E-15 | 0.02 | 6.99E-15 | 0.02 | 6.99E-15 |
| 0.03 | -2.2E-08 | 2.25E-14 | 0.03 | 2.25E-14 | 0.03 | 2.25E-14 |
| 0.045 | -3.7E-08 | 3.65E-14 | 0.045 | 3.65E-14 | 0.045 | 3.65E-14 |
| 0.0675 | -6E-09 | 5.97E-15 | 0.0675 | 5.97E-15 | 0.0675 | 5.97E-15 |
| 0.10125 | 5.06E-08 | 5.06E-14 | 0.10125 | 5.06E-14 | 0.10125 | 5.06E-14 |
| 0.151875 | -3.1E-07 | 3.1E-13 | 0.151875 | 3.1E-13 | 0.151875 | 3.1E-13 |
| 0.227812 | 7.75E-07 | 7.75E-13 | 0.227812 | 7.75E-13 | 0.227812 | 7.75E-13 |
| 0.327812 | 5.14E-06 | 5.14E-12 | 0.327812 | 5.14E-12 | 0.327812 | 5.14E-12 |
| 0.427812 | -2.5E-06 | 2.55E-12 | 0.427812 | 2.55E-12 | 0.427812 | 2.55E-12 |
| 0.527812 | 2.08E-06 | 2.08E-12 | 0.527812 | 2.08E-12 | 0.527812 | 2.08E-12 |
| 0.627813 | 2.19E-06 | 2.19E-12 | 0.627813 | 2.19E-12 | 0.627813 | 2.19E-12 |
| 0.727813 | -2.4E-06 | 2.38E-12 | 0.727813 | 2.38E-12 | 0.727813 | 2.38E-12 |
| 0.827812 | 4.45E-06 | 4.45E-12 | 0.827812 | 4.45E-12 | 0.827812 | 4.45E-12 |
| 0.927813 | 1.59E-06 | 1.59E-12 | 0.927813 | 1.59E-12 | 0.927813 | 1.59E-12 |
| 1.027812 | 5.66E-07 | 5.66E-13 | 1.027812 | 5.66E-13 | 1.027812 | 5.66E-13 |
| 1.127813 | -2E-06 | 1.99E-12 | 1.127813 | 1.99E-12 | 1.127813 | 1.99E-12 |
| 1.227813 | -3.5E-06 | 3.48E-12 | 1.227813 | 3.48E-12 | 1.227813 | 3.48E-12 |
| 1.327813 | 6.86E-07 | 6.86E-13 | 1.327813 | 6.86E-13 | 1.327813 | 6.86E-13 |
| 1.427812 | 4.15E-06 | 4.15E-12 | 1.427812 | 4.15E-12 | 1.427812 | 4.15E-12 |
| 1.527812 | 1.33E-06 | 1.33E-12 | 1.527812 | 1.33E-12 | 1.527812 | 1.33E-12 |
| 1.627813 | 2.22E-06 | 2.22E-12 | 1.627813 | 2.22E-12 | 1.627813 | 2.22E-12 |
| 1.727813 | 3.29E-06 | 3.29E-12 | 1.727813 | 3.29E-12 | 1.727813 | 3.29E-12 |
| 1.827813 | 1.3E-06 | 1.3E-12 | 1.827813 | 1.3E-12 | 1.827813 | 1.3E-12 |
| 1.927812 | -1.2E-06 | 1.23E-12 | 1.927812 | 1.23E-12 | 1.927812 | 1.23E-12 |
| 2.027812 | -4E-07 | 4.04E-13 | 2.027812 | 4.04E-13 | 2.027812 | 4.04E-13 |
| 2.127812 | -2.2E-06 | 2.16E-12 | 2.127812 | 2.16E-12 | 2.127812 | 2.16E-12 |
| 2.227813 | 2.85E-06 | 2.85E-12 | 2.227813 | 2.85E-12 | 2.227813 | 2.85E-12 |
| 2.327812 | 1.67E-06 | 1.67E-12 | 2.327812 | 1.67E-12 | 2.327812 | 1.67E-12 |
| 2.427813 | 3.16E-06 | 3.16E-12 | 2.427813 | 3.16E-12 | 2.427813 | 3.16E-12 |
| 2.527812 | 1.12E-06 | 1.12E-12 | 2.527812 | 1E-12 | 2.527812 | 1.12E-12 |
| 2.627812 | -1.5E+08 | 149.4885 | 2.627812 | 228.0642 | 2.627812 | 305.0775 |
| 2.727813 | -4E+08 | 395.9285 | 2.727813 | 447.9921 | 2.727813 | 498.7522 |
| 2.827812 | -5.6E+08 | 559.9997 | 2.827812 | 599.9756 | 2.827812 | 638.7417 |
| 2.927813 | -6.8E+08 | 683.7391 | 2.927813 | 717.0478 | 2.927813 | 749.1002 |
| 3.027812 | -7.3E+08 | 731.233 | 3.027812 | 786.2965 | 3.027812 | 835.4321 |
| 3.127812 | -6.2E+08 | 622.0225 | 3.127812 | 672.0103 | 3.127812 | 717.3575 |
| 3.227813 | -5.8E+08 | 576.6321 | 3.227813 | 624.0849 | 3.227813 | 667.7059 |
| 3.327812 | -5.5E+08 | 554.8288 | 3.327812 | 601.0093 | 3.327812 | 643.7098 |
| 3.427813 | -5.4E+08 | 542.2648 | 3.427813 | 587.6808 | 3.427813 | 629.7667 |
| 3.527812 | -5.3E+08 | 533.5774 | 3.527812 | 578.395 | 3.527812 | 619.999 |
| 3.627812 | -5.3E+08 | 526.639 | 3.627812 | 571.0004 | 3.627812 | 612.1918 |
| 3.727813 | -5.2E+08 | 520.6649 | 3.727813 | 564.6091 | 3.727813 | 605.4305 |
| 3.827812 | -5.2E+08 | 515.3494 | 3.827812 | 558.8954 | 3.827812 | 599.3803 |

| | | | | | | | | |
|---|---|---|---|---|---|---|---|---|
| 3.927813 | -5.1E+08 | 510.5132 | 3.927813 | 553.7183 | | 3.927813 | 593.8942 | |
| 4.027812 | -5.1E+08 | 506.0802 | 4.027812 | 548.9682 | | 4.027812 | 588.8553 | |
| 4.127812 | -5E+08 | 502.0134 | 4.127812 | 544.5959 | | 4.127812 | 584.2159 | |
| 4.227812 | -5E+08 | 498.2639 | 4.227812 | 540.5724 | | 4.227812 | 579.9387 | |
| 4.327813 | -4.9E+08 | 494.7972 | 4.327813 | 536.8537 | | 4.327813 | 575.993 | |
| 4.427813 | -4.9E+08 | 491.588 | 4.427813 | 533.4089 | | 4.427813 | 572.3383 | |
| 4.527812 | -4.9E+08 | 488.6141 | 4.527812 | 530.2142 | | 4.527812 | 568.9464 | |
| 4.627812 | -4.9E+08 | 485.8547 | 4.627812 | 527.2483 | | 4.627812 | 565.795 | |
| 4.727812 | -4.8E+08 | 483.2899 | 4.727812 | 524.4907 | | 4.727812 | 562.8634 | |
| 4.827813 | -4.8E+08 | 480.9012 | 4.827813 | 521.922 | | 4.827813 | 560.1321 | |
| 4.927813 | -4.8E+08 | 478.672 | 4.927813 | 519.5245 | | 4.927813 | 557.5824 | |
| 5.027812 | -4.8E+08 | 476.5871 | 5.027812 | 517.2821 | | 5.027812 | 555.1973 | |
| 5.127812 | -4.7E+08 | 474.6335 | 5.127812 | 515.1805 | | 5.127812 | 552.9616 | |
| 5.227812 | -4.7E+08 | 472.7992 | 5.227812 | 513.2069 | | 5.227812 | 550.8618 | |
| 5.327813 | -4.7E+08 | 471.0737 | 5.327813 | 511.35 | | 5.327813 | 548.8858 | |
| 5.427813 | -4.7E+08 | 469.4472 | 5.427813 | 509.5993 | | 5.427813 | 547.0224 | |
| 5.527812 | -4.7E+08 | 467.9111 | 5.527812 | 507.9455 | | 5.527812 | 545.2617 | |
| 5.627812 | -4.7E+08 | 466.4573 | 5.627812 | 506.3799 | | 5.627812 | 543.5947 | |
| 5.727812 | -4.7E+08 | 465.0785 | 5.727812 | 504.8949 | | 5.727812 | 542.013 | |
| 5.827813 | -4.6E+08 | 463.7683 | 5.827813 | 503.4833 | | 5.827813 | 540.5093 | |
| 5.927813 | -4.6E+08 | 462.5206 | 5.927813 | 502.1389 | | 5.927813 | 539.0769 | |
| 6.027812 | -4.6E+08 | 461.33 | 6.027812 | 500.8558 | | 6.027812 | 537.7095 | |
| 6.127812 | -4.6E+08 | 460.1918 | 6.127812 | 499.6288 | | 6.127812 | 536.4017 | |
| 6.227812 | -4.6E+08 | 459.1015 | 6.227812 | 498.4532 | | 6.227812 | 535.1485 | |
| 6.327813 | -4.6E+08 | 458.055 | 6.327813 | 497.3248 | | 6.327813 | 533.9452 | |
| 6.427813 | -4.6E+08 | 457.0488 | 6.427813 | 496.2395 | | 6.427813 | 532.7878 | |
| 6.527812 | -4.6E+08 | 456.0796 | 6.527812 | 495.194 | | 6.527812 | 531.6726 | |
| 6.627812 | -4.6E+08 | 455.1444 | 6.627812 | 494.1849 | | 6.627812 | 530.5961 | |
| 6.727812 | -4.5E+08 | 454.2405 | 6.727812 | 493.2095 | | 6.727812 | 529.5553 | |
| 6.827813 | -4.5E+08 | 453.3654 | 6.827813 | 492.265 | | 6.827813 | 528.5473 | |
| 6.927813 | -4.5E+08 | 452.5169 | 6.927813 | 491.3491 | | 6.927813 | 527.5697 | |
| 7.027812 | -4.5E+08 | 451.693 | 7.027812 | 490.4596 | | 7.027812 | 526.6202 | |
| 7.127812 | -4.5E+08 | 450.8918 | 7.127812 | 489.5945 | | 7.127812 | 525.6967 | |
| 7.227812 | -4.5E+08 | 450.1118 | 7.227812 | 488.7521 | | 7.227812 | 524.7972 | |
| 7.327813 | -4.5E+08 | 449.3513 | 7.327813 | 487.9308 | | 7.327813 | 523.9201 | |
| 7.427813 | -4.5E+08 | 448.609 | 7.427813 | 487.129 | | 7.427813 | 523.0637 | |
| 7.527812 | -4.5E+08 | 447.8837 | 7.527812 | 486.3454 | | 7.527812 | 522.2268 | |
| 7.627812 | -4.5E+08 | 447.1742 | 7.627812 | 485.5789 | | 7.627812 | 521.408 | |
| 7.727812 | -4.5E+08 | 446.4795 | 7.727812 | 484.8283 | | 7.727812 | 520.6061 | |
| 7.827813 | -4.5E+08 | 445.7987 | 7.827813 | 484.0926 | | 7.827813 | 519.82 | |
| 7.927813 | -4.5E+08 | 445.1308 | 7.927813 | 483.3709 | | 7.927813 | 519.0488 | |
| 8.027813 | -4.4E+08 | 444.4752 | 8.027813 | 482.6623 | | 8.027813 | 518.2916 | |
| 8.127812 | -4.4E+08 | 443.8311 | 8.127812 | 481.9661 | | 8.127812 | 517.5476 | |
| 8.227813 | -4.4E+08 | 443.1979 | 8.227813 | 481.2816 | | 8.227813 | 516.816 | |
| 8.327812 | -4.4E+08 | 442.5749 | 8.327812 | 480.6082 | | 8.327812 | 516.0962 | |
| 8.427813 | -4.4E+08 | 441.9617 | 8.427813 | 479.9453 | | 8.427813 | 515.3876 | |
| 8.527813 | -4.4E+08 | 441.3578 | 8.527813 | 479.2923 | | 8.527813 | 514.6896 | |

| | | |
|---|---|---|
| 8.627812 | -4.4E+08 | 440.7626 |
| 8.727813 | -4.4E+08 | 440.1758 |
| 8.827812 | -4.4E+08 | 439.5971 |
| 8.927813 | -4.4E+08 | 439.026 |
| 9.027813 | -4.4E+08 | 438.4623 |
| 9.127812 | -4.4E+08 | 437.9056 |
| 9.227813 | -4.4E+08 | 437.3558 |
| 9.327812 | -4.4E+08 | 436.8124 |
| 9.427813 | -4.4E+08 | 436.2755 |
| 9.527813 | -4.4E+08 | 435.7446 |
| 9.627812 | -4.4E+08 | 435.2197 |
| 9.727813 | -4.3E+08 | 434.7005 |
| 9.827812 | -4.3E+08 | 434.1869 |
| 9.927813 | -4.3E+08 | 433.6787 |
| 10 | -4.3E+08 | 433.3152 |

| | |
|---|---|
| 8.627812 | 478.6488 |
| 8.727813 | 478.0144 |
| 8.827812 | 477.3886 |
| 8.927813 | 476.7711 |
| 9.027813 | 476.1615 |
| 9.127812 | 475.5595 |
| 9.227813 | 474.9649 |
| 9.327812 | 474.3773 |
| 9.427813 | 473.7965 |
| 9.527813 | 473.2224 |
| 9.627812 | 472.6546 |
| 9.727813 | 472.0931 |
| 9.827812 | 471.5376 |
| 9.927813 | 470.9879 |
| 10 | 470.5947 |

| | |
|---|---|
| 8.627812 | 514.0017 |
| 8.727813 | 513.3235 |
| 8.827812 | 512.6544 |
| 8.927813 | 511.9942 |
| 9.027813 | 511.3424 |
| 9.127812 | 510.6987 |
| 9.227813 | 510.0628 |
| 9.327812 | 509.4345 |
| 9.427813 | 508.8135 |
| 9.527813 | 508.1995 |
| 9.627812 | 507.5923 |
| 9.727813 | 506.9918 |
| 9.827812 | 506.3977 |
| 9.927813 | 505.8099 |
| 10 | 505.3893 |

Raw data of Figure 4.12

**Compare-relaxation result-viscohyper-elasticvisco**

| elastic visco | | |
|---|---|---|
| time | stress | stress (mpa) |
| 0 | 0 | 0 |
| 0.01 | 6.31E-11 | 6.31E-17 |
| 0.02 | 1.04E-10 | 1.04E-16 |
| 0.03 | 3.59E-10 | 3.59E-16 |
| 0.045 | 2.74E-10 | 2.74E-16 |
| 0.0675 | -4.7E-11 | 4.66E-17 |
| 0.10125 | -4.7E-10 | 4.73E-16 |
| 0.151875 | 3.04E-10 | 3.04E-16 |
| 0.227812 | 1.9E-10 | 1.9E-16 |
| 0.327812 | -3.4E-10 | 3.38E-16 |
| 0.427812 | -2.9E-10 | 2.91E-16 |
| 0.527812 | -4.7E-10 | 4.72E-16 |
| 0.627813 | -4.6E-11 | 4.59E-17 |
| 0.727813 | -4.9E-10 | 4.85E-16 |
| 0.827812 | -2.5E-10 | 2.46E-16 |
| 0.927813 | 1.18E-10 | 1.18E-16 |
| 1.027812 | -3.8E-10 | 3.77E-16 |
| 1.127813 | 5.17E-10 | 5.17E-16 |
| 1.227813 | 1.63E-10 | 1.63E-16 |
| 1.327813 | -2.9E-10 | 2.86E-16 |
| 1.427812 | -3.3E-10 | 3.3E-16 |
| 1.527812 | -2.3E-10 | 2.32E-16 |
| 1.627813 | -3.8E-10 | 3.8E-16 |
| 1.727813 | -6.5E-10 | 6.52E-16 |
| 1.827813 | -2.3E-10 | 2.34E-16 |
| 1.927812 | 2.09E-10 | 2.09E-16 |
| 2.027812 | 4E-10 | 4E-16 |
| 2.127812 | 4.04E-10 | 4.04E-16 |
| 2.227813 | 5.88E-10 | 5.88E-16 |
| 2.327812 | 1.16E-10 | 1.16E-16 |
| 2.427813 | 7.46E-12 | 7.46E-18 |
| 2.527812 | 3.61E-10 | 3.61E-16 |
| 2.627812 | -4.7E+07 | 47.3901 |
| 2.727813 | -1.4E+08 | 141.8042 |
| 2.827812 | -2.3E+08 | 232.7053 |
| 2.927813 | -3.3E+08 | 327.3327 |
| 3.027812 | -4E+08 | 396.6156 |
| 3.127812 | -3.7E+08 | 373.9059 |
| 3.227813 | -3.6E+08 | 362.0898 |
| 3.327812 | -3.5E+08 | 354.7769 |
| 3.427813 | -3.5E+08 | 349.4374 |
| 3.527812 | -3.5E+08 | 345.0747 |

| viscohyper | | |
|---|---|---|
| Time | stress | Stress (Mpa) |
| 0 | 0 | 0 |
| 0.01 | -3.7E-10 | 3.71E-16 |
| 0.02 | -7E-09 | 6.99E-15 |
| 0.03 | -2.2E-08 | 2.25E-14 |
| 0.045 | -3.7E-08 | 3.65E-14 |
| 0.0675 | -6E-09 | 5.97E-15 |
| 0.10125 | 5.06E-08 | 5.06E-14 |
| 0.151875 | -3.1E-07 | 3.1E-13 |
| 0.227812 | 7.75E-07 | 7.75E-13 |
| 0.327812 | 5.14E-06 | 5.14E-12 |
| 0.427812 | -2.5E-06 | 2.55E-12 |
| 0.527812 | 2.08E-06 | 2.08E-12 |
| 0.627813 | 2.19E-06 | 2.19E-12 |
| 0.727813 | -2.4E-06 | 2.38E-12 |
| 0.827812 | 4.45E-06 | 4.45E-12 |
| 0.927813 | 1.59E-06 | 1.59E-12 |
| 1.027812 | 5.66E-07 | 5.66E-13 |
| 1.127813 | -2E-06 | 1.99E-12 |
| 1.227813 | -3.5E-06 | 3.48E-12 |
| 1.327813 | 6.86E-07 | 6.86E-13 |
| 1.427812 | 4.15E-06 | 4.15E-12 |
| 1.527812 | 1.33E-06 | 1.33E-12 |
| 1.627813 | 2.22E-06 | 2.22E-12 |
| 1.727813 | 3.29E-06 | 3.29E-12 |
| 1.827813 | 1.3E-06 | 1.3E-12 |
| 1.927812 | -1.2E-06 | 1.23E-12 |
| 2.027812 | -4E-07 | 4.04E-13 |
| 2.127812 | -2.2E-06 | 2.16E-12 |
| 2.227813 | 2.85E-06 | 2.85E-12 |
| 2.327812 | 1.67E-06 | 1.67E-12 |
| 2.427813 | 3.16E-06 | 3.16E-12 |
| 2.527812 | 1.12E-06 | 1.12E-12 |
| 2.627812 | -1.5E+08 | 149.4885 |
| 2.727813 | -4E+08 | 395.9285 |
| 2.827812 | -5.6E+08 | 559.9997 |
| 2.927813 | -6.8E+08 | 683.7391 |
| 3.027812 | -7.3E+08 | 731.233 |
| 3.127812 | -6.2E+08 | 622.0225 |
| 3.227813 | -5.8E+08 | 576.6321 |
| 3.327812 | -5.5E+08 | 554.8288 |
| 3.427813 | -5.4E+08 | 542.2648 |
| 3.527812 | -5.3E+08 | 533.5774 |

| | | |
|---|---|---|
| 3.627812 | -3.4E+08 | 341.2812 |
| 3.727813 | -3.4E+08 | 337.8803 |
| 3.827812 | -3.3E+08 | 334.7872 |
| 3.927813 | -3.3E+08 | 331.9546 |
| 4.027812 | -3.3E+08 | 329.3512 |
| 4.127812 | -3.3E+08 | 326.9531 |
| 4.227812 | -3.2E+08 | 324.7404 |
| 4.327813 | -3.2E+08 | 322.6958 |
| 4.427813 | -3.2E+08 | 320.8038 |
| 4.527812 | -3.2E+08 | 319.0507 |
| 4.627812 | -3.2E+08 | 317.4237 |
| 4.727812 | -3.2E+08 | 315.9117 |
| 4.827813 | -3.1E+08 | 314.5043 |
| 4.927813 | -3.1E+08 | 313.1921 |
| 5.027812 | -3.1E+08 | 311.9667 |
| 5.127812 | -3.1E+08 | 310.8178 |
| 5.227812 | -3.1E+08 | 309.7436 |
| 5.327813 | -3.1E+08 | 308.7354 |
| 5.427813 | -3.1E+08 | 307.787 |
| 5.527812 | -3.1E+08 | 306.8933 |
| 5.627812 | -3.1E+08 | 306.0496 |
| 5.727812 | -3.1E+08 | 305.2515 |
| 5.827813 | -3E+08 | 304.4952 |
| 5.927813 | -3E+08 | 303.7771 |
| 6.027812 | -3E+08 | 303.094 |
| 6.127812 | -3E+08 | 302.4429 |
| 6.227812 | -3E+08 | 301.8212 |
| 6.327813 | -3E+08 | 301.2263 |
| 6.427813 | -3E+08 | 300.6562 |
| 6.527812 | -3E+08 | 300.1088 |
| 6.627812 | -3E+08 | 299.5824 |
| 6.727812 | -3E+08 | 299.0752 |
| 6.827813 | -3E+08 | 298.5857 |
| 6.927813 | -3E+08 | 298.1126 |
| 7.027812 | -3E+08 | 297.6547 |
| 7.127812 | -3E+08 | 297.2107 |
| 7.227812 | -3E+08 | 296.7797 |
| 7.327813 | -3E+08 | 296.3608 |
| 7.427813 | -3E+08 | 295.9529 |
| 7.527812 | -3E+08 | 295.5555 |
| 7.627812 | -3E+08 | 295.1678 |
| 7.727812 | -2.9E+08 | 294.7891 |
| 7.827813 | -2.9E+08 | 294.4188 |
| 7.927813 | -2.9E+08 | 294.0565 |
| 8.027813 | -2.9E+08 | 293.7016 |
| 8.127812 | -2.9E+08 | 293.3536 |
| 8.227813 | -2.9E+08 | 293.0122 |

| | | |
|---|---|---|
| 3.627812 | -5.3E+08 | 526.639 |
| 3.727813 | -5.2E+08 | 520.6649 |
| 3.827812 | -5.2E+08 | 515.3494 |
| 3.927813 | -5.1E+08 | 510.5132 |
| 4.027812 | -5.1E+08 | 506.0802 |
| 4.127812 | -5E+08 | 502.0134 |
| 4.227812 | -5E+08 | 498.2639 |
| 4.327813 | -4.9E+08 | 494.7972 |
| 4.427813 | -4.9E+08 | 491.588 |
| 4.527812 | -4.9E+08 | 488.6141 |
| 4.627812 | -4.9E+08 | 485.8547 |
| 4.727812 | -4.8E+08 | 483.2899 |
| 4.827813 | -4.8E+08 | 480.9012 |
| 4.927813 | -4.8E+08 | 478.672 |
| 5.027812 | -4.8E+08 | 476.5871 |
| 5.127812 | -4.7E+08 | 474.6335 |
| 5.227812 | -4.7E+08 | 472.7992 |
| 5.327813 | -4.7E+08 | 471.0737 |
| 5.427813 | -4.7E+08 | 469.4472 |
| 5.527812 | -4.7E+08 | 467.9111 |
| 5.627812 | -4.7E+08 | 466.4573 |
| 5.727812 | -4.7E+08 | 465.0785 |
| 5.827813 | -4.6E+08 | 463.7683 |
| 5.927813 | -4.6E+08 | 462.5206 |
| 6.027812 | -4.6E+08 | 461.33 |
| 6.127812 | -4.6E+08 | 460.1918 |
| 6.227812 | -4.6E+08 | 459.1015 |
| 6.327813 | -4.6E+08 | 458.055 |
| 6.427813 | -4.6E+08 | 457.0488 |
| 6.527812 | -4.6E+08 | 456.0796 |
| 6.627812 | -4.6E+08 | 455.1444 |
| 6.727812 | -4.5E+08 | 454.2405 |
| 6.827813 | -4.5E+08 | 453.3654 |
| 6.927813 | -4.5E+08 | 452.5169 |
| 7.027812 | -4.5E+08 | 451.693 |
| 7.127812 | -4.5E+08 | 450.8918 |
| 7.227812 | -4.5E+08 | 450.1118 |
| 7.327813 | -4.5E+08 | 449.3513 |
| 7.427813 | -4.5E+08 | 448.609 |
| 7.527812 | -4.5E+08 | 447.8837 |
| 7.627812 | -4.5E+08 | 447.1742 |
| 7.727812 | -4.5E+08 | 446.4795 |
| 7.827813 | -4.5E+08 | 445.7987 |
| 7.927813 | -4.5E+08 | 445.1308 |
| 8.027813 | -4.4E+08 | 444.4752 |
| 8.127812 | -4.4E+08 | 443.8311 |
| 8.227813 | -4.4E+08 | 443.1979 |

| | | |
|---|---|---|
| 8.327812 | -2.9E+08 | 292.677 |
| 8.427813 | -2.9E+08 | 292.3476 |
| 8.527813 | -2.9E+08 | 292.0237 |
| 8.627812 | -2.9E+08 | 291.7052 |
| 8.727813 | -2.9E+08 | 291.3916 |
| 8.827812 | -2.9E+08 | 291.0827 |
| 8.927813 | -2.9E+08 | 290.7783 |
| 9.027813 | -2.9E+08 | 290.4783 |
| 9.127812 | -2.9E+08 | 290.1824 |
| 9.227813 | -2.9E+08 | 289.8905 |
| 9.327812 | -2.9E+08 | 289.6024 |
| 9.427813 | -2.9E+08 | 289.3179 |
| 9.527813 | -2.9E+08 | 289.037 |
| 9.627812 | -2.9E+08 | 288.7595 |
| 9.727813 | -2.9E+08 | 288.4853 |
| 9.827812 | -2.9E+08 | 288.2142 |
| 9.927813 | -2.9E+08 | 287.9461 |
| 10 | -2.9E+08 | 287.7548 |

| | | |
|---|---|---|
| 8.327812 | -4.4E+08 | 442.5749 |
| 8.427813 | -4.4E+08 | 441.9617 |
| 8.527813 | -4.4E+08 | 441.3578 |
| 8.627812 | -4.4E+08 | 440.7626 |
| 8.727813 | -4.4E+08 | 440.1758 |
| 8.827812 | -4.4E+08 | 439.5971 |
| 8.927813 | -4.4E+08 | 439.026 |
| 9.027813 | -4.4E+08 | 438.4623 |
| 9.127812 | -4.4E+08 | 437.9056 |
| 9.227813 | -4.4E+08 | 437.3558 |
| 9.327812 | -4.4E+08 | 436.8124 |
| 9.427813 | -4.4E+08 | 436.2755 |
| 9.527813 | -4.4E+08 | 435.7446 |
| 9.627812 | -4.4E+08 | 435.2197 |
| 9.727813 | -4.3E+08 | 434.7005 |
| 9.827812 | -4.3E+08 | 434.1869 |
| 9.927813 | -4.3E+08 | 433.6787 |
| 10 | -4.3E+08 | 433.3152 |